4 Non overconstrained *T3*-type TPMs with coupled motions

Equation (1.15) indicates that *non overconstrained* solutions of *T3*-type TPMs with *coupled motions* and q independent loops meet the condition $\sum_{1}^{p} f_i = 3 + 6q$. Various solutions fulfil this condition along with $S_F = 3$, $(R_F) = (\mathbf{v}_1, \mathbf{v}_2, \mathbf{v}_3)$ and $N_F = 0$. They can have identical limbs or limbs with different structures and may be actuated by linear or rotating motors.

4.1 Basic solutions with linear actuators

In the basic non overconstrained TPMs with *linear actuators* and coupled motions $F \leftarrow G_1–G_2–G_3$, the moving platform $n \equiv n_{Gi}$ ($i = 1, 2, 3$) is connected to the reference platform $1 \equiv 1_{Gi} \equiv 0$ by three limbs with five degrees of connectivity. No idle mobilities exist in these *basic solutions*.

The various types of limbs with five degrees of connectivity and no idle mobilities are systematized in Figs. 4.1 and 4.2. They are actuated by linear motors mounted on the fixed base (Fig. 4.1) or on a moving link (Fig. 4.2). The prismatic joints between links 2 and 3 (Fig. 4.2c–f) and 3 and 4 (Fig. 4.2a, b) are actuated in the solutions with the linear actuator non adjacent to the fixed base.

Various solutions of TPMs with coupled motions and no idle mobilities can be obtained by using three limbs with identical or different topologies presented in Figs. 4.1 and 4.2. We only show solutions with identical limb type as illustrated in Figs. 4.3–4.9. The limb topology and connecting conditions in these solutions are systematized in Table 4.1.

The actuated prismatic joints adjacent to the fixed base in the three limbs have orthogonal directions (Figs. 4.3–4.5) in the solutions using the limbs systematized in Fig. 4.1. The axes of the first unactuated revolute joints of the three limbs have orthogonal directions (Figs. 4.6, 4.7a, 4.8 and 4.9) or are parallel to one plane (Fig. 4.7b) in the solutions using the limbs systematized in Fig. 4.2.

G. Gogu, *Structural Synthesis of Parallel Robots: Part 2: Translational Topologies with Two and Three Degrees of Freedom,* Solid Mechanics and Its Applications 159, 365–469.

For the solutions in Figs. 4.3–4.9, Eqs. (1.2)–(1.8) and (1.17) give the following structural parameters: $M_{Gi} = S_{Gi} = 3$, $(R_{G1}) = (\boldsymbol{v}_x, \boldsymbol{v}_y, \boldsymbol{v}_y, \boldsymbol{\omega}_\beta, \boldsymbol{\omega}_\delta)$, $(R_{G2}) = (\boldsymbol{v}_x, \boldsymbol{v}_y, \boldsymbol{v}_y, \boldsymbol{\omega}_\alpha, \boldsymbol{\omega}_\delta)$, $(R_{G2}) = (\boldsymbol{v}_x, \boldsymbol{v}_y, \boldsymbol{v}_y, \boldsymbol{\omega}_\alpha, \boldsymbol{\omega}_\beta)$, $(R_F) = (\boldsymbol{v}_x, \boldsymbol{v}_y, \boldsymbol{v}_y)$, $S_F = 3$, $r_F = 12$, $M_F = 3$, $N_F = 0$ and $T_F = 0$.

Table 4.1. Limb topology and connecting conditions of the non overconstrained TPM with no idle mobilities and linear actuators presented in Figs. 4.3–4.9

No.	TPM type	Limb topology	Connecting conditions
1	$3\text{-}\underline{P}RRRR$ (Fig. 4.3a)	$\underline{P} \perp R \parallel R \perp R \parallel R$ (Fig. 4.1a)	Actuated $\underline{P}$ joints adjacent to the fixed base have orthogonal directions
2	$3\text{-}\underline{P}RRRR$ (Fig. 4.3b)	$\underline{P} \perp R \perp R \parallel R \perp R$ (Fig. 4.1b)	Idem No. 1
3	$3\text{-}\underline{P}RRRR$ (Fig. 4.4a)	$\underline{P} \parallel R \parallel R \perp R \parallel R$ (Fig. 4.1c)	Idem No. 1
4	$3\text{-}\underline{P}RRRR$ (Fig. 4.4b)	$\underline{P} \parallel R \perp R \parallel R \perp R$ (Fig. 4.1d)	Idem No. 1
5	$3\text{-}\underline{P}RRRR$ (Fig. 4.5)	$\underline{P} \perp R \perp R \parallel R \perp R$ (Fig. 4.1e)	Idem No. 1
6	$3\text{-}RR\underline{P}RR$ (Fig. 4.6)	$R \perp R \parallel \underline{P} \parallel R \perp R$ (Fig. 4.2a)	Actuated $\underline{P}$ joints non adjacent to the fixed base and the first revolute joints of the three legs have orthogonal axes
7	$3\text{-}RR\underline{P}RR$ (Fig. 4.7a)	$R \perp R \perp \underline{P} \perp^{\parallel} R \perp R$ (Fig. 4.2b)	Idem No. 6
8	$3\text{-}RR\underline{P}RR$ (Fig. 4.7b)	$R \perp R \perp \underline{P} \perp^{\parallel} R \perp R$ (Fig. 4.2b)	Actuated $\underline{P}$ joints non adjacent to the fixed base and the first revolute joints of the three legs are parallel to one plane
9	$3\text{-}R\underline{P}RRR$ (Fig. 4.8a)	$R \perp \underline{P} \perp^{\perp} R \parallel R \perp R$ (Fig. 4.2c)	Idem No. 6
10	$3\text{-}R\underline{P}RRR$ (Fig. 4.8b)	$R \perp \underline{P} \parallel R \parallel R \perp R$ (Fig. 4.2d)	Idem No. 6
11	$3\text{-}R\underline{P}RRR$ (Fig. 4.9a)	$R \perp \underline{P} \perp^{\parallel} R \perp R \parallel R$ (Fig. 4.2e)	Idem No. 6
12	$3\text{-}R\underline{P}RRR$ (Fig. 4.9b)	$R \parallel \underline{P} \perp R \parallel R \perp R$ (Fig. 4.2f)	Idem No. 6

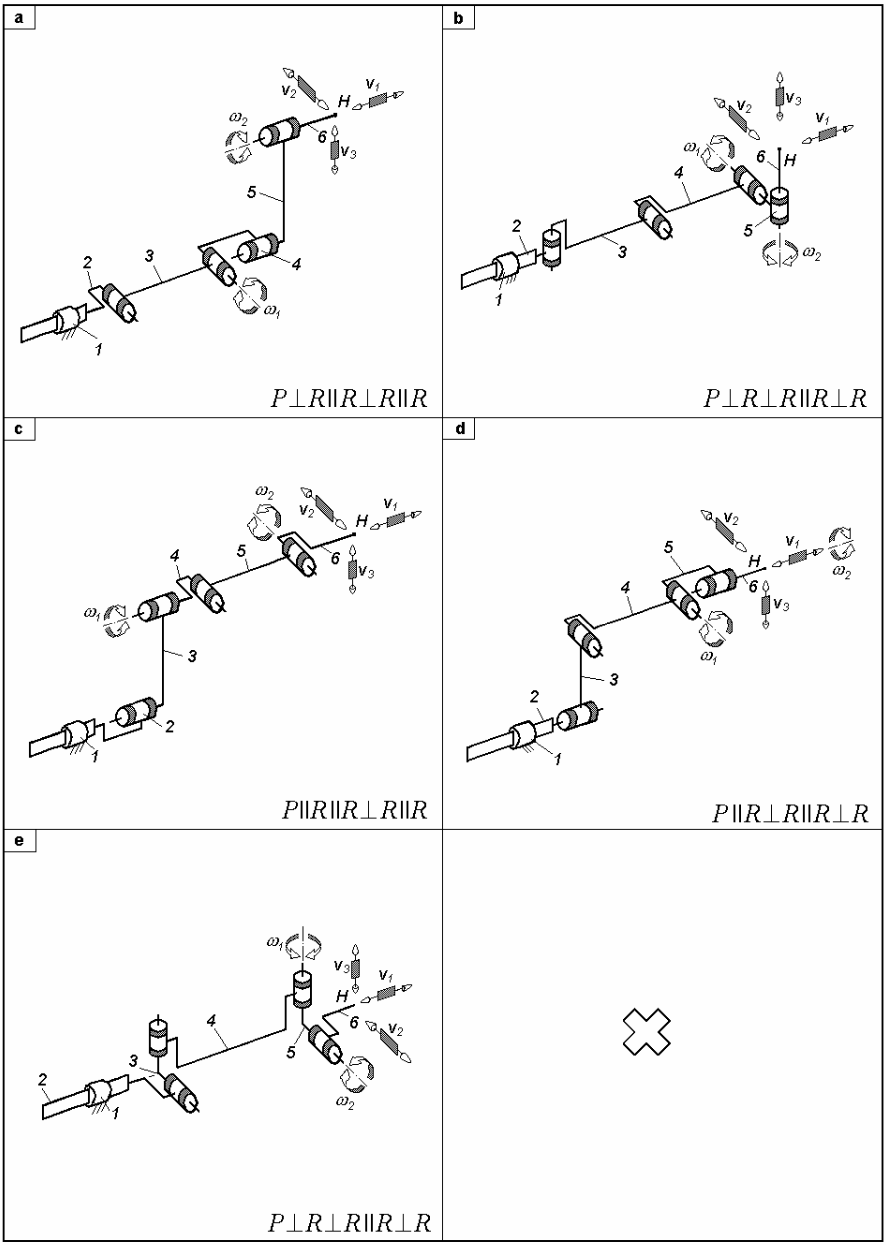

Fig. 4.1. Simple limbs for non overconstrained TPMs with coupled motions defined by $M_G = S_G = 5$, $(R_G) = (\boldsymbol{v}_1, \boldsymbol{v}_2, \boldsymbol{v}_3, \boldsymbol{\omega}_1, \boldsymbol{\omega}_2)$ and actuated by linear motors mounted on the fixed base

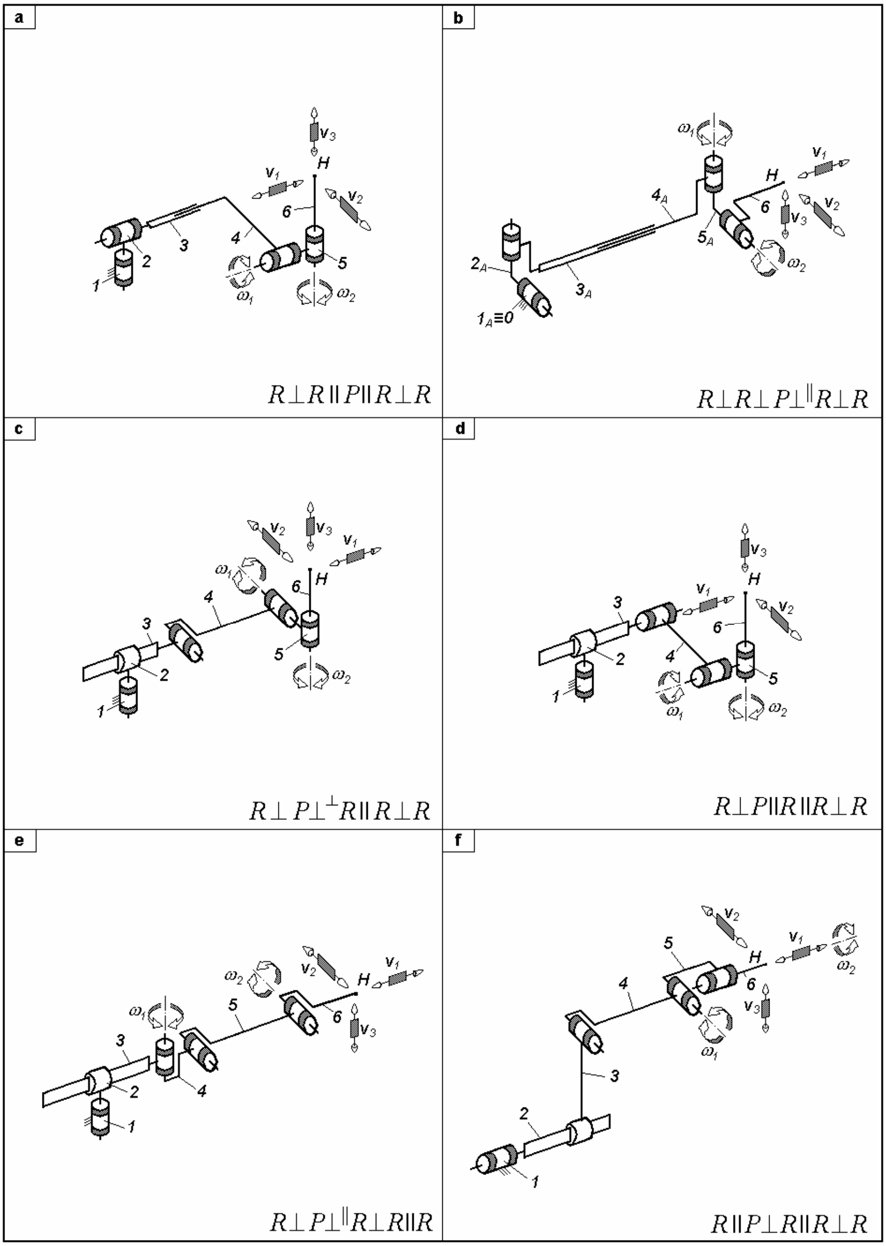

Fig. 4.2. Simple limbs for non overconstrained TPMs with coupled motions defined by $M_G = S_G = 5$, $(R_G) = (\boldsymbol{v}_1, \boldsymbol{v}_2, \boldsymbol{v}_3, \boldsymbol{\omega}_1, \boldsymbol{\omega}_2)$ and actuated by linear motors non adjacent to the fixed base

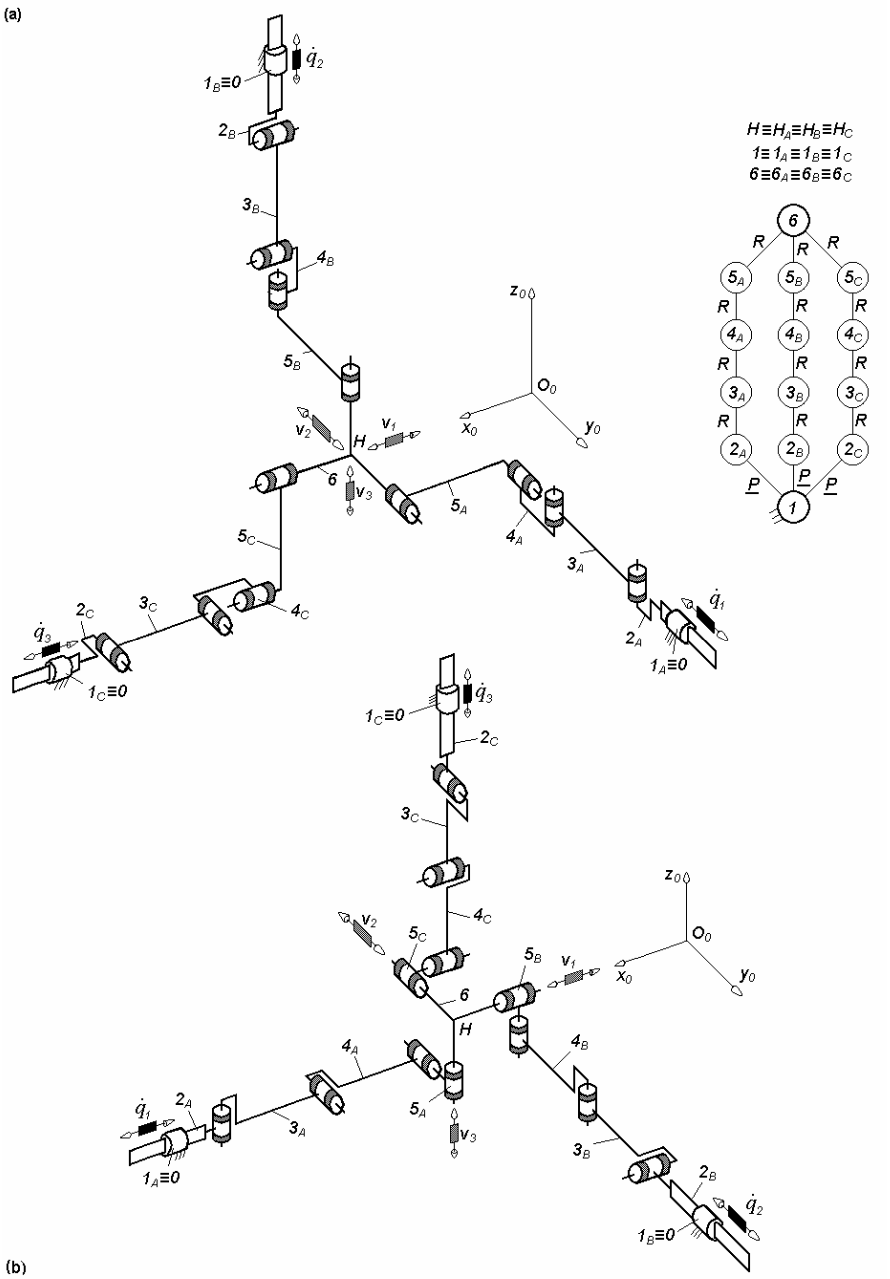

Fig. 4.3. *3-$\underline{P}$RRRR*-type non overconstrained TPMs with coupled motions and linear actuators mounted on the fixed base, limb topology $\underline{P}\perp R\|R\perp R\|R$ (**a**) and $\underline{P}\perp R\perp R\|R\perp R$ (**b**)

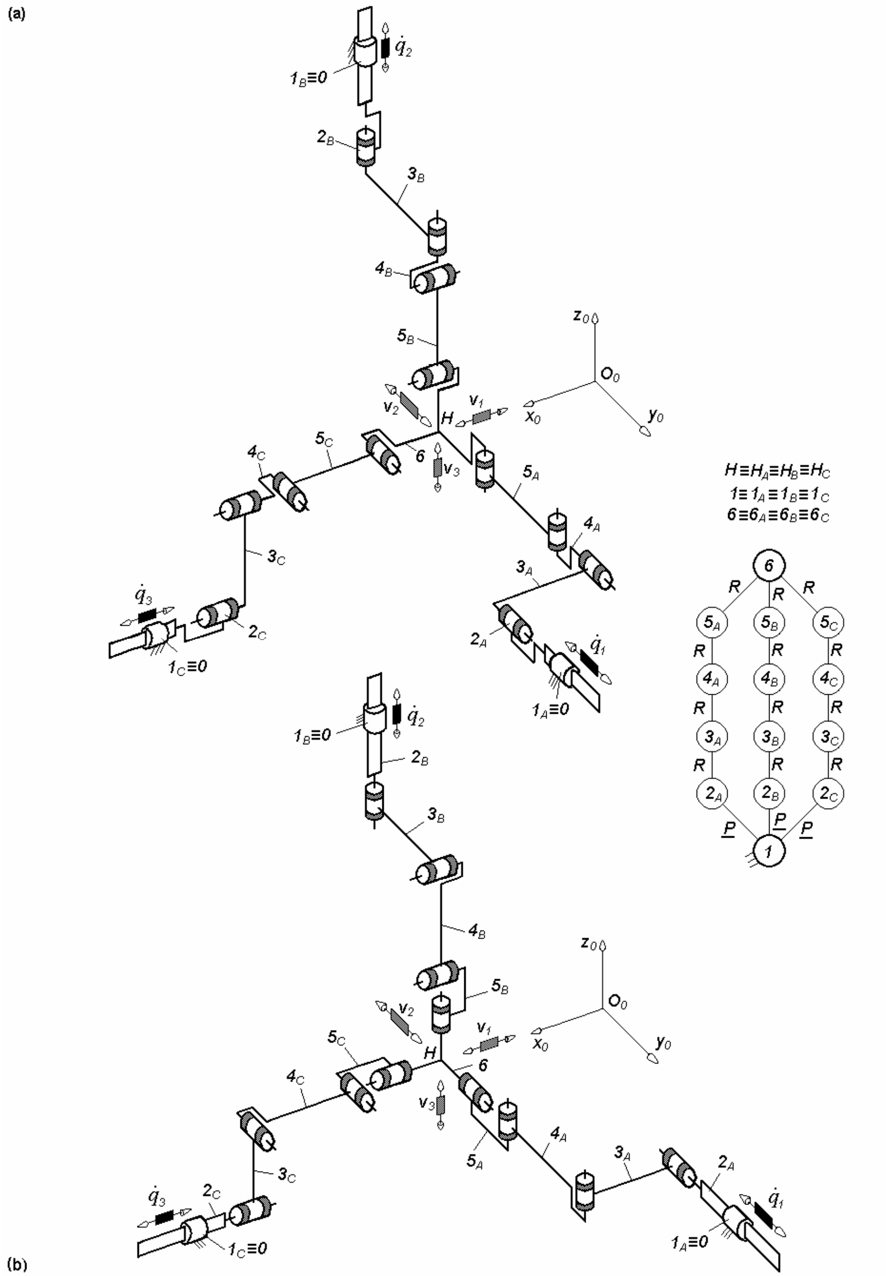

Fig. 4.4. *3-PRRRR*-type non overconstrained TPMs with coupled motions and linear actuators mounted on the fixed base, limb topology $\underline{P}||R||R\perp R||R$ (**a**) and $\underline{P}||R\perp R||R\perp R$ (**b**)

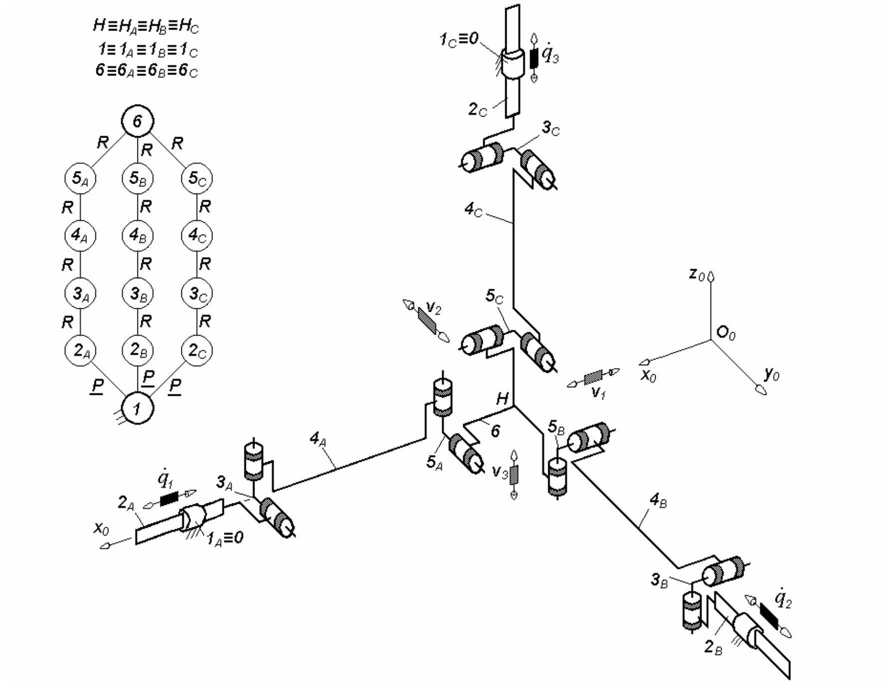

Fig. 4.5. *3-<u>P</u>RRRR*-type non overconstrained TPM with coupled motions and linear actuators mounted on the fixed base, limb topology $\underline{P}\perp R\perp R||R\perp^{||}R$

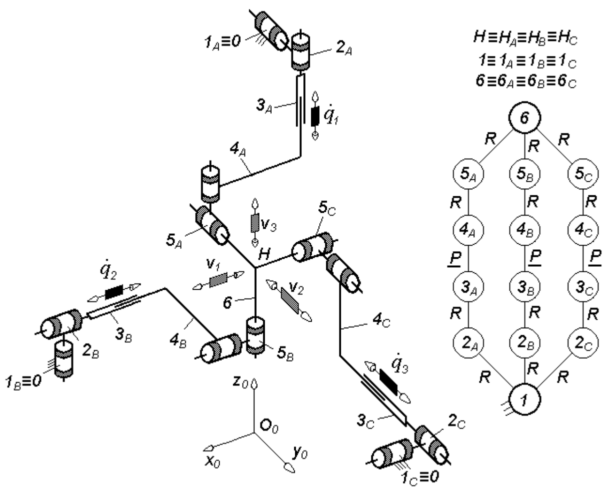

Fig. 4.6. *3-RR<u>P</u>RR*-type non overconstrained TPM with coupled motions and linear actuators non adjacent to the fixed base, limb topology $R\perp R||\underline{P}\|R\perp^{||}R$

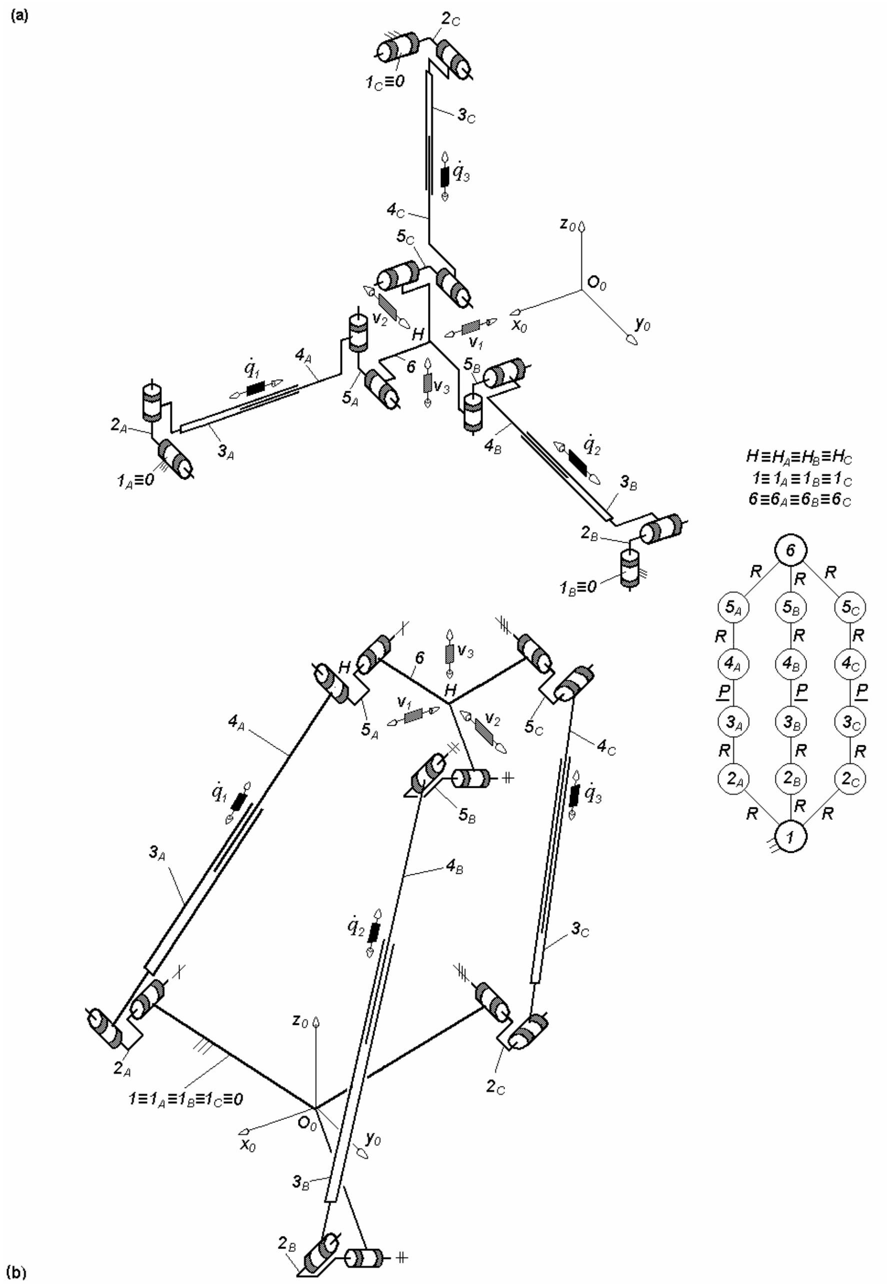

Fig. 4.7. *3-RRPRR*-type non overconstrained TPMs with coupled motions and linear actuators non adjacent to the fixed base mounted on the fixed base, limb topology $R \perp R \perp \underline{P} \perp^{\parallel} R \perp R$

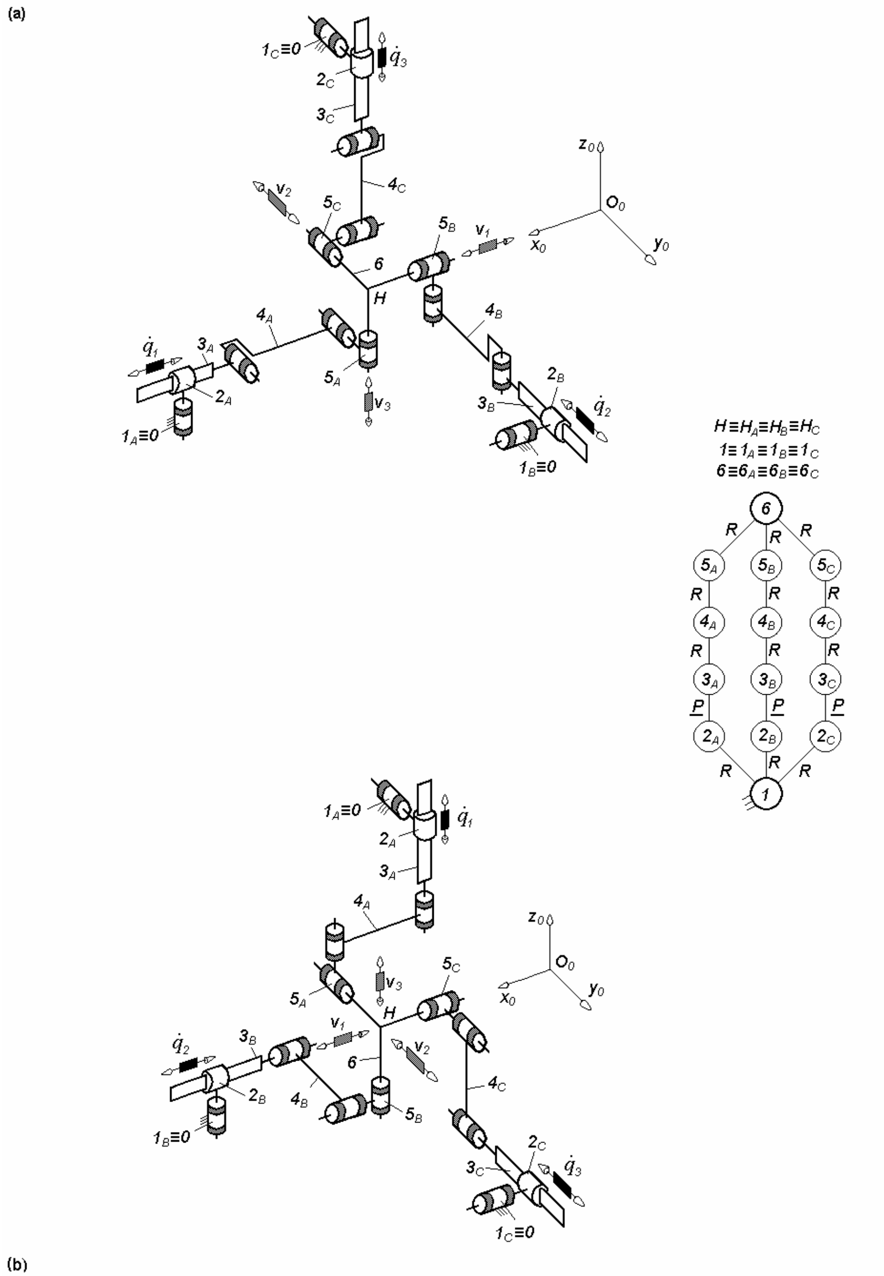

Fig. 4.8. *3-RPRRR*-type non overconstrained TPMs with coupled motions and linear actuators non adjacent to the fixed base, limb topology $R \perp \underline{P} \perp^{\perp} R||R \perp^{||} R$ (**a**) and $R \perp \underline{P}||R||R \perp^{||} R$ (**b**)

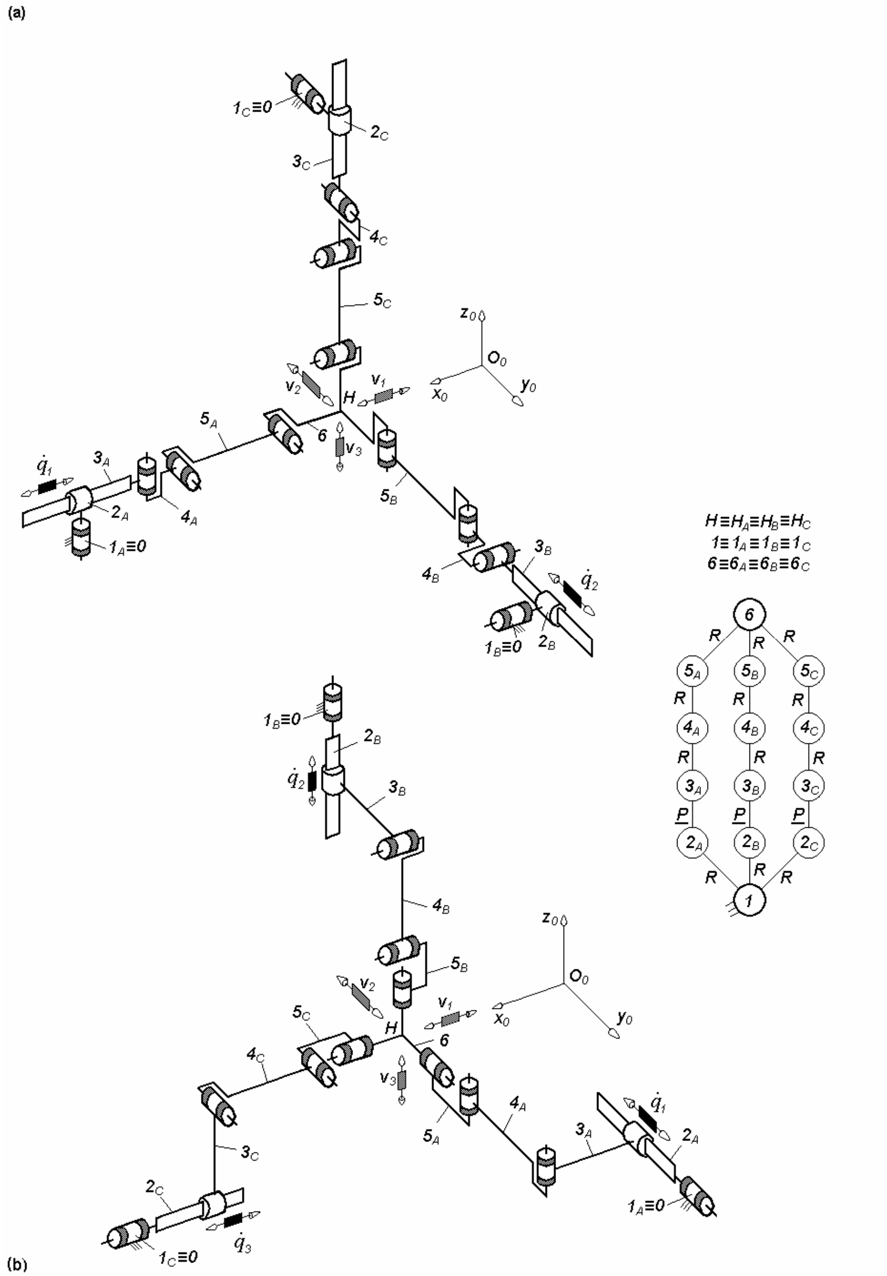

Fig. 4.9. *3-RPRRR*-type non overconstrained TPMs with coupled motions and linear actuators non adjacent to the fixed base, limb topology $R\perp\underline{P}\perp^{\|}R\perp R\|R$ (**a**) and $R\|\underline{P}\perp R\|R\perp^{\|}R$ (**b**)

4.2 Derived solutions with linear actuators

Non overconstrained solutions $F \leftarrow G_1\text{–}G_2\text{–}G_2$ with linear actuators and coupled motions can also be derived from the overconstrained solutions presented in Figs. 3.6–3.23 by introducing the required *idle mobilities*. They have the linear actuators mounted on the fixed base (Figs. 4.10–4.22) or between two moving links (Figs. 4.23–4.28). The limb topology of these non overconstrained solutions ($N_F = 0$) are systematized in Tables 4.2 and 4.3 and the structural parameters in Tables 4.4–4.8.

For example, the non overconstrained solutions in Fig. 4.10 are derived from the overconstrained solutions in Fig. 3.6 by introducing two rotational idle mobilities outside the parallelogram loop and one translational and two rotational idle mobilities in each parallelogram loop. They are introduced by replacing two revolute joints by spherical ones in each parallelogram loop and the prismatic joints by cylindrical ones. The prismatic joints in Fig. 3.6 are also replaced by cylindrical joints in Fig. 4.10. We may note that the two spherical joints adjacent to link 5 introduce one translational and two rotational idle mobilities in each parallelogram loop and also provide an idle rotational mobility of link 5. Attention must be paid when introducing the idle mobilities so as not to modify the mobility of the parallel mechanism and the connectivity of the moving platform.

Table 4.2. Limb topology of the derived non overconstrained TPMs with idle mobilities and linear actuators mounted on the fixed base presented in Figs. 4.10–4.22

No.	Basic TPM type	N_F	Derived TPM with $N_F = 0$ type	Limb topology
1	$3\text{-}\underline{P}PaP$ (Fig. 3.6)	*15*	$3\text{-}\underline{P}Pa^{ss}C^*$ (Fig. 4.10)	$\underline{P} \perp Pa^{ss} \| C^*$
2	$3\text{-}\underline{P}PPa$ (Fig. 3.7)	*15*	$3\text{-}\underline{P}C^*Pa^{ss}$ (Fig. 4.11)	$\underline{P} \perp C^* \| Pa^{ss}$
3	$3\text{-}\underline{P}Pa^{cc}$ (Fig. 3.8)	*12*	$3\text{-}\underline{P}R^*R^*Pa^{scc}$ (Fig. 4.12)	$\underline{P} \perp R^* \perp^{\perp} R^* \perp^{\|} Pa^{scc}$
4	$3\text{-}\underline{P}Pa^{cc}$ (Fig. 3.9)	*12*	$3\text{-}\underline{P}R^*Pa^{ccs}R^*$ (Fig. 4.13)	$\underline{Pa} \perp R^* \perp^{\perp} Pa^{ccs} \| R^*$
5	$3\text{-}\underline{P}PaPa$ (Fig. 3.10a)	*24*	$3\text{-}\underline{P}Pa^{ss}Pa^{ss}$ (Fig. 4.14a)	$\underline{P} \perp Pa^{ss} \perp^{\perp} Pa^{ss}$
6	$3\text{-}\underline{P}PaPa$ (Fig. 3.10b)	*24*	$3\text{-}\underline{P}Pa^{ss}Pa^{ss}$ (Fig. 4.14b)	$\underline{P} \perp Pa^{ss} \perp^{\|} Pa^{ss}$
7	$3\text{-}\underline{P}PaPa$ (Fig. 3.11a)	*24*	$3\text{-}\underline{P}Pa^{ss}Pa^{ss}$ (Fig. 4.15a)	$\underline{P} \| Pa^{ss} \perp Pa^{ss}$
8	$3\text{-}\underline{P}Pr$ (Fig. 3.11b)	*12*	$3\text{-}\underline{P}Pr^*R^*R^*$ (Fig. 4.15b)	$\underline{P}Pr^*R^* \perp R^*$
9	$3\text{-}\underline{P}RC$ (Fig. 3.12a)	*3*	$3\text{-}\underline{P}RCR^*$ (Fig. 4.16a)	$\underline{P} \perp R \| C \perp^{\|} R^*$
10	$3\text{-}\underline{P}CR$ (Fig. 3.12b)	*3*	$3\text{-}\underline{P}CRR^*$ (Fig. 4.16b)	$\underline{P} \perp C \| R \perp^{\|} R^*$
11	$3\text{-}\underline{P}RC$ (Fig. 3.13)	*3*	$3\text{-}\underline{P}RR^*C$ (Fig. 4.17)	$\underline{P} \perp R \perp R^* \perp^{\|} C$
12	$3\text{-}\underline{P}CR$ (Fig. 3.14)	*3*	$3\text{-}\underline{P}CR^*R$ (Fig. 4.18)	$\underline{P} \perp C \perp R^* \perp^{\|} R$
13	$3\text{-}\underline{P}RPaR$ (Fig. 3.15a)	*12*	$3\text{-}\underline{P}R^*RPa^{ss}$ (Fig. 4.19a)	$\underline{P} \perp R^* \perp^{\|} R \perp Pa^{ss}$
14	$3\text{-}\underline{P}RPaR$ (Fig. 3.15b)	*12*	$3\text{-}\underline{P}R^*RPa^{ss}$ (Fig. 4.19b)	$\underline{P} \| R^* \perp R \perp Pa^{ss}$
15	$3\text{-}\underline{P}RPaR$ (Fig. 3.15a, b)	*12*	$3\text{-}\underline{P}Pa^{4s}$ (Fig. 4.20a, b	$\underline{P}\text{-}Pa^{4s}$
16	$3\text{-}\underline{P}RRPa$ (Fig. 3.16a)	*12*	$3\text{-}\underline{P}RPa^{ss}R^*$ (Fig. 4.21a)	$\underline{P} \perp R \perp^{\|} Pa^{ss} \| R^*$
17	$3\text{-}\underline{P}RRPa$ (Fig. 3.16b)	*12*	$3\text{-}\underline{P}RRPa^{ss}$ (Fig. 4.21b)	$\underline{P} \| R \| R \perp Pa^{ss}$
18	$3\text{-}\underline{P}PaRR$ (Fig. 3.17a)	*12*	$3\text{-}\underline{P}R^*Pa^{ss}R$ (Fig. 4.22a)	$\underline{P} \perp R^* \| Pa^{ss} \perp R$
19	$3\text{-}\underline{P}PaRR$ (Fig. 3.17b)	*12*	$3\text{-}\underline{P}R^*Pa^{ss}R$ (Fig. 4.22b	$\underline{P} \| R^* \| Pa^{ss} \perp R$

Table 4.3. Limb topology of the derived TPMs with idle mobilities and linear actuators mounted on a moving link presented in Figs. 4.23–4.28

No.	Basic TPM type	N_F	Derived TPM with $N_F = 0$ type	Limb topology
1	$3\text{-}R\underline{P}C$ (Fig. 3.18a)	3	$3\text{-}R\underline{C}C$ (Fig. 4.23a)	$R\perp\underline{C}\perp^{\|\|}C$
2	$3\text{-}C\underline{P}R$ (Fig. 3.18b)	3	$3\text{-}C\underline{C}R$ (Fig. 4.23b)	$C\perp\underline{C}\perp^{\|\|}R$
3	$3\text{-}R\underline{P}C$ (Fig. 3.19)	3	$3\text{-}R\underline{C}C$ (Fig. 4.24)	$R\perp\underline{C}\perp^{\|\|}C$
4	$3\text{-}C\underline{P}R$ (Fig. 3.20)	3	$3\text{-}C\underline{C}R$ (Fig. 4.25)	$C\perp\underline{C}\perp^{\|\|}R$
5	$3\text{-}P\underline{P}RR$ (Fig. 3.21)	3	$3\text{-}P\underline{P}RRR*$ (Fig. 4.26)	$P\perp\underline{P}\perp^{\|\|}R\|\|R\perp^{\|\|}R*$
6	$3\text{-}RPa\underline{P}R$ (Fig. 3.22a)	12	$3\text{-}RPa*\underline{P}RR*$ (Fig. 4.27a)	$R\perp Pa*\perp^{\perp}\underline{P}\perp R\perp R*$
7	$3\text{-}RPa\underline{P}R$ (Fig. 3.22b)	12	$3\text{-}RPa^{ss}\underline{P}R$ (Fig. 4.28a)	$R\perp Pa^{ss}\perp^{\|\|}\underline{P}\|\|R$
8	$3\text{-}RPaR\underline{P}$ (Fig. 3.23a)	12	$3\text{-}RPa^{ss}R*\underline{P}$ (Fig. 4.27b)	$3\text{-}R\perp Pa^{ss}\perp R*\perp\underline{P}$
9	$3\text{-}RPaR\underline{P}$ (Fig. 3.23b)	12	$3\text{-}RPa^{ss}R\underline{P}$ (Fig. 4.28b)	$3\text{-}R\perp Pa^{ss}\perp^{\|\|}R\|\|\underline{P}$

Table 4.4. Bases of the operational velocities spaces of the limbs isolated from the parallel mechanisms presented in Figs. 4.10–4.28

No.	Parallel mechanism	Basis (R_{G1})	(R_{G2})	(R_{G3})
1	Figs. 4.10–4.14, 4.15a, 4.24, 4.28	$(\boldsymbol{v}_1,\boldsymbol{v}_2,\boldsymbol{v}_3,\boldsymbol{\omega}_\beta,\boldsymbol{\omega}_\delta)$	$(\boldsymbol{v}_1,\boldsymbol{v}_2,\boldsymbol{v}_3,\boldsymbol{\omega}_\alpha,\boldsymbol{\omega}_\delta)$	$(\boldsymbol{v}_1,\boldsymbol{v}_2,\boldsymbol{v}_3,\boldsymbol{\omega}_\alpha,\boldsymbol{\omega}_\beta)$
2	Figs. 4.15b, 4.16–4.18, 4.19b, 4.21b, 4.22, 4.23, 4.26–4.27	$(\boldsymbol{v}_1,\boldsymbol{v}_2,\boldsymbol{v}_3,\boldsymbol{\omega}_\alpha,\boldsymbol{\omega}_\beta)$	$(\boldsymbol{v}_1,\boldsymbol{v}_2,\boldsymbol{v}_3,\boldsymbol{\omega}_\beta,\boldsymbol{\omega}_\delta)$	$(\boldsymbol{v}_1,\boldsymbol{v}_2,\boldsymbol{v}_3,\boldsymbol{\omega}_\alpha,\boldsymbol{\omega}_\delta)$
3	Fig. 4.19a	$(\boldsymbol{v}_1,\boldsymbol{v}_2,\boldsymbol{v}_3,\boldsymbol{\omega}_\beta,\boldsymbol{\omega}_\delta)$	$(\boldsymbol{v}_1,\boldsymbol{v}_2,\boldsymbol{v}_3,\boldsymbol{\omega}_\alpha,\boldsymbol{\omega}_\beta)$	$(\boldsymbol{v}_1,\boldsymbol{v}_2,\boldsymbol{v}_3,\boldsymbol{\omega}_\alpha,\boldsymbol{\omega}_\delta)$
4	Fig. 4.20	$(\boldsymbol{v}_1,\boldsymbol{v}_2,\boldsymbol{v}_3,\boldsymbol{\omega}_\alpha,\boldsymbol{\omega}_\delta)$	$(\boldsymbol{v}_1,\boldsymbol{v}_2,\boldsymbol{v}_3,\boldsymbol{\omega}_\alpha,\boldsymbol{\omega}_\beta)$	$(\boldsymbol{v}_1,\boldsymbol{v}_2,\boldsymbol{v}_3,\boldsymbol{\omega}_\beta,\boldsymbol{\omega}_\delta)$
5	Fig. 4.21a	$(\boldsymbol{v}_1,\boldsymbol{v}_2,\boldsymbol{v}_3,\boldsymbol{\omega}_\beta,\boldsymbol{\omega}_\delta)$	$(\boldsymbol{v}_1,\boldsymbol{v}_2,\boldsymbol{v}_3,\boldsymbol{\omega}_\alpha,\boldsymbol{\omega}_\delta)$	$(\boldsymbol{v}_1,\boldsymbol{v}_2,\boldsymbol{v}_3,\boldsymbol{\omega}_\alpha,\boldsymbol{\omega}_\beta)$

Table 4.5. Structural parameters[a] of translational parallel mechanisms in Figs. 4.10–4.15

No.	Structural parameter	Solution *3-PPa^ss C** (Fig. 4.10) *3-PC*Pa^ss* (Fig. 4.11)	*3-PR*R*Pa^scc* (Fig. 4.12) *3-PR*Pa^ccs R** (Fig. 4.13)	*3-PPa^ss Pa^ss* (Fig. 4.14) *3-PPa^ss Pa^ss* (Fig. 4.15a) *3-PPr*R*R** (Fig. 4.15b)
1	M	14	17	20
2	P_1	6	7	9
3	P_2	6	7	9
4	P_3	6	7	9
5	P	18	21	27
6	Q	5	5	8
7	K_1	0	0	0
8	K_2	3	3	3
9	K	3	3	3
10	(R_{Gi}) $(i = 1,2,3)$	See Table 4.4	See Table 4.4	See Table 4.4
11	S_{G1}	5	5	5
12	S_{G2}	5	5	5
13	S_{G3}	5	5	5
14	r_{G1}	6	6	12
15	r_{G2}	6	6	12
16	r_{G3}	6	6	12
17	M_{G1}	5	5	5
18	M_{G2}	5	5	5
19	M_{G3}	5	5	5
20	(R_F)	$(\boldsymbol{v}_1, \boldsymbol{v}_2, \boldsymbol{v}_3)$	$(\boldsymbol{v}_1, \boldsymbol{v}_2, \boldsymbol{v}_3)$	$(\boldsymbol{v}_1, \boldsymbol{v}_2, \boldsymbol{v}_3)$
21	S_F	3	3	3
22	r_l	18	18	36
23	r_F	30	30	48
24	M_F	3	3	3
25	N_F	0	0	0
26	T_F	0	0	0
27	$\sum_{j=1}^{p_1} f_j$	11	11	17
28	$\sum_{j=1}^{p_2} f_j$	11	11	17
29	$\sum_{j=1}^{p_3} f_j$	11	11	17
30	$\sum_{j=1}^{p} f_j$	33	33	51

[a]See footnote of Table 2.1 for the nomenclature of structural parameters

Table 4.6. Structural parameters[a] of translational parallel mechanisms in Figs. 4.16–4.20

No.	Structural parameter	Solution 3-*PRCR**(Fig. 4.16a) 3-*PCRR**(Fig. 4.16b) 3-*PRR*C*(Fig. 4.17) 3-*PCR*R*(Fig. 4.18)	3-*PR*RPa*^{ss} (Fig. 4.19)	*PPa*^{4s} (Fig. 4.20)
1	m	11	17	11
2	P_1	4	7	5
3	P_2	4	7	5
4	P_3	4	7	5
5	P	12	21	15
6	Q	2	5	5
7	K_1	3	0	0
8	K_2	0	3	3
9	K	3	3	3
10	(R_{Gi}) $(i = 1,2,3)$	See Table 4.4	See Table 4.4	See Table 4.4
11	S_{G1}	5	5	5
12	S_{G2}	5	5	5
13	S_{G3}	5	5	5
14	r_{G1}	0	6	6
15	r_{G2}	0	6	6
16	r_{G3}	0	6	6
17	M_{G1}	5	5	7
18	M_{G2}	5	5	7
19	M_{G3}	5	5	7
20	(R_F)	$(\boldsymbol{v}_1, \boldsymbol{v}_2, \boldsymbol{v}_3)$	$(\boldsymbol{v}_1, \boldsymbol{v}_2, \boldsymbol{v}_3)$	$(\boldsymbol{v}_1, \boldsymbol{v}_2, \boldsymbol{v}_3)$
21	S_F	3	3	3
22	r_l	0	18	18
23	r_F	12	30	30
24	M_F	3	3	9
25	N_F	0	0	0
26	T_F	0	0	6
27	$\sum_{j=1}^{p_1} f_j$	5	11	13
28	$\sum_{j=1}^{p_2} f_j$	5	11	13
29	$\sum_{j=1}^{p_3} f_j$	5	11	13
30	$\sum_{j=1}^{p} f_j$	15	33	39

[a]See footnote of Table 2.1 for the nomenclature of structural parameters

Table 4.7. Structural parameters[a] of translational parallel mechanisms in Figs. 4.21–4.26

No.	Structural parameter	Solution *3-PRPa^ss R** (Fig. 4.21a) *3-PRRPa^ss* (Fig. 4.21b) *3-PR*Pa^ss R* (Fig. 4.22)	*3-RCC* (Figs. 4.23a, 4.24) *3-CCR* (Figs. 4.23b, 4.25)	*3-PPRRR** (Fig. 4.26)
1	m	17	8	14
2	p_1	7	3	5
3	p_2	7	3	5
4	p_3	7	3	5
5	p	21	9	15
6	q	5	2	2
7	k_1	0	3	3
8	k_2	3	0	0
9	k	3	3	3
10	(R_{Gi}) $(i = 1,2,3)$	See Table 4.4	See Table 4.4	See Table 4.4
11	S_{G1}	5	5	5
12	S_{G2}	5	5	5
13	S_{G3}	5	5	5
14	r_{G1}	6	0	0
15	r_{G2}	6	0	0
16	r_{G3}	6	0	0
17	M_{G1}	5	5	5
18	M_{G2}	5	5	5
19	M_{G3}	5	5	5
20	(R_F)	$(\boldsymbol{v}_1, \boldsymbol{v}_2, \boldsymbol{v}_3)$	$(\boldsymbol{v}_1, \boldsymbol{v}_2, \boldsymbol{v}_3)$	$(\boldsymbol{v}_1, \boldsymbol{v}_2, \boldsymbol{v}_3)$
21	S_F	3	3	3
22	r_l	18	0	0
23	r_F	30	12	12
24	M_F	3	3	3
25	N_F	0	0	0
26	T_F	0	0	0
27	$\sum_{j=1}^{p_1} f_j$	11	5	5
28	$\sum_{j=1}^{p_2} f_j$	11	5	5
29	$\sum_{j=1}^{p_3} f_j$	11	5	5
30	$\sum_{j=1}^{p} f_j$	33	15	15

[a]See footnote of Table 2.1 for the nomenclature of structural parameters

Table 4.8. Structural parameters[a] of translational parallel mechanisms in Figs. 4.27 and 4.28

No.	Structural parameter	Solution *3-RPa*<u>P</u>RR** (Fig. 4.27a)	*3-RPa^ss R*<u>P</u>* (Fig. 4.27b) *3-RPa^ss <u>P</u>R* (Fig. 4.28a) *3-RPa^ss R<u>P</u>* (Fig. 4.28b)
1	M	20	17
2	p_1	8	7
3	p_2	8	7
4	p_3	8	7
5	p	24	21
6	q	5	5
7	k_1	0	0
8	k_2	3	3
9	k	3	3
10	(R_{Gi}) $(i = 1,2,3)$	See Table 4.4	See Table 4.4
11	S_{G1}	5	5
12	S_{G2}	5	5
13	S_{G3}	5	5
14	r_{G1}	6	6
15	r_{G2}	6	6
16	r_{G3}	6	6
17	M_{G1}	5	5
18	M_{G2}	5	5
19	M_{G3}	5	5
20	(R_F)	$(\boldsymbol{v}_1, \boldsymbol{v}_2, \boldsymbol{v}_3)$	$(\boldsymbol{v}_1, \boldsymbol{v}_2, \boldsymbol{v}_3)$
21	S_F	3	3
22	r_l	18	18
23	r_F	30	3
24	M_F	3	3
25	N_F	0	0
26	T_F	0	0
27	$\sum_{j=1}^{p_1} f_j$	11	11
28	$\sum_{j=1}^{p_2} f_j$	11	11
29	$\sum_{j=1}^{p_3} f_j$	11	11
30	$\sum_{j=1}^{p} f_j$	33	33

[a]See footnote of Table 2.1 for the nomenclature of structural parameters

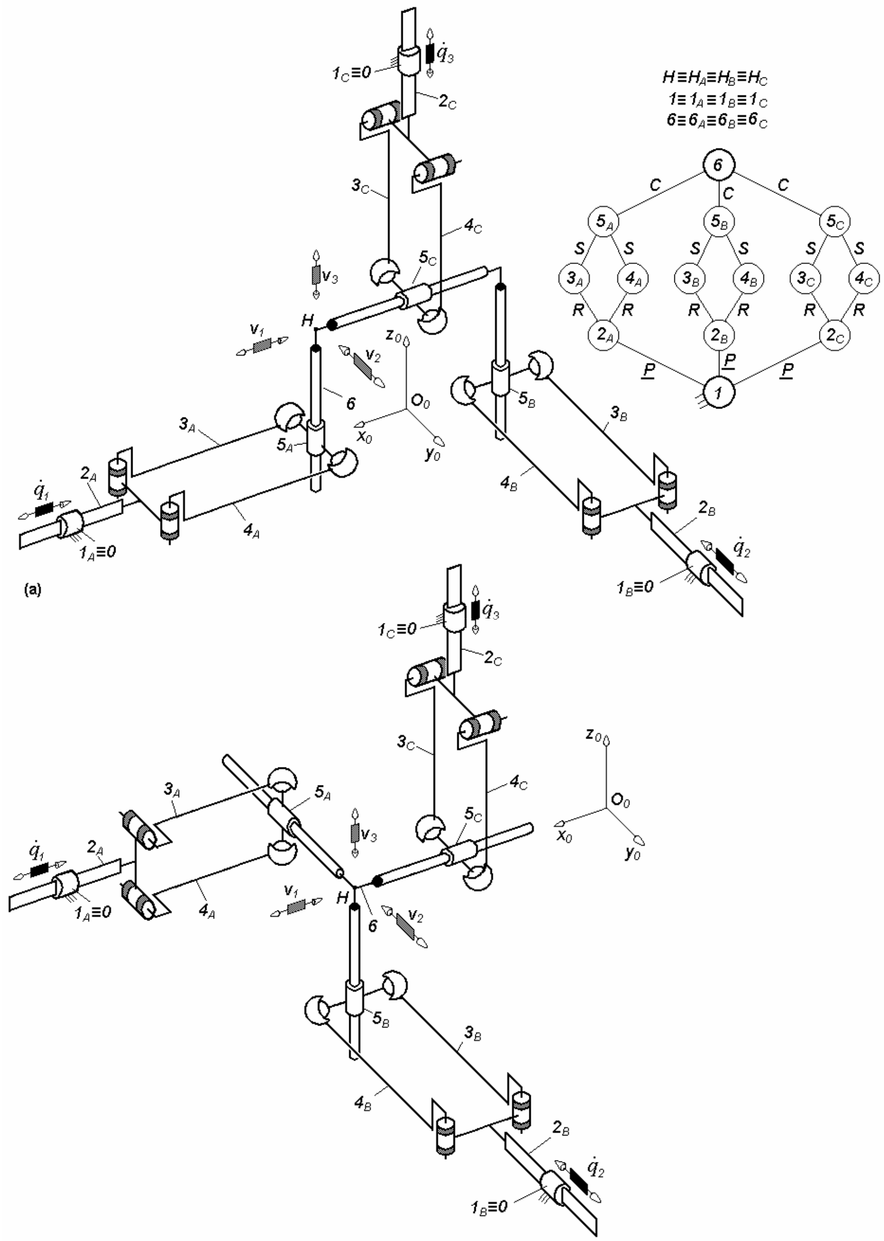

Fig. 4.10. *3-<u>P</u>Pa^ss C**-type non overconstrained TPMs with coupled motions and linear actuators mounted on the fixed base, limb topology $\underline{P} \perp Pa^{ss} || C^*$

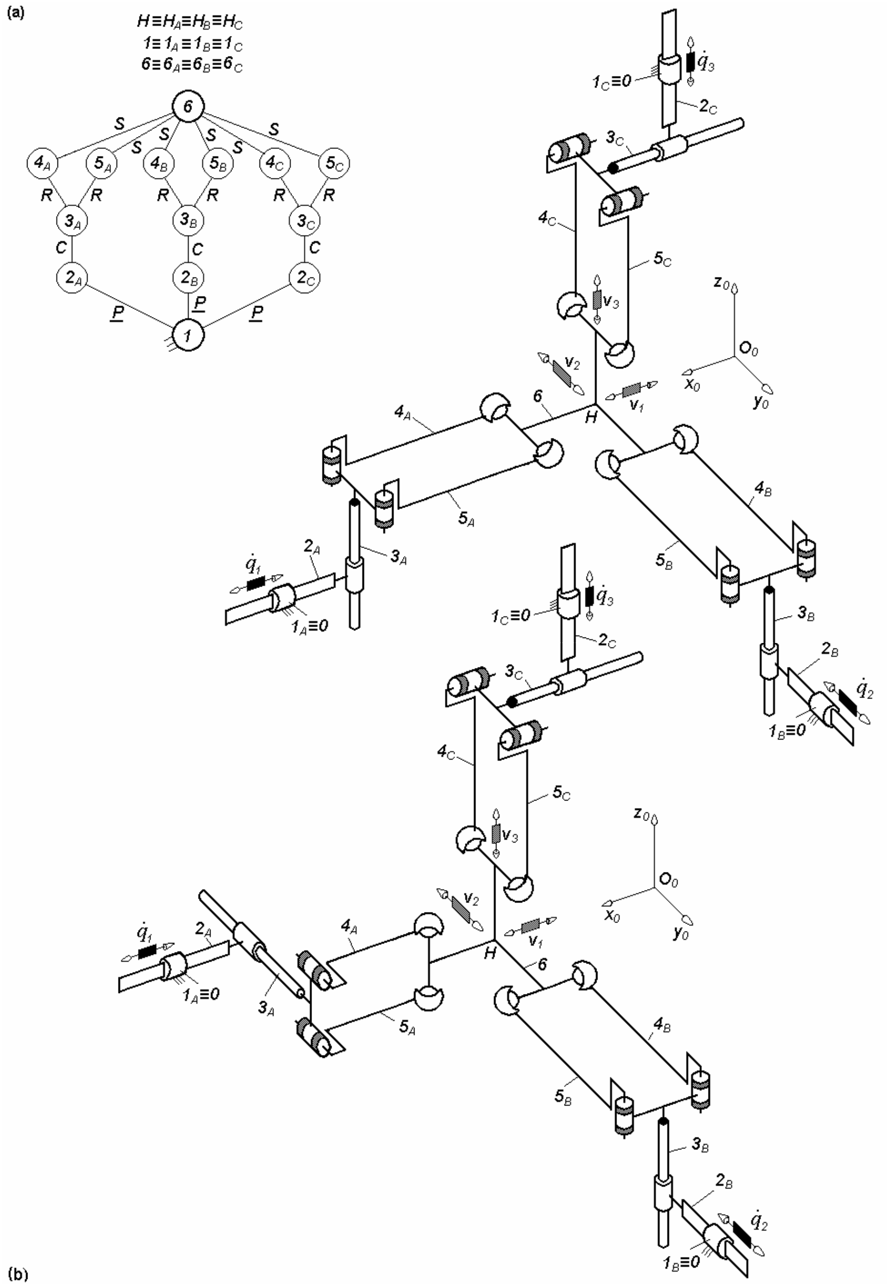

Fig. 4.11. *3-PC*Pa^ss*-type non overconstrained TPMs with coupled motions and linear actuators mounted on the fixed base, limb topology $\underline{P} \perp C^{*}||Pa^{ss}$

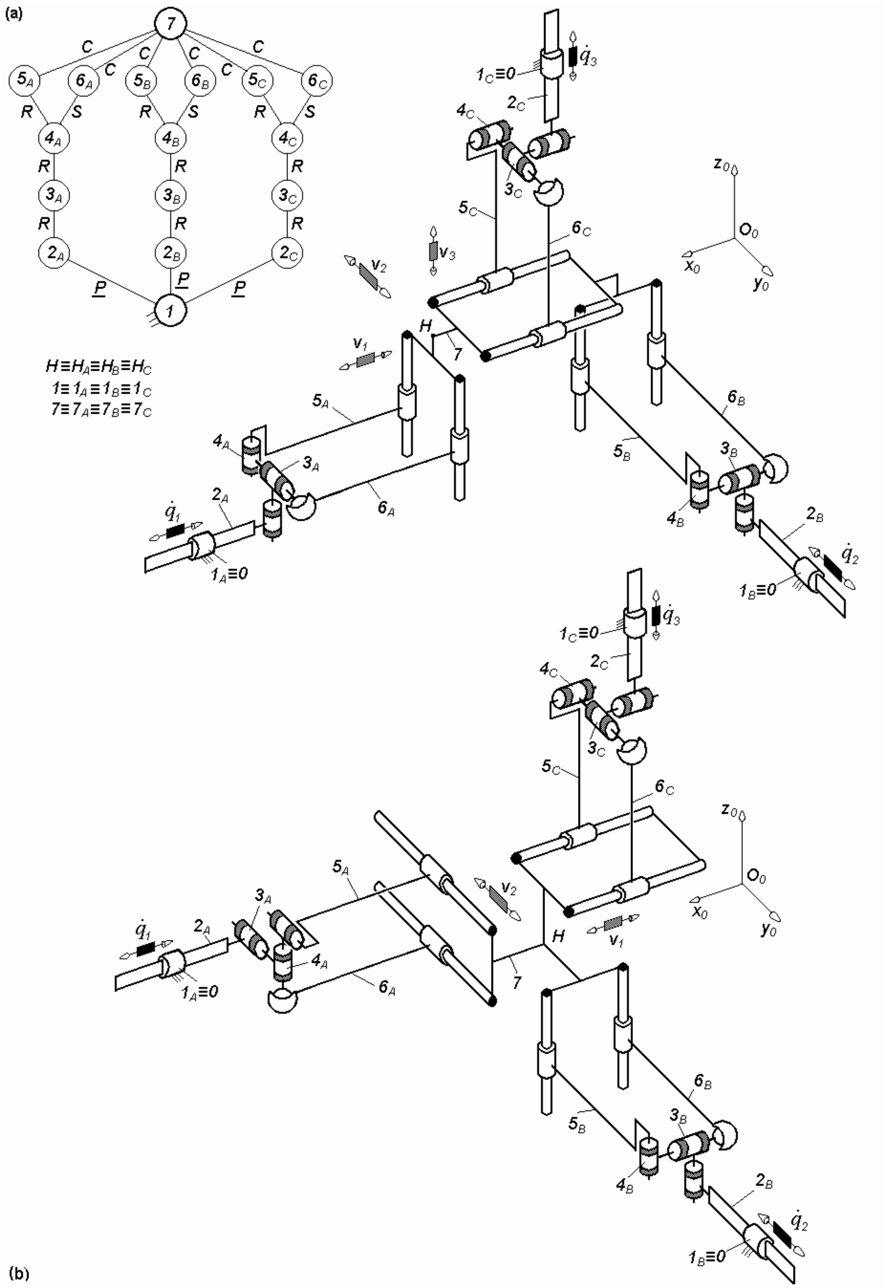

Fig. 4.12. *3-*$\underline{P}R^{*}R^{*}Pa^{scc}$-type non overconstrained TPMs with coupled motions and linear actuators mounted on the fixed base, limb topology $\underline{P}\perp R^{*}\perp^{\perp} R^{*}\perp^{\parallel} Pa^{scc}$

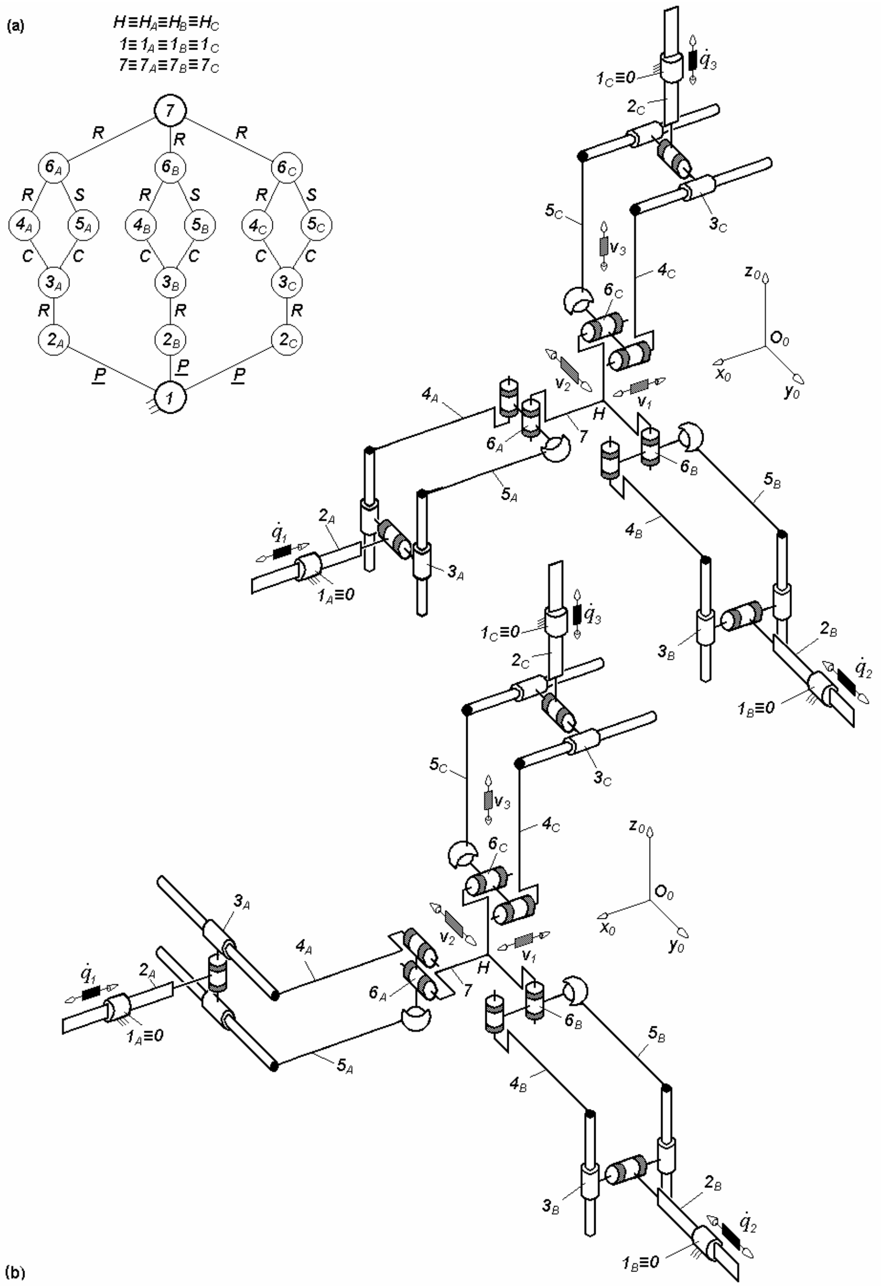

Fig. 4.13. *3-$\underline{P}R^*Pa^{ccs}R^*$*-type non overconstrained TPMs with coupled motions and linear actuators mounted on the fixed base, limb topology $\underline{Pa}\perp R^*\perp^{\perp} Pa^{ccs}||R^*$

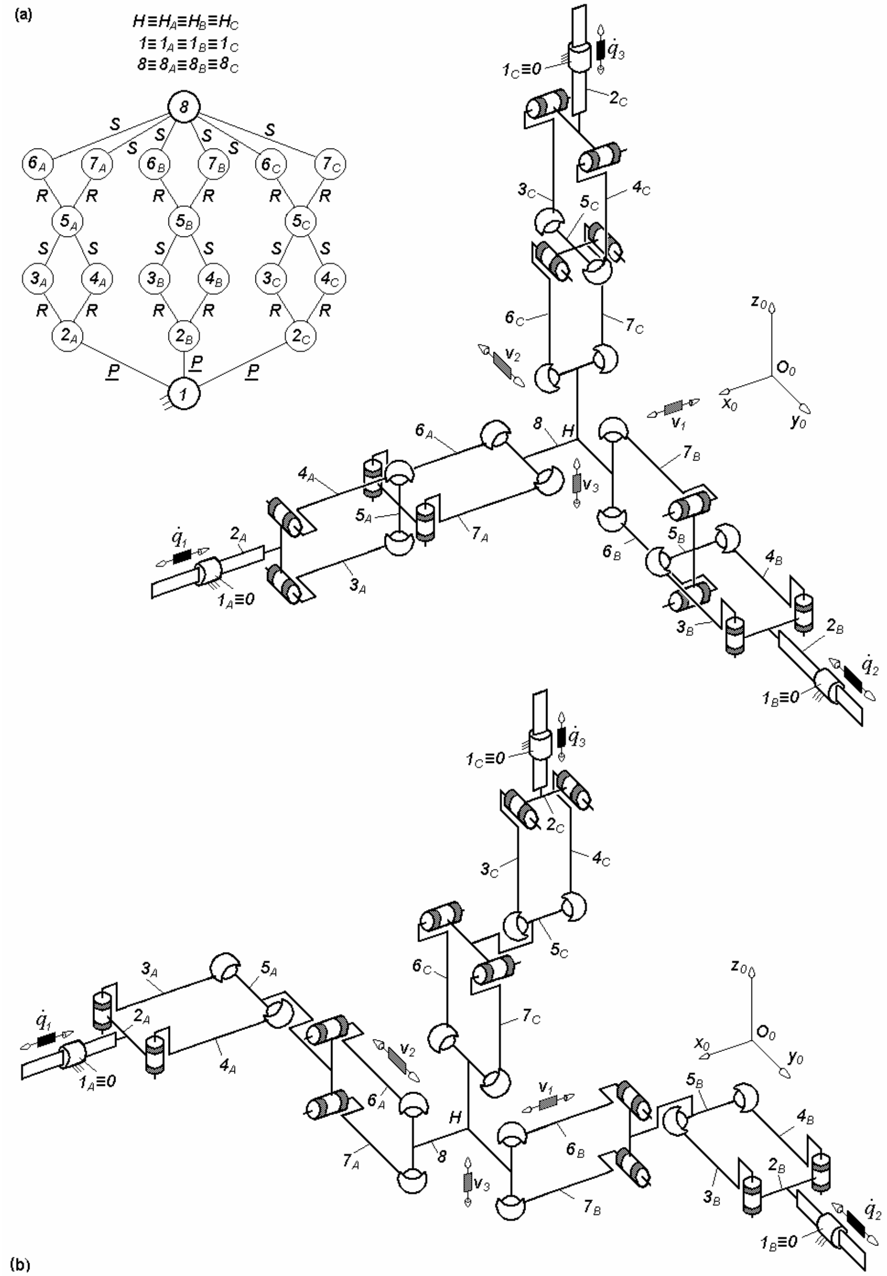

Fig. 4.14. *3-$\underline{P}Pa^{ss}Pa^{ss}$*-type non overconstrained TPMs with coupled motions and linear actuators mounted on the fixed base, limb topology $\underline{P} \perp Pa^{ss} \perp^{\perp} Pa^{ss}$ (**a**) and $\underline{P} \perp Pa^{ss} \perp^{\|} Pa^{ss}$ (**b**)

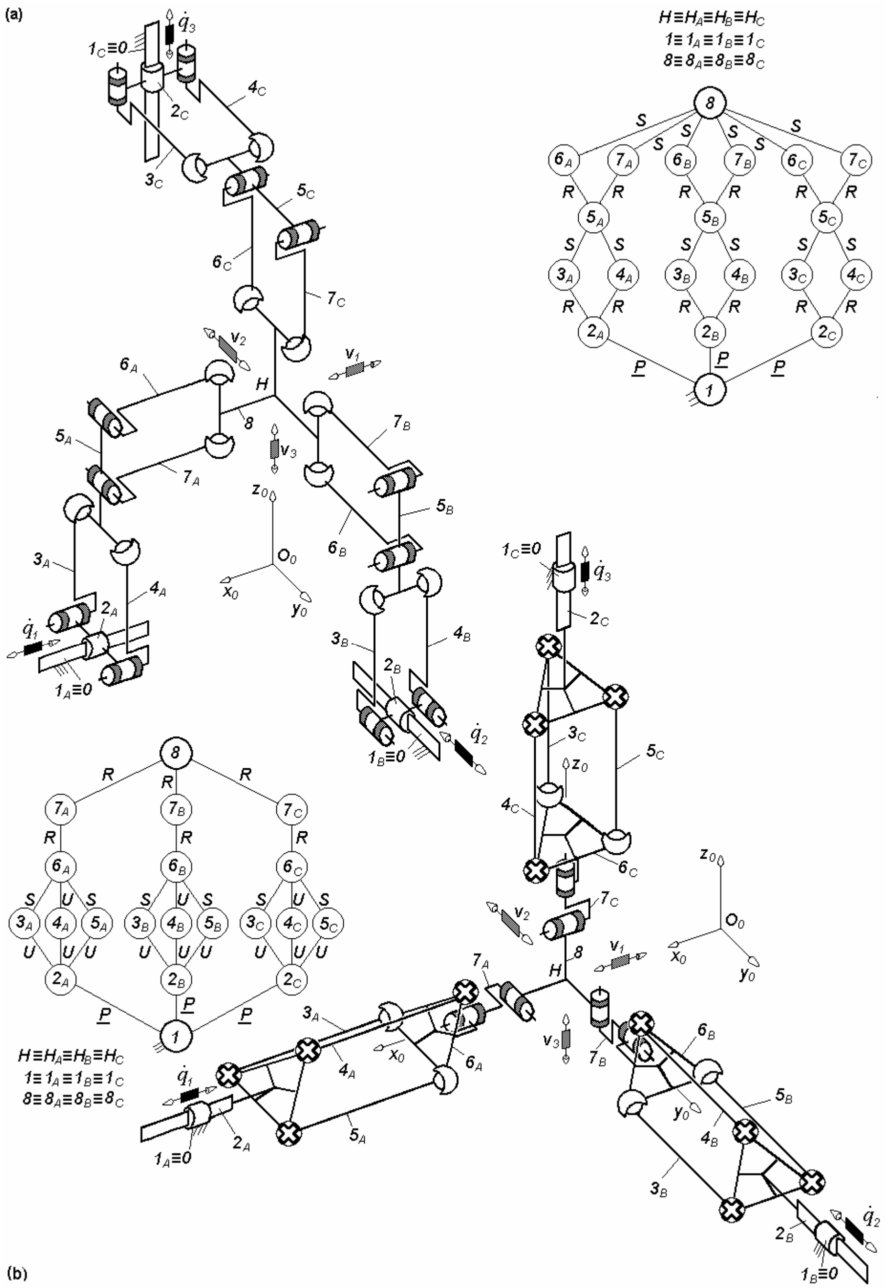

Fig. 4.15. Non overconstrained TPMs of types *3-PPa^ss^Pa^ss^* (**a**) and *3-PPr*R*R** (**b**) with coupled motions and linear actuators mounted on the fixed base, limb topology $\underline{P}||Pa^{ss} \perp Pa^{ss}$ (**a**) and $\underline{P}Pr^{*}R^{*} \perp R^{*}$ (**b**)

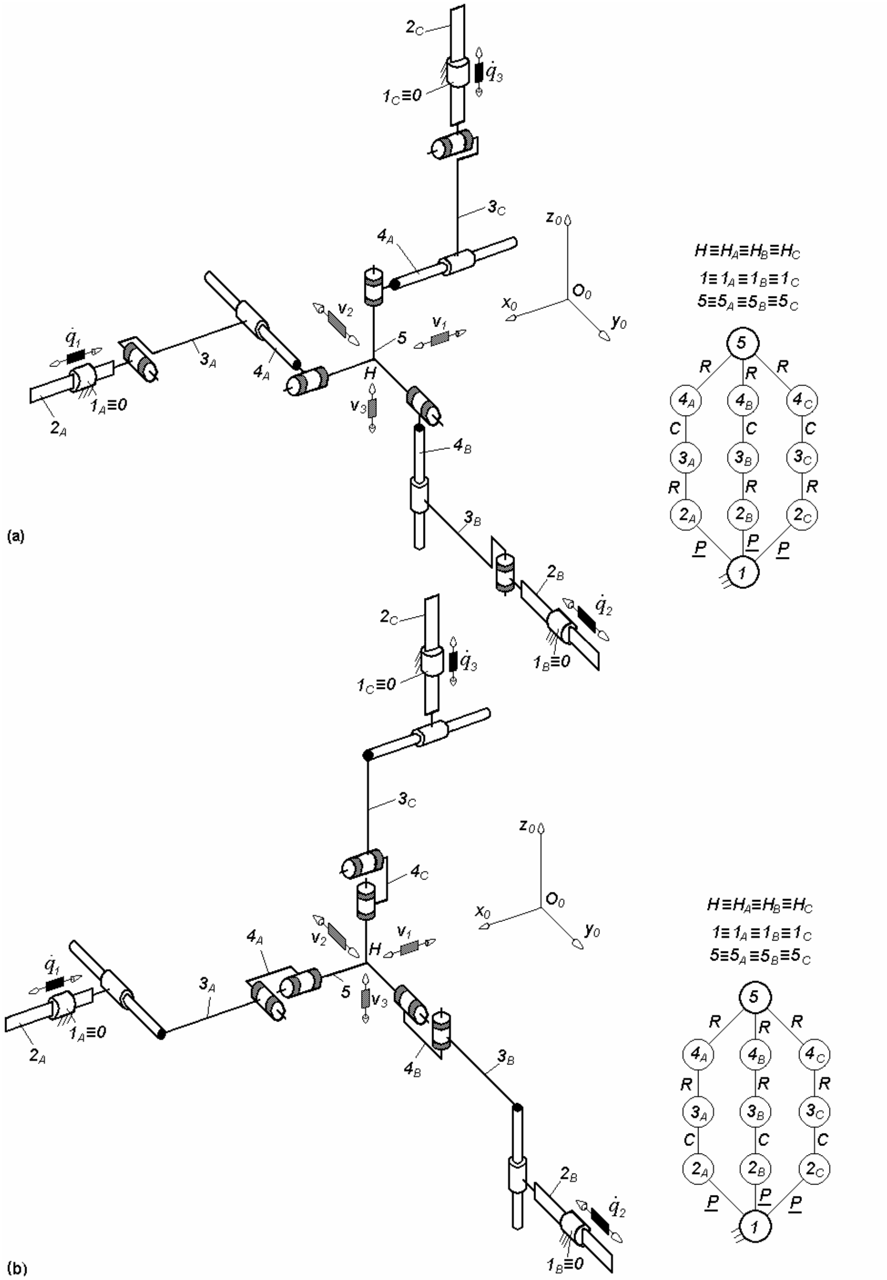

Fig. 4.16. Non overconstrained TPMs of types *3-*$\underline{P}$*RCR** (**a**) and *3-*$\underline{P}$*CRR**(**b**) with coupled motions and linear actuators mounted on the fixed base, limb topology $\underline{P} \perp R || C \perp^{||} R^*$ (**a**) and $\underline{P} \perp C || R \perp^{||} R^*$(**b**)

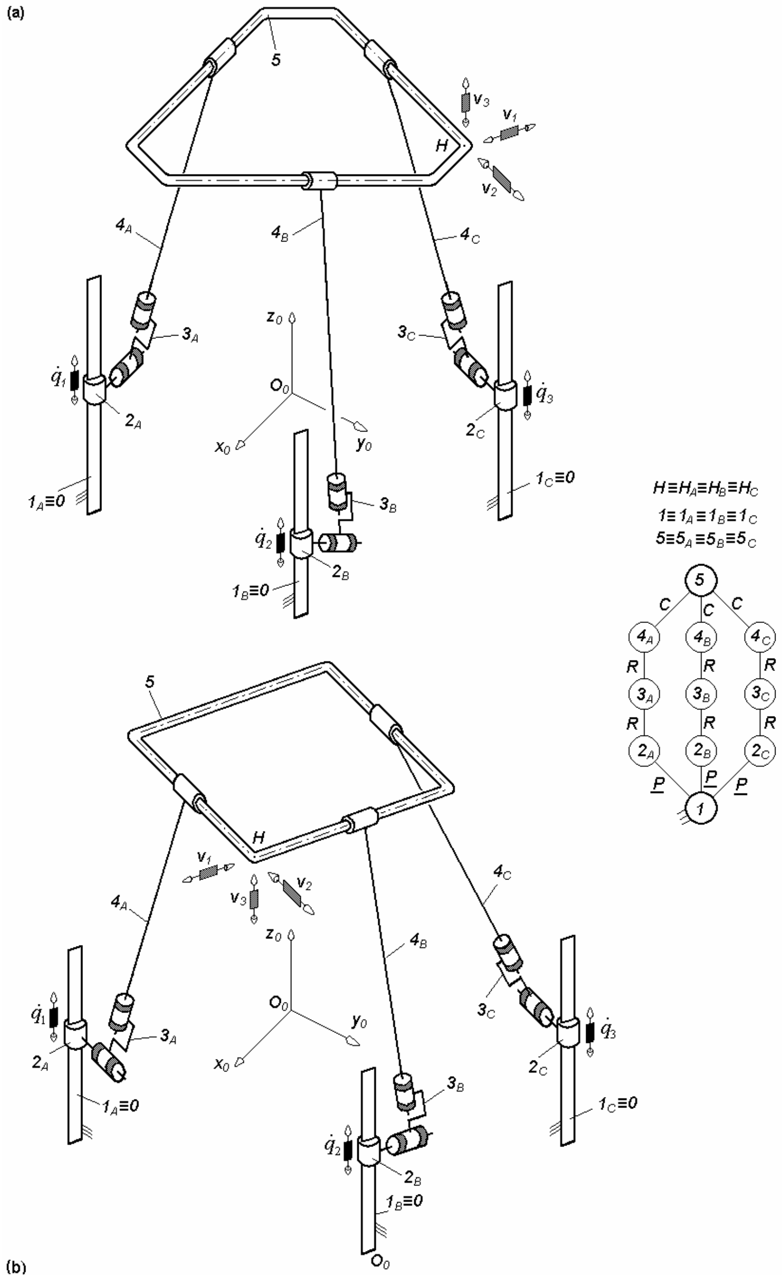

Fig. 4.17. *3-PRR*C*-type non overconstrained TPMs with coupled motions and linear actuators mounted on the fixed base, limb topology $\underline{P}\perp R\perp R^{*}\perp^{\parallel}C$

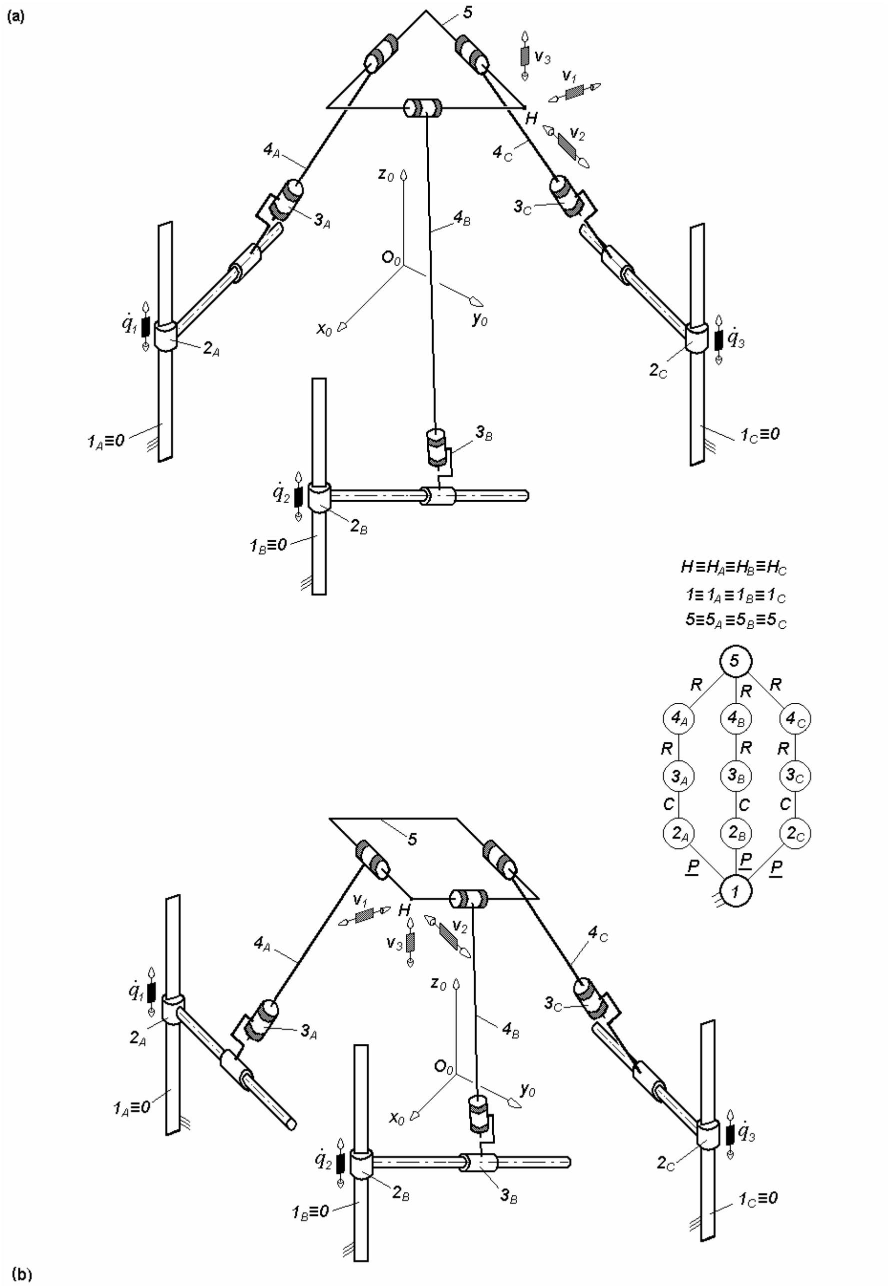

Fig. 4.18. *3-PCR*R*-type non overconstrained TPMs with coupled motions and linear actuators mounted on the fixed base, limb topology $\underline{P} \perp C \perp R^* \perp^{\parallel} R$

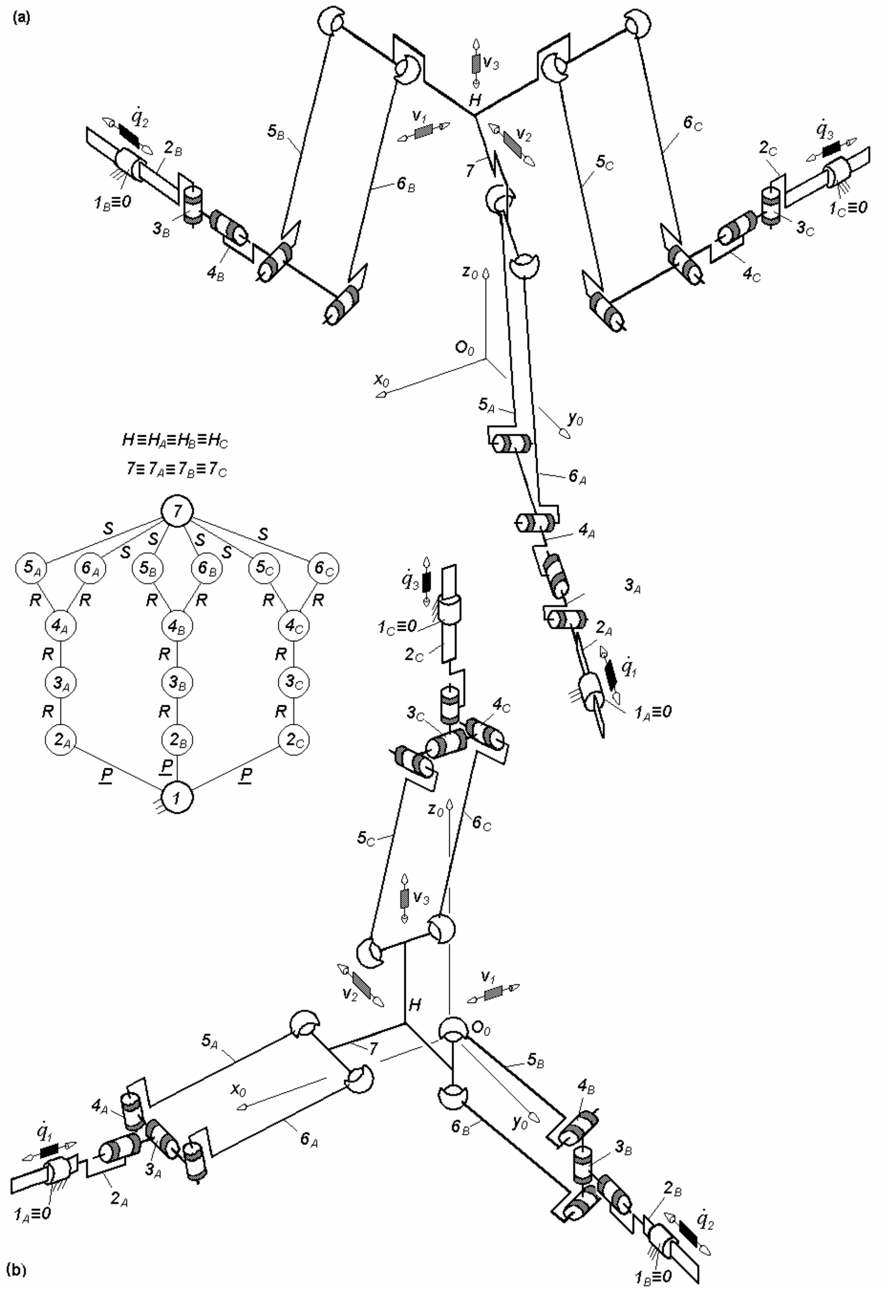

Fig. 4.19. $3\text{-}\underline{P}R^{*}RPa^{ss}$-type non overconstrained TPMs with coupled motions and linear actuators mounted on the fixed base, limb topology $\underline{P}\perp R^{*}\perp^{\parallel}R\perp Pa^{ss}$ (**a**) and $\underline{P}\parallel R^{*}\perp R\perp Pa^{ss}$ (**b**)

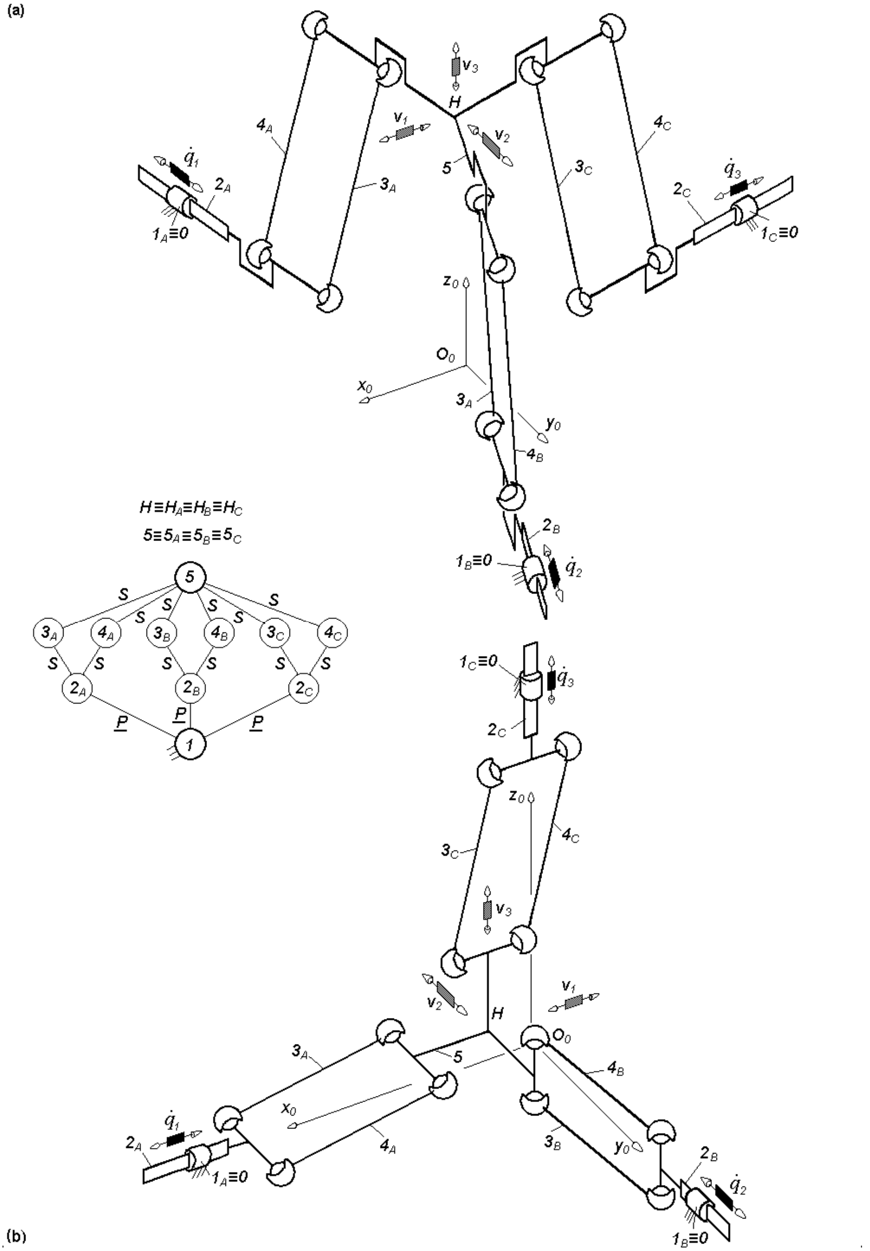

Fig. 4.20. *3-PPa*^{4s}-type non overconstrained TPMs with coupled motions and linear actuators mounted on the fixed base with 6 internal mobilities of links 3_A, 4_A, 3_B, 4_B, 3_C, and 4_C

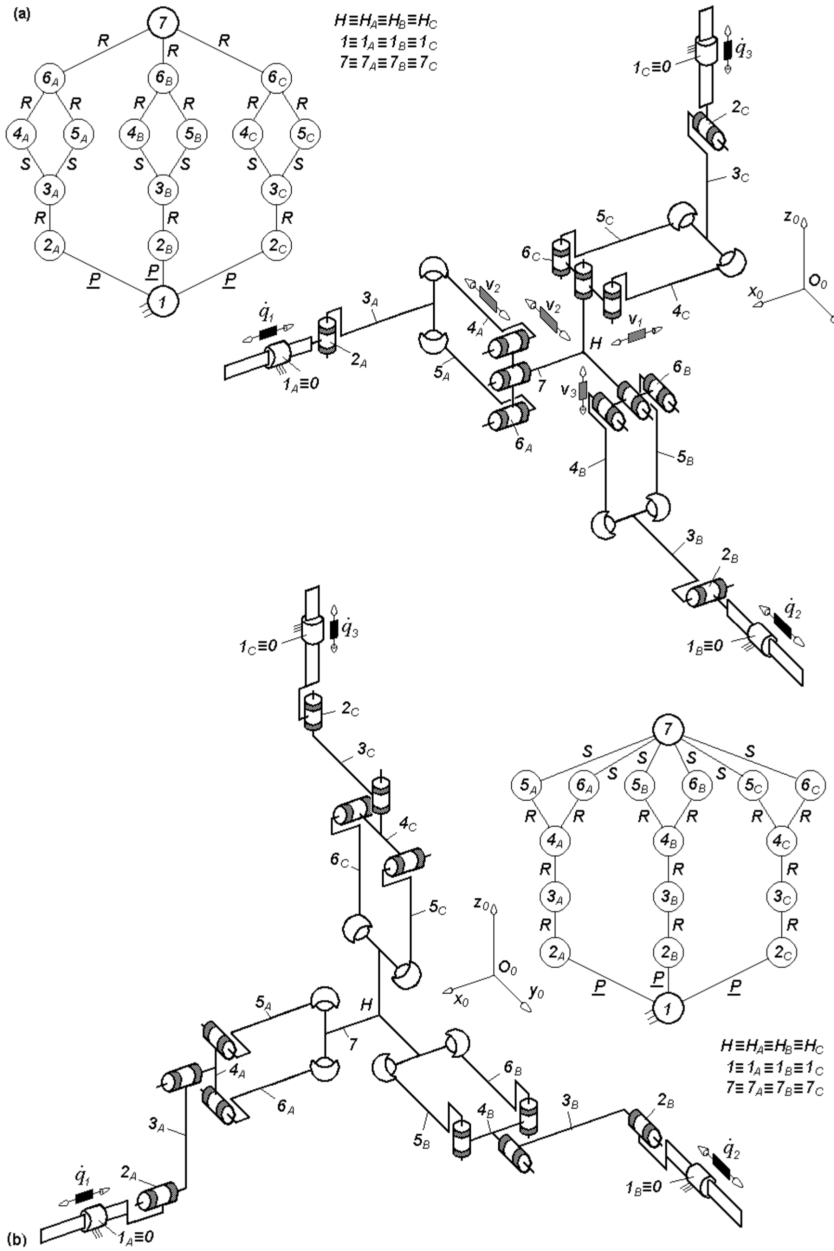

Fig. 4.21. Non overconstrained TPMs of types *3-*$\underline{P}$*RPa*^{ss}*R** (**a**) and *3-*$\underline{P}$*RRPa*^{ss} (**b**) with coupled motions and linear actuators mounted on the fixed base, limb topology $\underline{P} \perp R \perp {}^{||}Pa^{ss}||R^*$ (**a**) and $\underline{P}||R||R \perp Pa^{ss}$ (**b**)

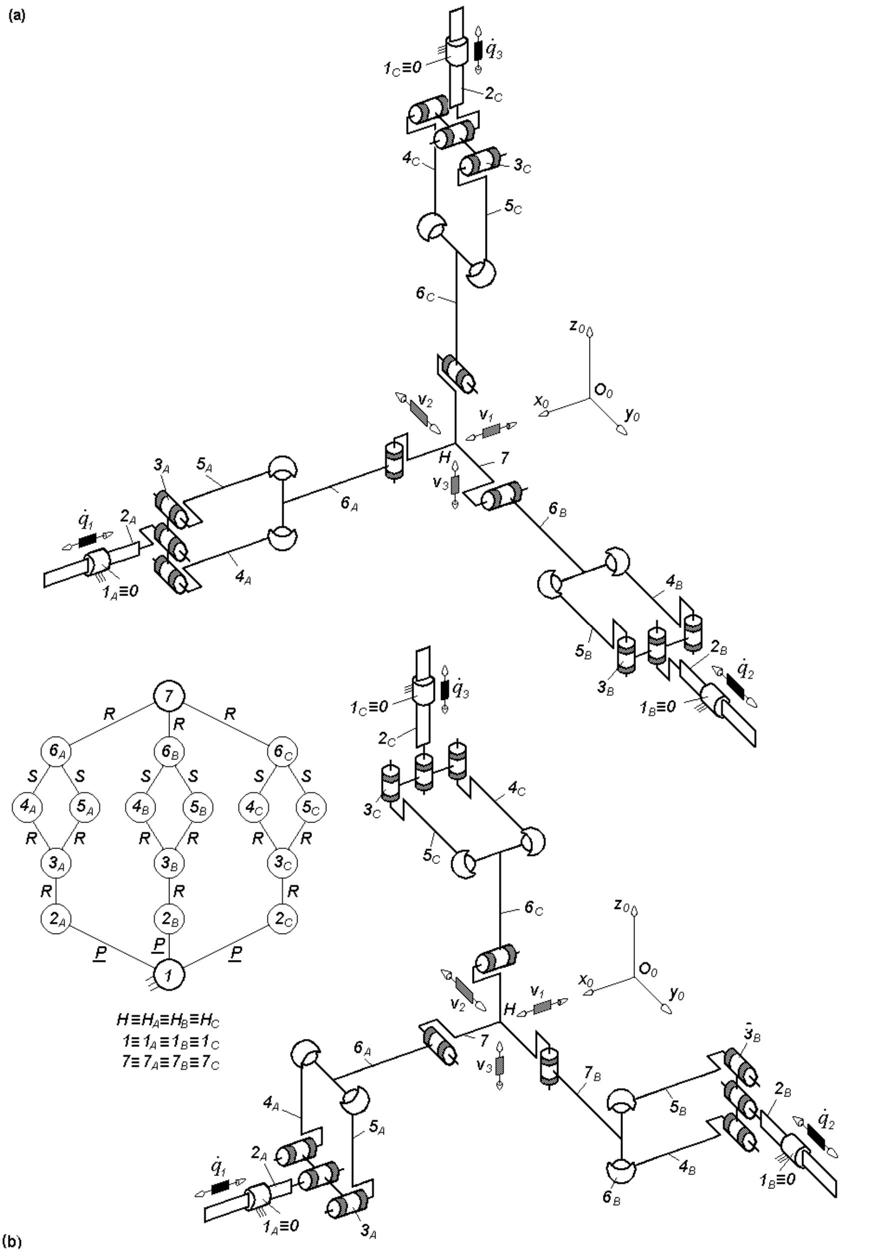

Fig. 4.22. *3-PR*Pa^ss R*-type non overconstrained TPMs with coupled motions and linear actuators mounted on the fixed base, limb topology $\underline{P} \perp R^*||Pa^{ss} \perp R$ (**a**) and $\underline{P}||R^*||Pa^{ss} \perp R$ (**b**)

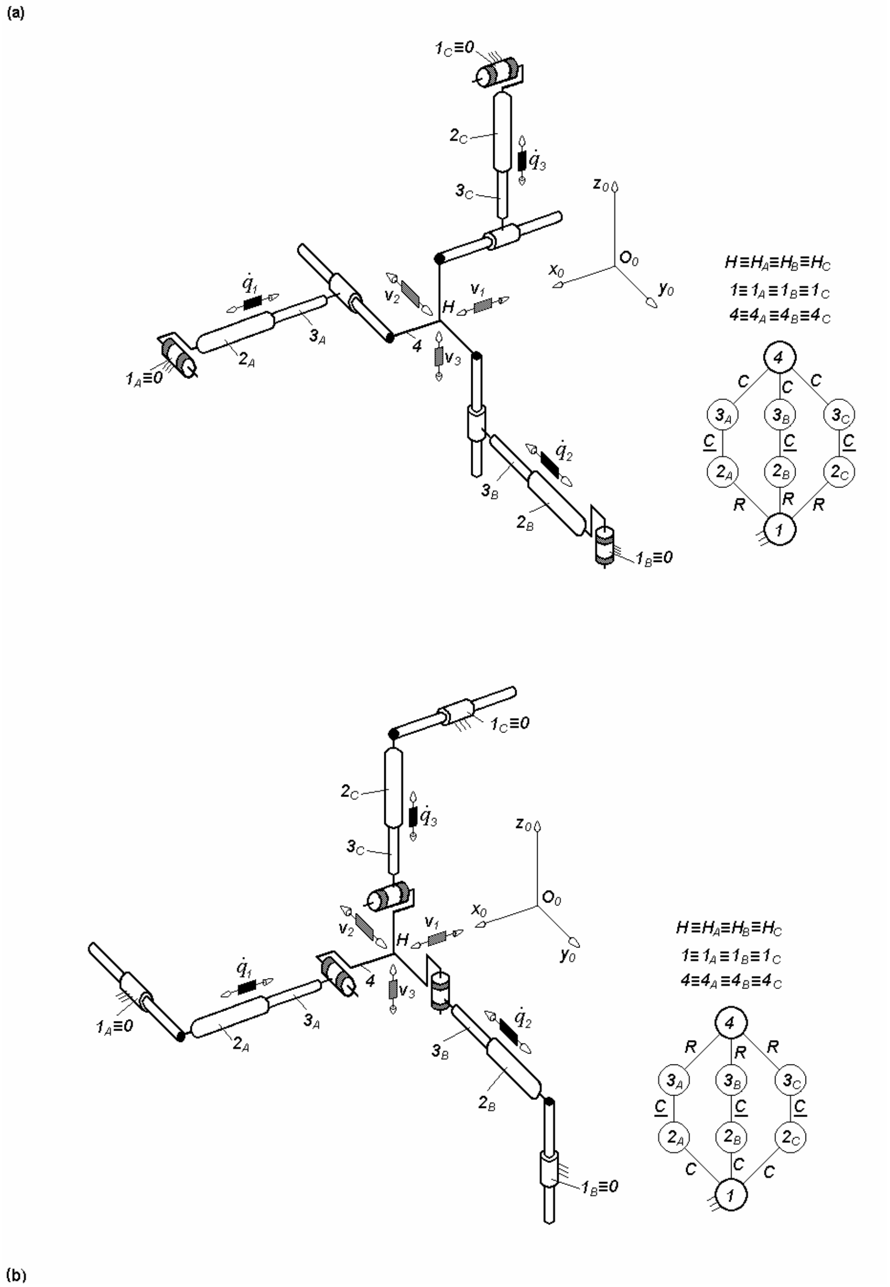

Fig. 4.23. Non overconstrained TPMs of types *3-R*$\underline{C}$*C* (**a**) and *3-C*$\underline{C}$*R* (**b**) with coupled motions and linear actuators combined in cylindrical joints non adjacent to the fixed base, limb topology $R\perp\underline{C}\perp^{\parallel}C$ (**a**) and $C\perp\underline{C}\perp^{\parallel}R$ (**b**)

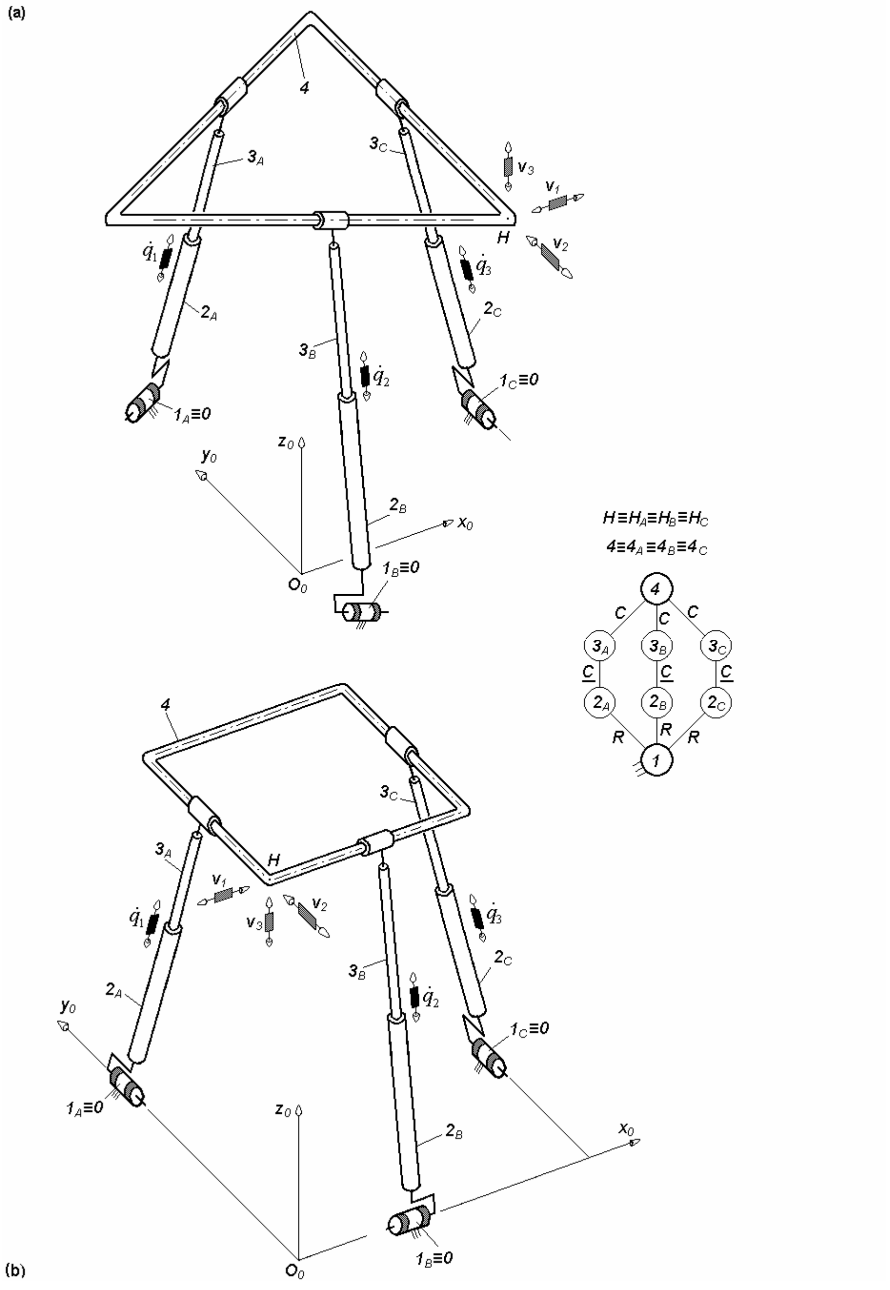

Fig. 4.24. *3-RCC*-type non overconstrained TPMs with coupled motions and linear actuators combined in cylindrical joints non adjacent to the fixed base, limb topology $R \perp \underline{C} \perp^{\parallel} C$

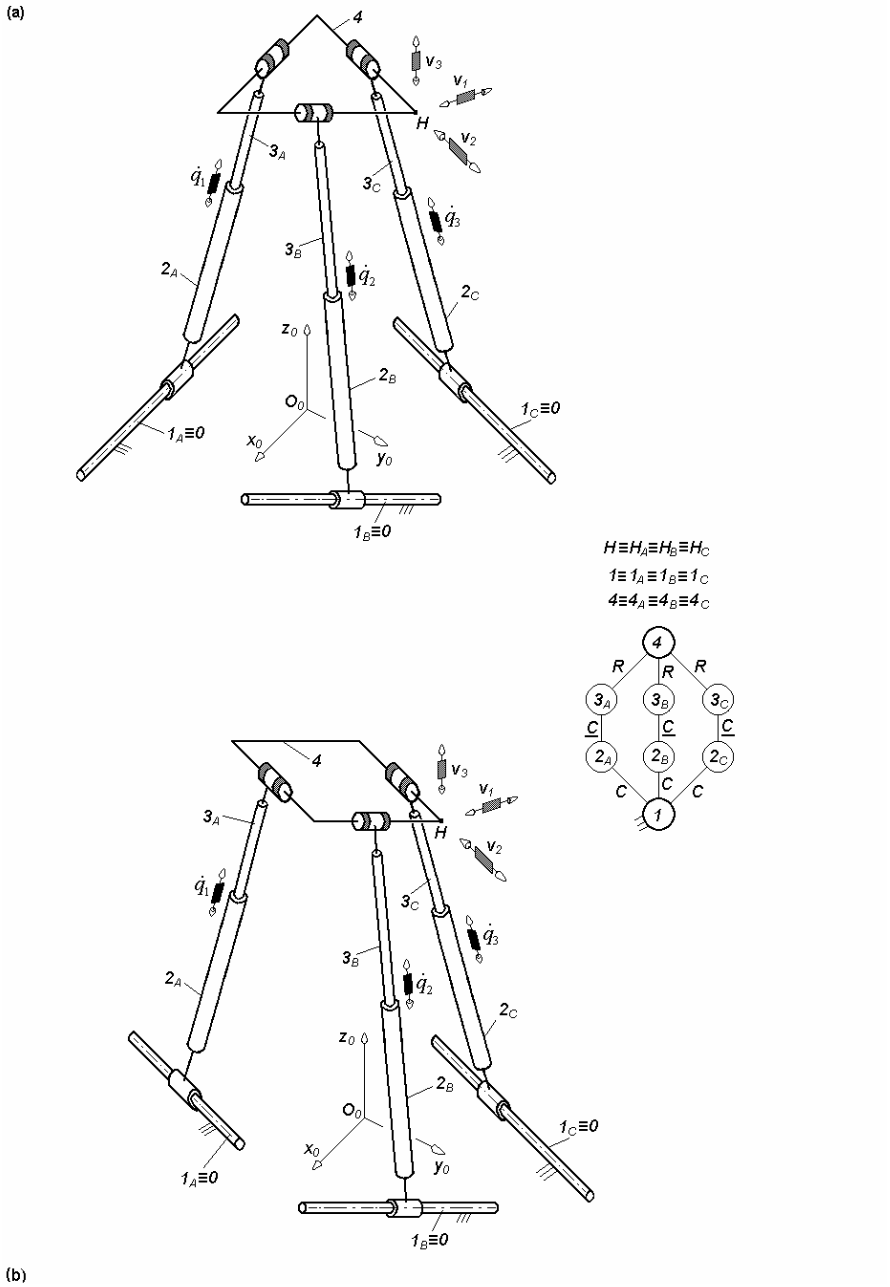

Fig. 4.25. *3-C*<u>*C*</u>*R*-type non overconstrained TPMs with coupled motions and linear actuators combined in cylindrical joints non adjacent to the fixed base, limb topology $C\perp \underline{C}\perp^{\parallel}R$

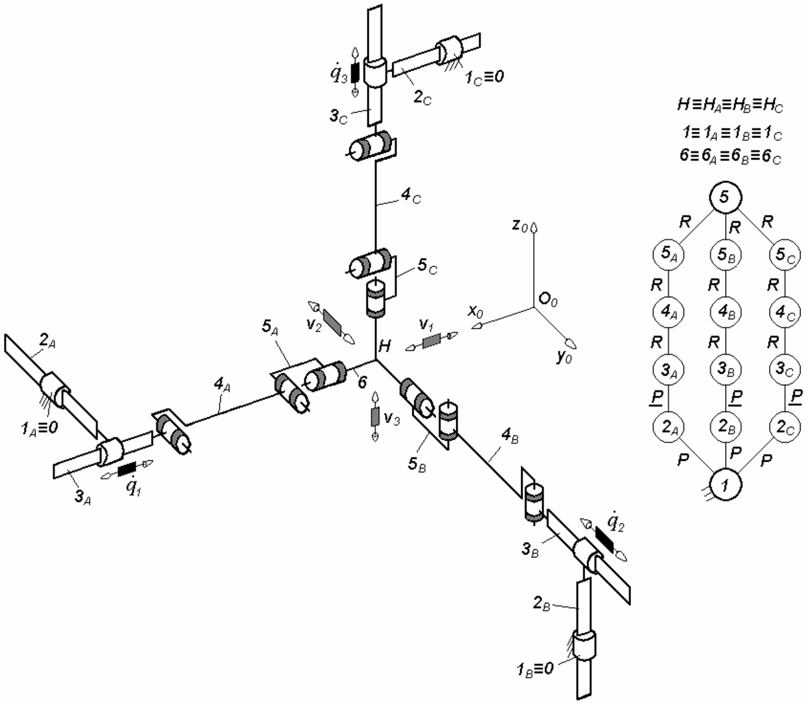

Fig. 4.26. *3-PPRRR**-type non overconstrained TPM with coupled motions and linear actuators non adjacent to the fixed base, limb topology $P\perp \underline{P}\perp^{||}R||R\perp^{||}R*$

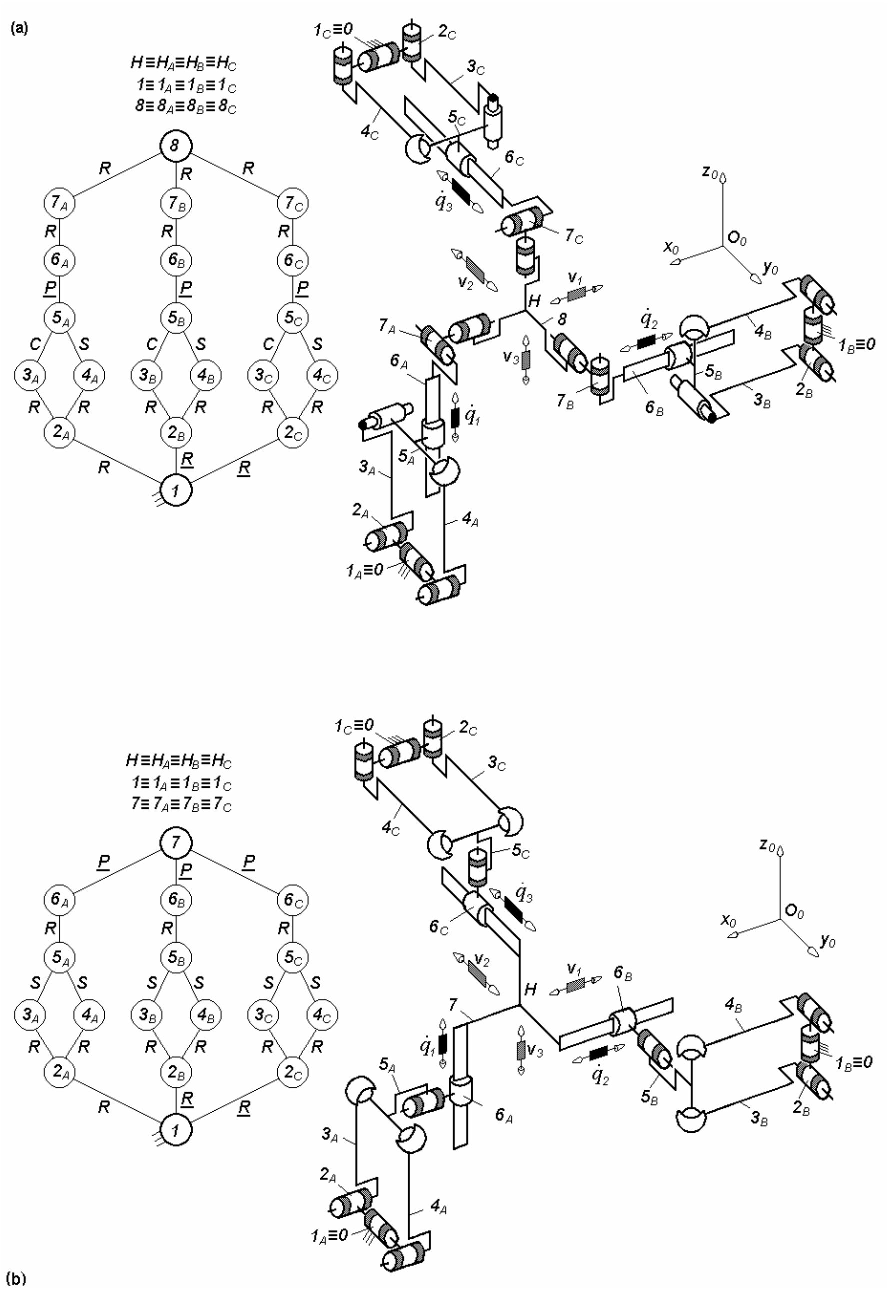

Fig. 4.27. Non overconstrained TPMs of types *3-RPa*PRR** (**a**) and *3-RPa^ss R*P* (**b**) with coupled motions and linear actuators non adjacent to the fixed base, limb topology $R \perp Pa^* \perp^{\perp} \underline{P} \perp R \perp R^*$ (**a**) and $R \perp Pa^{ss} \perp R^* \perp \underline{P}$ (**b**)

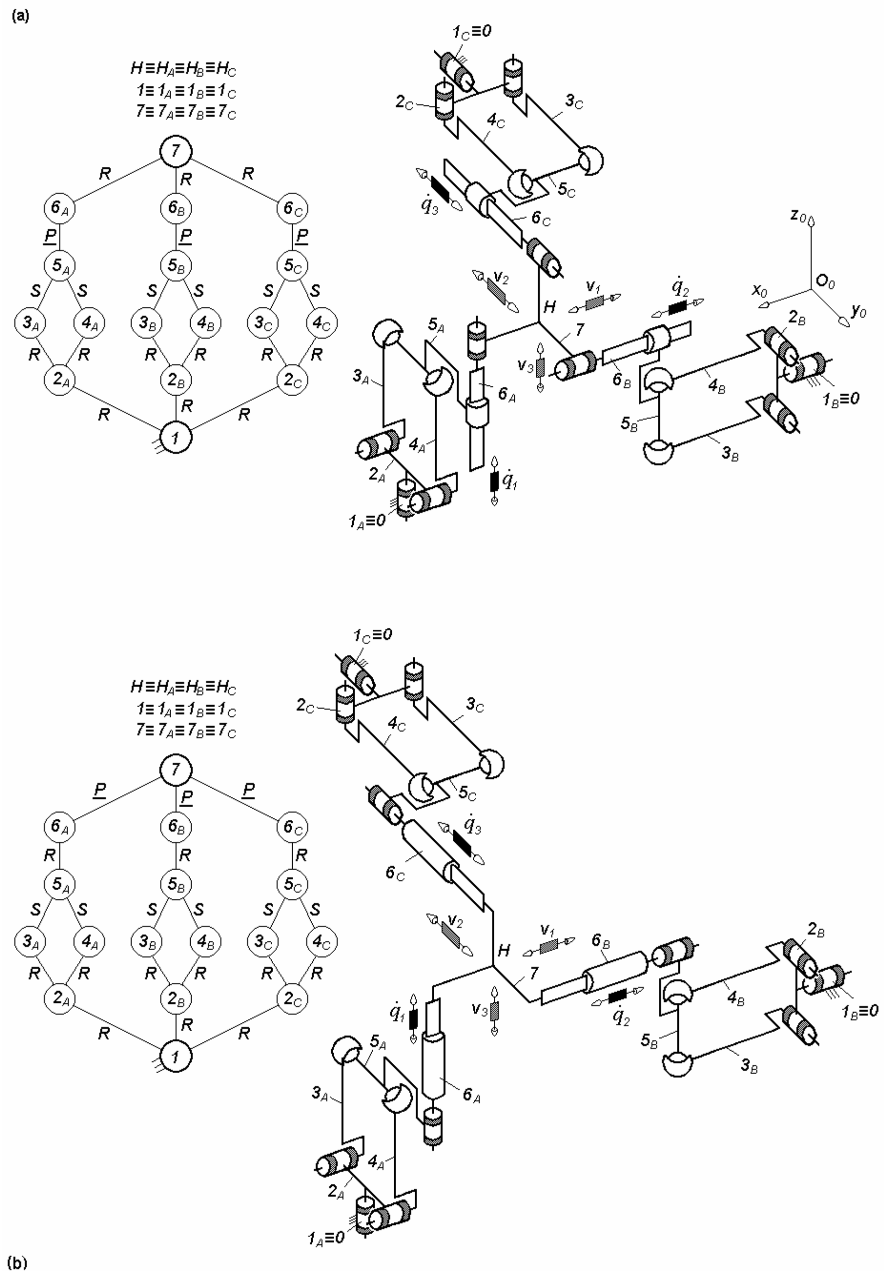

Fig. 4.28. Non overconstrained TPMs of types $3\text{-}RPa^{ss}\underline{P}R$ (**a**) and $3\text{-}RPa^{ss}R\underline{P}$ (**b**) with coupled motions and linear actuators non adjacent to the fixed base, limb topology $R \perp Pa^{ss} \perp^{||} \underline{P} || R$ (**a**) and $R \perp Pa^{ss} \perp^{||} R || \underline{P}$ (**b**)

4.3 Basic solutions with rotating actuators

In the *basic* non overconstrained TPMs with *rotating actuators* and coupled motions $F \leftarrow G_1–G_2–G_3$, the moving platform $n \equiv n_{Gi}$ ($i = 1, 2, 3$) is connected to the reference platform $1 \equiv 1_{Gi} \equiv 0$ by three limbs with five degrees of connectivity. No idle mobilities exist in these basic solutions.

The various types of limbs with five degrees of connectivity and no idle mobilities are systematized in Fig. 4.29. They are simple kinematic chains that can be actuated by rotating motors mounted on the fixed base. The limbs presented in Fig. 4.2 can also be used when the first revolute joint is actuated instead of the prismatic joint (see Figs. 4.6–4.9).

Various solutions of TPMs with coupled motions and no idle mobilities can be obtained by using three limbs with identical or different topologies presented in Figs. 4.2 and 4.29. We only show solutions with identical limb type as illustrated in Figs. 4.30–4.35. The limb topology and connecting conditions in these solutions are systematized in Table 4.9 and the structural parameters of the solutions are presented in Table 4.10.

The actuated revolute joints adjacent to the fixed base in the three limbs have orthogonal directions (Figs. 4.30b, 4.31–4.35) or are parallel to one plane (Fig. 4.30a).

Table 4.9. Limb topology and connecting conditions of the non overconstrained TPM with no idle mobilities and rotating actuators presented in Figs. 4.30–4.35

No.	TPM type	Limb topology	Connecting conditions
1	$3\text{-}\underline{R}RRRR$ (Fig. 4.30a)	$\underline{R}\|\|R\perp R\|\|R\perp R$ (Fig. 4.29a)	Actuated $\underline{R}$ joints adjacent to the fixed base and their axes are parallel to one plane
2	$3\text{-}\underline{R}RRRR$ (Fig. 4.30b)	$\underline{R}\|\|R\perp R\|\|R\perp R$ (Fig. 4.29a)	Actuated $\underline{R}$ joints adjacent to the fixed base and their axes are reciprocally orthogonal
3	$3\text{-}\underline{R}RRRR$ (Fig. 4.31a)	$\underline{R}\|\|R\|\|R\perp R\|\|R$ (Fig. 4.29b)	Idem No. 2
4	$3\text{-}\underline{R}RRRR$ (Fig. 4.31b)	$\underline{R}\perp R\|\|R\perp R\|\|R$ (Fig. 4.29c)	Idem No. 2
5	$3\text{-}\underline{R}RRRR$ (Fig. 4.32a)	$\underline{R}\perp R\|\|R\|\|R\perp R$ (Fig. 4.29d)	Idem No. 2
6	$3\text{-}\underline{R}RRRP$ (Fig. 4.32b)	$\underline{R}\perp R\|\|R\perp R\perp P$ (Fig. 4.29e)	Idem No. 2
7	$3\text{-}\underline{R}RPRR$ (Fig. 4.33a)	$\underline{R}\perp R\perp {}^{\|\|}P\perp R\perp R$ (Fig. 4.29f)	Idem No. 2
8	$3\text{-}\underline{R}RRPR$ (Fig. 4.33b)	$\underline{R}\perp R\|\|R\perp R\perp P$ (Fig. 4.29g)	Idem No. 2
9	$3\text{-}\underline{R}CRR$ (Fig. 4.34a)	$\underline{R}\perp C\|\|R\perp R$ (Fig. 4.29j)	Idem No. 2
10	$3\text{-}\underline{R}RCR$ (Fig. 4.34b)	$\underline{R}\perp R\|\|C\perp R$ (Fig. 4.29m)	Idem No. 2
11	$3\text{-}\underline{R}RRC$ (Fig. 4.35a)	$\underline{R}\|\|R\perp R\|\|C$ (Fig. 4.29p)	Idem No. 2
12	$3\text{-}\underline{R}RRC$ (Fig. 4.35b)	$\underline{R}\perp R\|\|R\perp C$ (Fig. 4.29s)	Idem No. 2

Table 4.10. Structural parameters[a] of translational parallel mechanisms in Figs. 4.30–4.35

No.	Structural parameter	Solution 3-*R*RRRR (Figs. 4.30, 4.31)	3-*R*RRRR, 3-*R*RRRP (Fig. 4.32) 3-*R*RPRR, 3-*R*RRPR (Fig. 4.33)	3-*R*CRR, 3-*R*RCR (Fig. 4.34) 3-*R*RRC (Fig. 4.35)
1	m	14	14	11
2	p_1	5	5	4
3	p_2	5	5	4
4	p_3	5	5	4
5	p	15	15	12
6	q	2	2	2
7	k_1	3	3	3
8	k_2	0	0	0
9	k	3	3	3
10	(R_{G1})	$(\boldsymbol{v}_1,\boldsymbol{v}_2,\boldsymbol{v}_3,\boldsymbol{\omega}_\beta,\boldsymbol{\omega}_\delta)$	$(\boldsymbol{v}_1,\boldsymbol{v}_2,\boldsymbol{v}_3,\boldsymbol{\omega}_\alpha,\boldsymbol{\omega}_\beta)$	$(\boldsymbol{v}_1,\boldsymbol{v}_2,\boldsymbol{v}_3,\boldsymbol{\omega}_\beta,\boldsymbol{\omega}_\delta)$
11	(R_{G2})	$(\boldsymbol{v}_1,\boldsymbol{v}_2,\boldsymbol{v}_3,\boldsymbol{\omega}_\alpha,\boldsymbol{\omega}_\delta)$	$(\boldsymbol{v}_1,\boldsymbol{v}_2,\boldsymbol{v}_3,\boldsymbol{\omega}_\beta,\boldsymbol{\omega}_\delta)$	$(\boldsymbol{v}_1,\boldsymbol{v}_2,\boldsymbol{v}_3,\boldsymbol{\omega}_\alpha,\boldsymbol{\omega}_\delta)$
12	(R_{G3})	$(\boldsymbol{v}_1,\boldsymbol{v}_2,\boldsymbol{v}_3,\boldsymbol{\omega}_\alpha,\boldsymbol{\omega}_\beta)$	$(\boldsymbol{v}_1,\boldsymbol{v}_2,\boldsymbol{v}_3,\boldsymbol{\omega}_\alpha,\boldsymbol{\omega}_\delta)$	$(\boldsymbol{v}_1,\boldsymbol{v}_2,\boldsymbol{v}_3,\boldsymbol{\omega}_\alpha,\boldsymbol{\omega}_\beta)$
13	S_{G1}	5	5	5
14	S_{G2}	5	5	5
15	S_{G3}	5	5	5
16	r_{G1}	0	0	0
17	r_{G2}	0	0	0
18	r_{G3}	0	0	0
19	M_{G1}	5	5	5
20	M_{G2}	5	5	5
21	M_{G3}	5	5	5
22	(R_F)	$(\boldsymbol{v}_1,\boldsymbol{v}_2,\boldsymbol{v}_3)$	$(\boldsymbol{v}_1,\boldsymbol{v}_2,\boldsymbol{v}_3)$	$(\boldsymbol{v}_1,\boldsymbol{v}_2,\boldsymbol{v}_3)$
23	S_F	3	3	3
24	r_l	0	0	0
25	r_F	12	12	12
26	M_F	3	3	3
27	N_F	0	0	0
28	T_F	0	0	0
29	$\sum_{j=1}^{p_1} f_j$	5	5	5
30	$\sum_{j=1}^{p_2} f_j$	5	5	5
31	$\sum_{j=1}^{p_3} f_j$	5	5	5
32	$\sum_{j=1}^{p} f_j$	15	15	15

[a]See footnote of Table 2.1 for the nomenclature of structural parameters

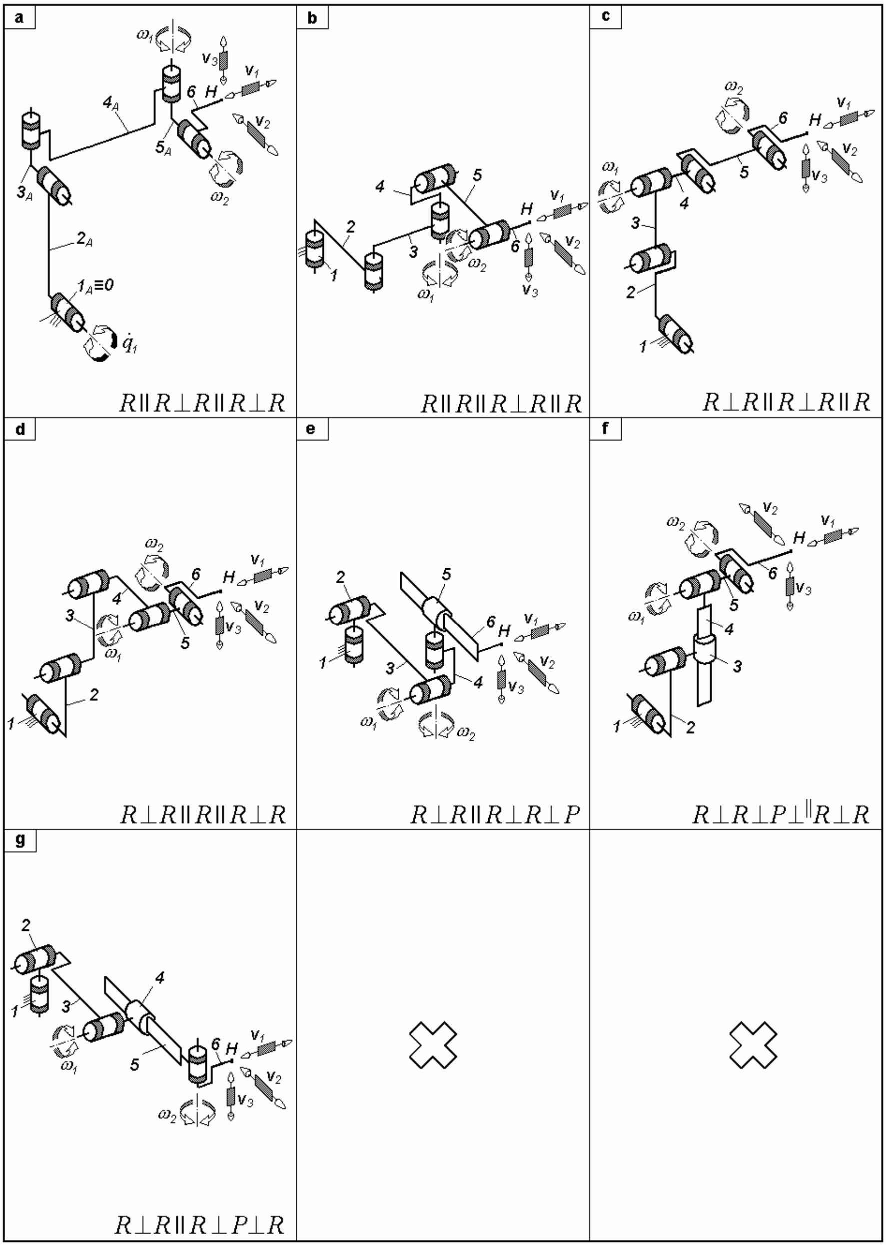

Fig. 4.29. Simple limbs for non overconstrained TPMs with coupled motions defined by $M_G = S_G = 5$, $(R_G) = (\boldsymbol{v}_1, \boldsymbol{v}_2, \boldsymbol{v}_3, \boldsymbol{\omega}_1, \boldsymbol{\omega}_2)$ and actuated by rotating motors mounted on the fixed base

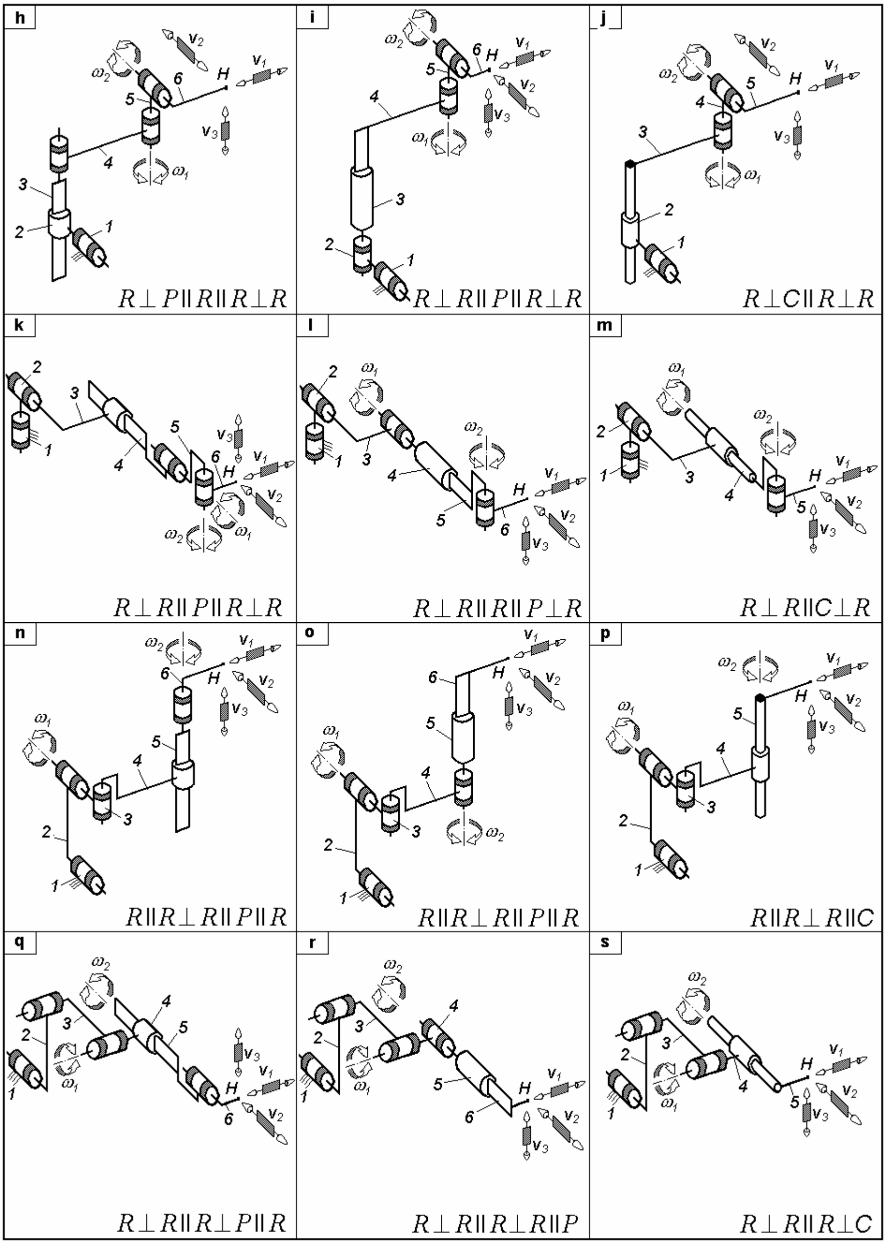
h
R⊥P||R||R⊥R
i
R⊥R||P||R⊥R
j
R⊥C||R⊥R
k
R⊥R||P||R⊥R
l
R⊥R||R||P⊥R
m
R⊥R||C⊥R
n
R||R⊥R||P||R
o
R||R⊥R||P||R
p
R||R⊥R||C
q
R⊥R||R⊥P||R
r
R⊥R||R⊥R||P
s
R⊥R||R⊥C

Fig. 4.29. (cont.)

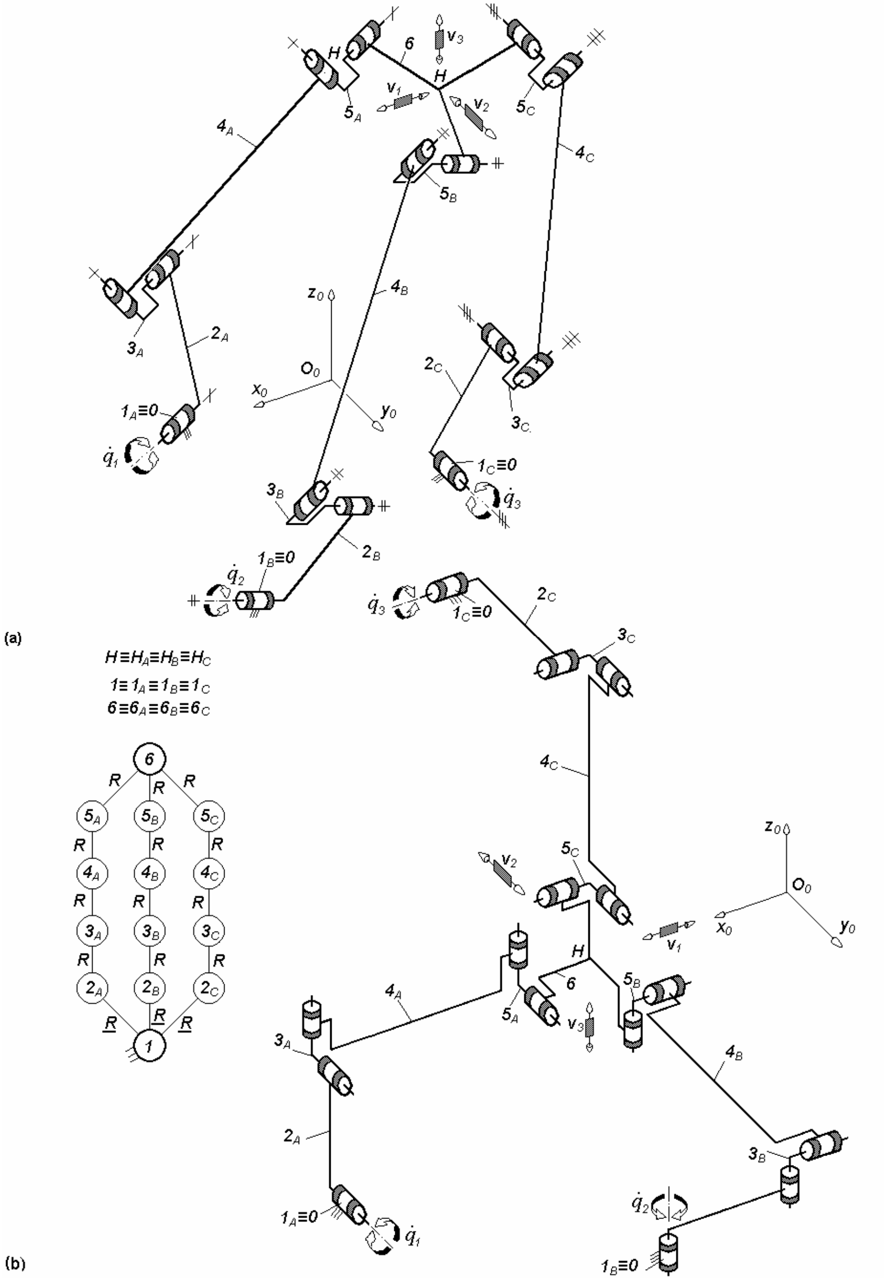

Fig. 4.30. *3-RRRRR*-type non overconstrained TPMs with coupled motions and rotating actuators mounted on the fixed base, limb topology $\underline{R}||R\perp R||R\perp^{||}R$

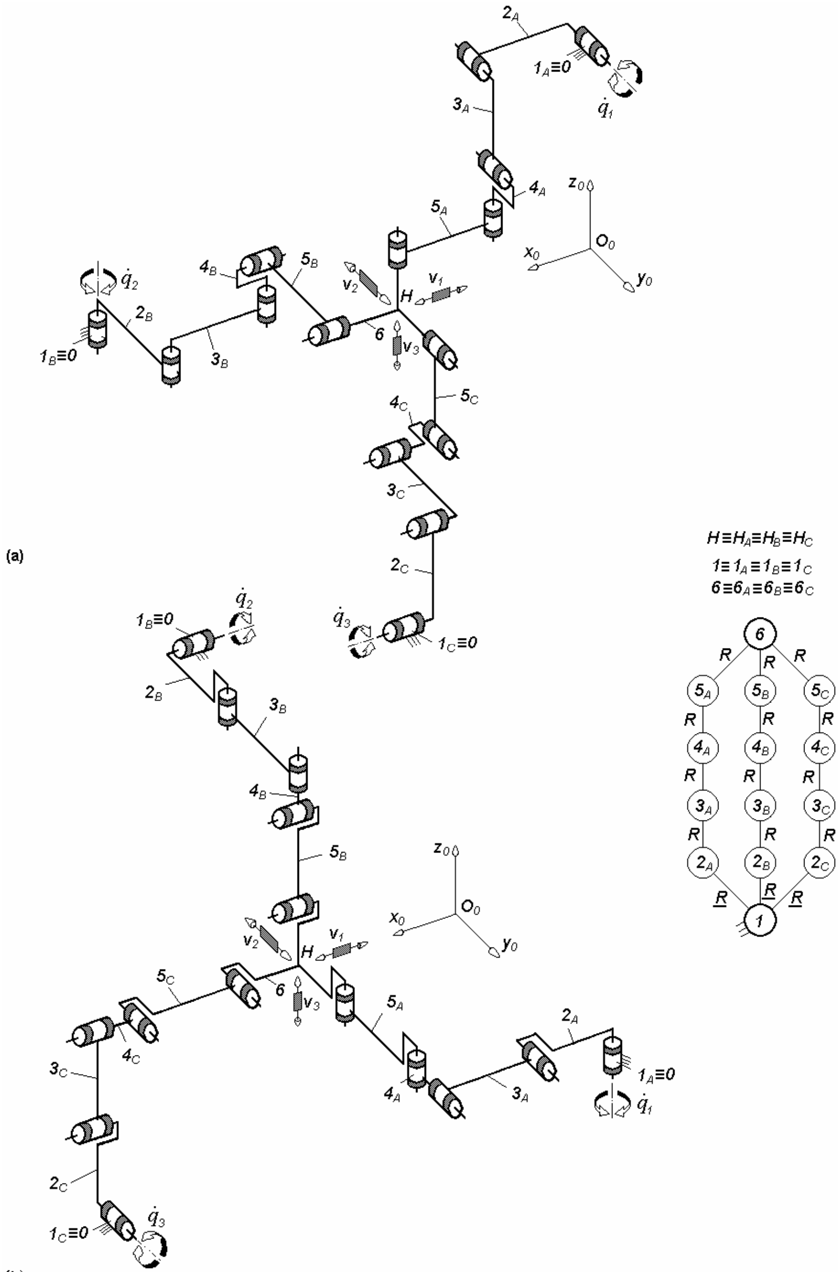

Fig. 4.31. *3-$\underline{R}RRRR$-type* non overconstrained TPMs with coupled motions and rotating actuators mounted on the fixed base, limb topology $\underline{R}||R||R \perp R||R$ (**a**) and $\underline{R} \perp R||R \perp R||R$ (**b**)

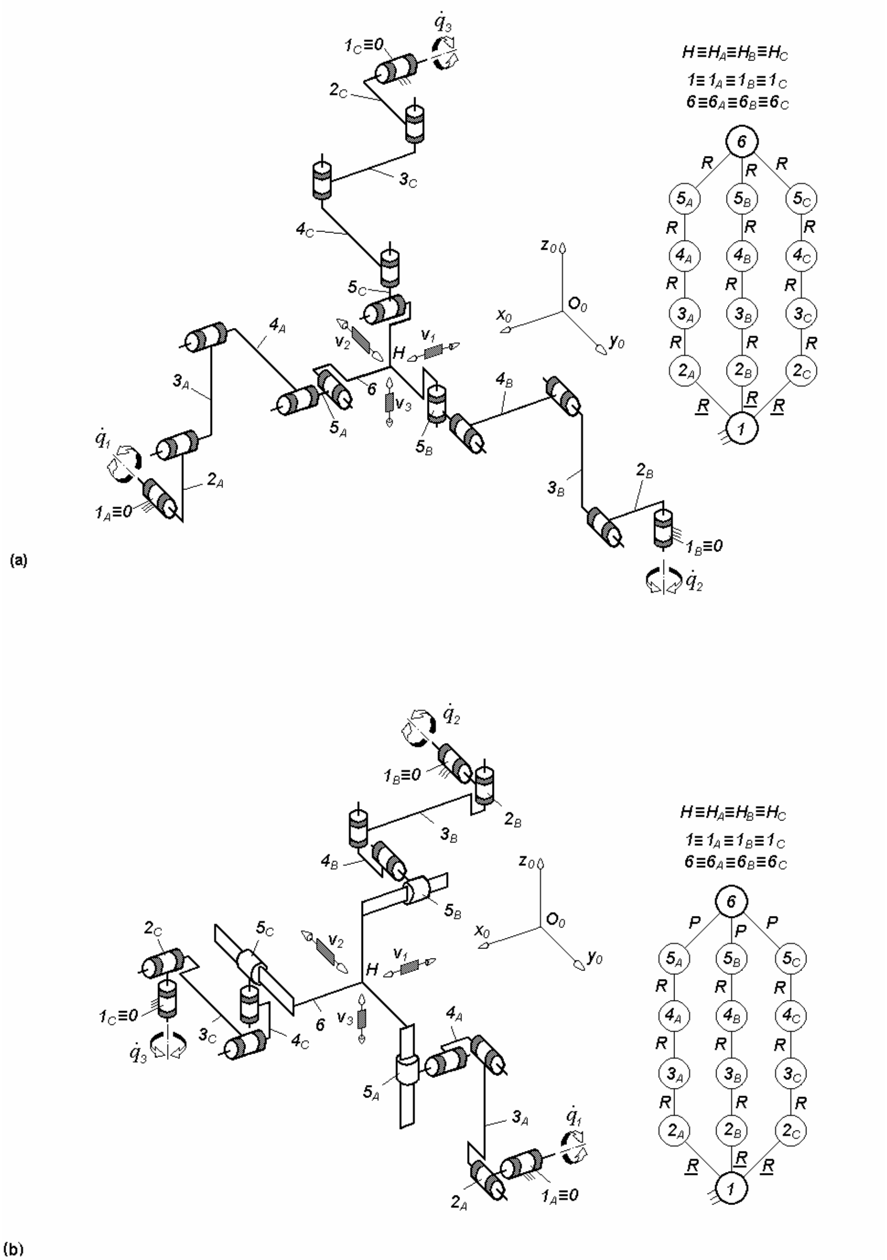

Fig. 4.32. Non overconstrained TPMs of types *3-*$\underline{R}$*RRRR* (**a**) and *3-*$\underline{R}$*RRRP* (**b**) with coupled motions and rotating actuators mounted on the fixed base, limb topology $\underline{R} \perp R||R||R \perp R$ (**a**) and $\underline{R} \perp R||R \perp R \perp P$ (**b**)

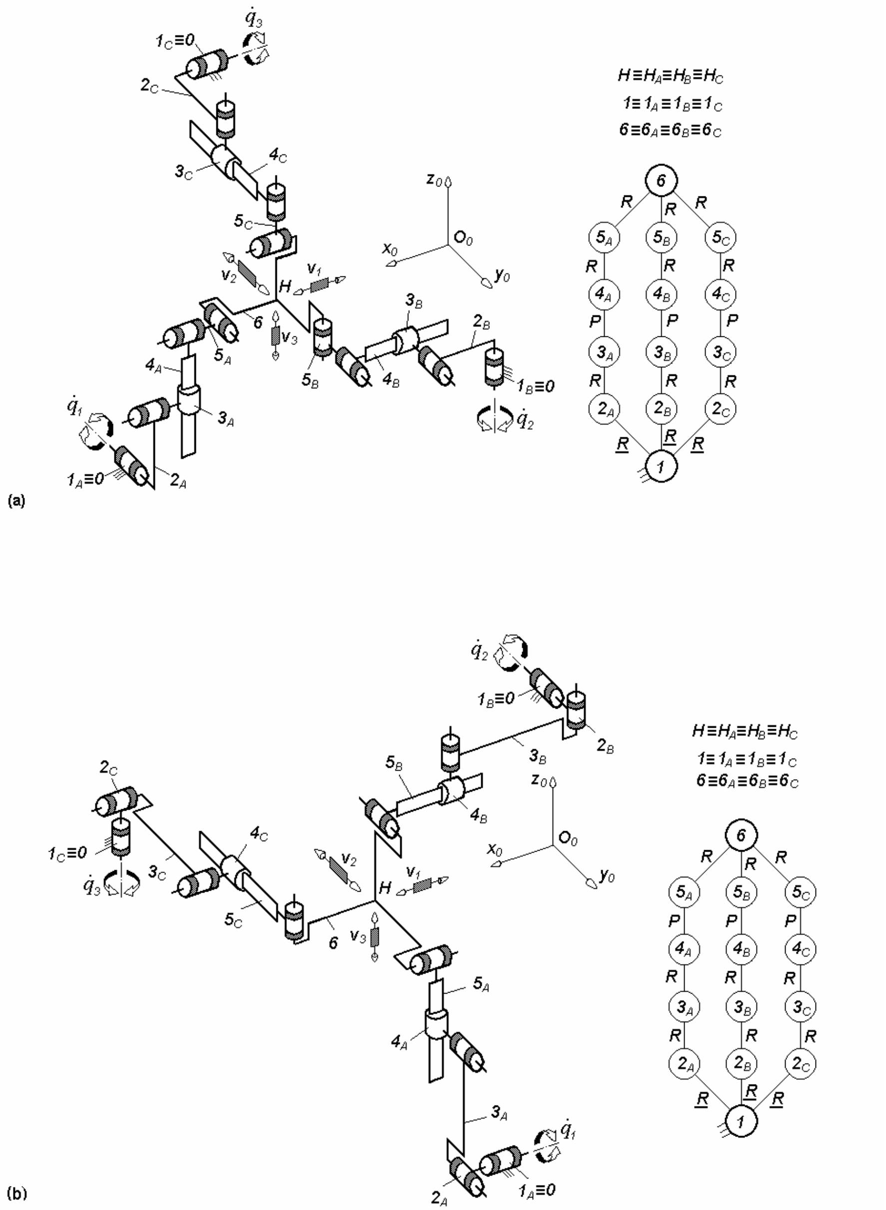

Fig. 4.33. Non overconstrained TPMs of types *3-<u>R</u>RPRR* (**a**) and *3-<u>R</u>RRPR* (**b**) with coupled motions and rotating actuators mounted on the fixed base, limb topology $\underline{R} \perp R \perp P \perp R \perp R$ (**a**) and $\underline{R} \perp R||R \perp R \perp P$ (**b**)

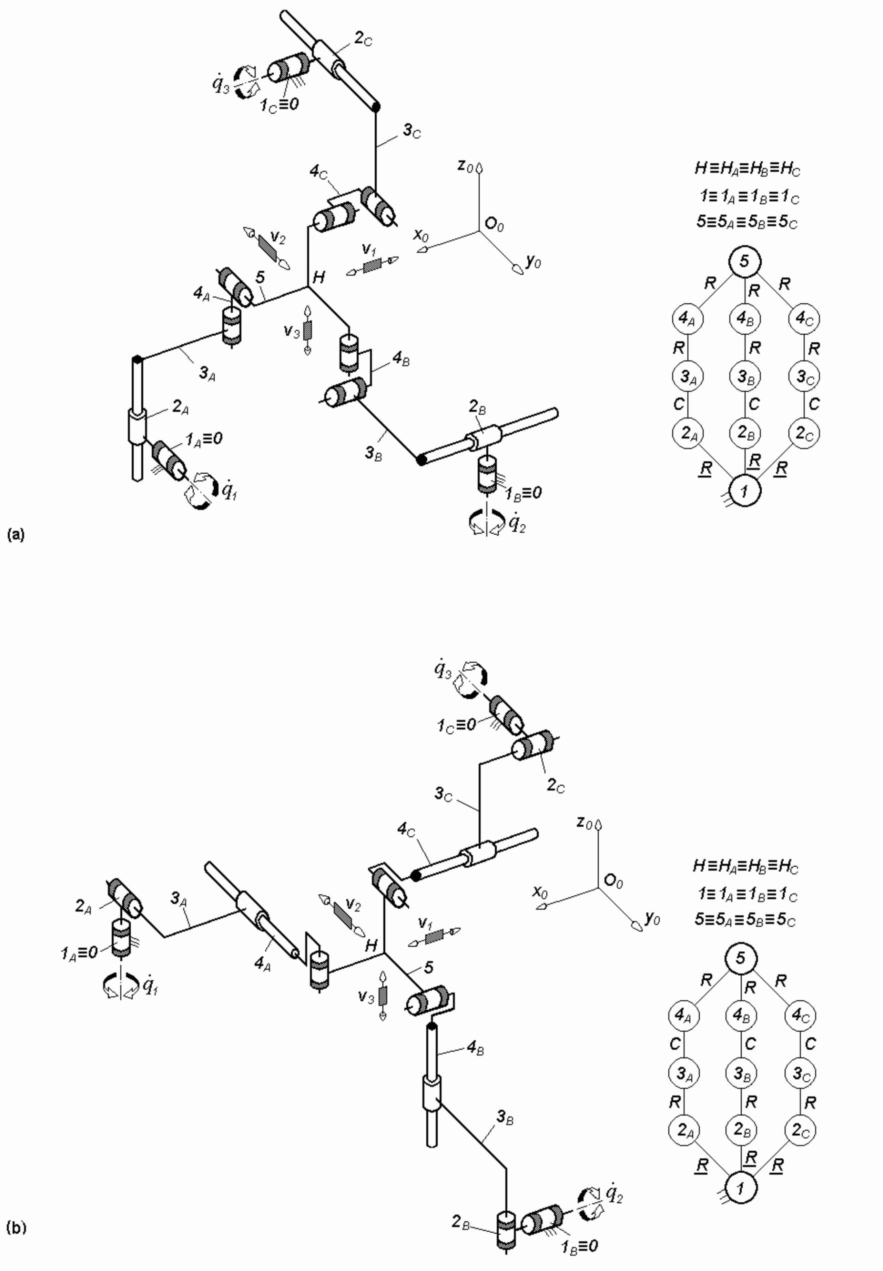

Fig. 4.34. Non overconstrained TPMs of types *3-<u>R</u>CRR* (**a**) and *3-<u>R</u>RCR* (**b**) with coupled motions and rotating actuators mounted on the fixed base: $\underline{R} \perp C||R \perp^{||} R$ (**a**) and $\underline{R} \perp R||C \perp^{||} R$ (**b**)

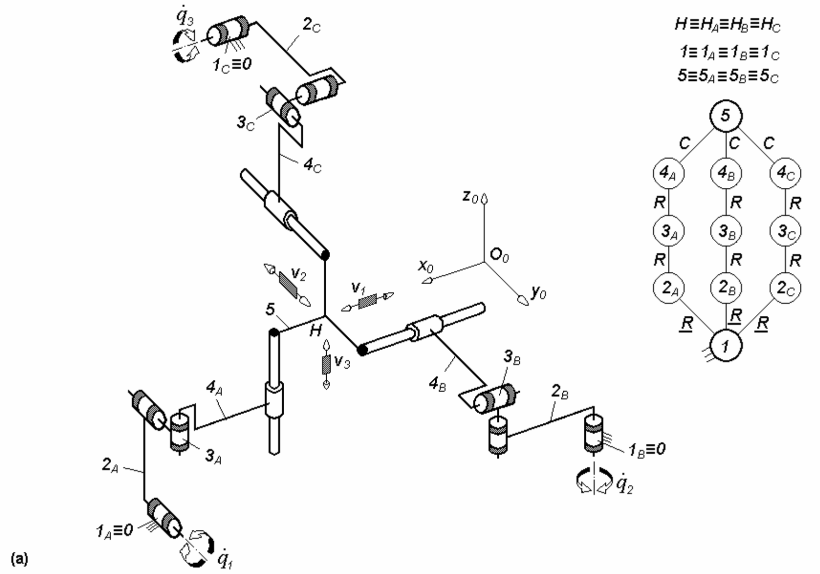

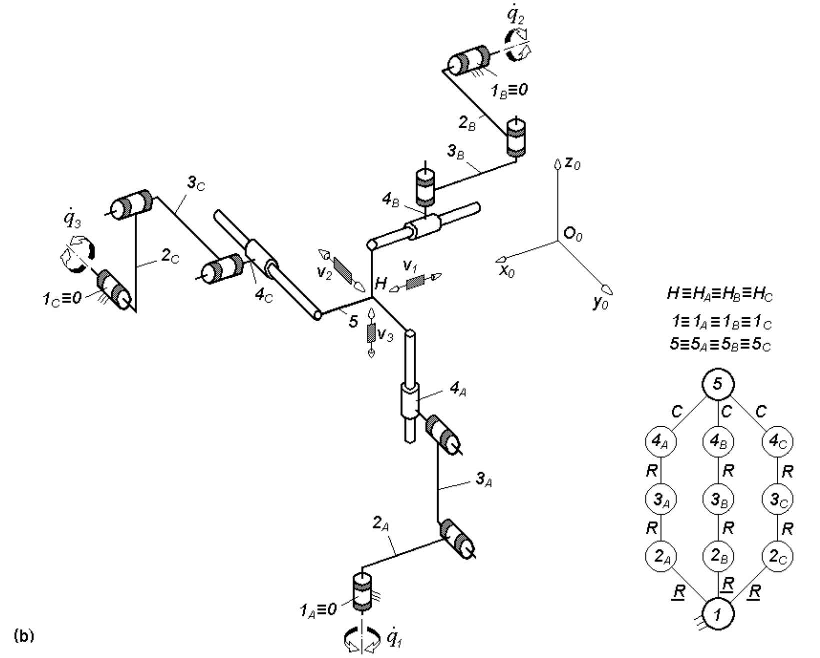

Fig. 4.35. *3-RRRC*-type non overconstrained TPMs with coupled motions and rotating actuators mounted on the fixed base limb topology $\underline{R}||R\perp R||C$ (**a**) and $\underline{R}\perp R||R\perp^{||}C$ (**b**)

4.4 Derived solutions with rotating actuators

Non overconstrained solutions $F \leftarrow G_1G_2\text{–}G_2$ with *rotating actuators* and *coupled motions* can be derived from the overconstrained solutions presented in Figs. 3.71–3.118 by introducing the required *idle mobilities*. They have the rotating actuators mounted on the fixed base (Figs. 4.36–4.82).

For example, the non overconstrained solutions in Fig. 4.36 are derived from the overconstrained solutions in Fig. 3.71 by introducing two rotational idle mobilities outside the parallelogram loop and one translational and two rotational idle mobilities in each parallelogram loop. They are introduced by replacing two revolute joints by one spherical and one cylindrical joint in the first parallelogram loop and by two spherical joints in the second parallelogram loop of each limb. The prismatic joints in Fig. 3.71 are also replaced by cylindrical ones in Fig. 4.36. We note that the two spherical joints adjacent to link 7 introduce one translational and two rotational idle mobilities in each parallelogram loop and also provide an idle rotational mobility of link 5. An idle mobility of rotation is combined in each cylindrical joint denoted by C*.

The limb topology and connecting conditions of the solutions in Figs. 4.36–4.82 are systematized in Table 4.11 and the structural parameters of the solutions are presented in Tables 4.12–4.18.

Table 4.11. Limb topology of the non overconstrained solutions ($N_F = 0$) of the derived TPMs with idle mobilities and rotating actuators mounted on the fixed base presented in Figs. 4.36–4.82

No.	Basic TPM type	N_F	Derived TPM with $N_F = 0$ type	Limb topology
1	$3\text{-}\underline{Pa}PaP$ (Fig. 3.71)	24	$3\text{-}\underline{Pa}^{cs}Pa^{ss}C^*$ (Fig. 4.36)	$\underline{Pa}^{cs}\perp Pa^{ss}\|C^*$
2	$3\text{-}\underline{Pa}PaP$ (Fig. 3.72)	24	$3\text{-}\underline{Pa}^{cs}Pa^{ss}C^*$ (Fig. 4.37)	$\underline{Pa}^{cs}\|Pa^{ss}\|C^*$
3	$3\text{-}\underline{Pa}PPa$ (Fig. 3.73)	24	$3\text{-}\underline{Pa}^{cs}C^*Pa^{ss}$ (Fig. 4.38)	$\underline{Pa}^{cs}\perp C^*\|Pa^{ss}$
4	$3\text{-}\underline{Pa}PPa$ (Fig. 3.74)	24	$3\text{-}\underline{Pa}^{cs}C^*Pa^{ss}$ (Fig. 4.39)	$\underline{Pa}^{cs}\|C^*\|Pa^{ss}$
5	$3\text{-}\underline{Pa}Pa^{cc}$ (Fig. 3.75)	21	$3\text{-}\underline{Pa}^{cs}R^*R^*Pa^{scc}$ (Fig. 4.40)	$\underline{Pa}^{cs}\|R^*\perp R^*\|Pa^{scc}$
6	$3\text{-}\underline{Pa}Pa^{cc}$ (Fig. 3.76	21	$3\text{-}\underline{Pa}^{cs}R^*Pa^{ccs}R^*$ (Fig. 4.41	$\underline{Pa}^{cs}\perp R^*\|Pa^{ccs}\perp^{\|}R^*$
7	$3\text{-}\underline{Pa}Pa^{cc}$ (Fig. 3.77	21	$3\text{-}\underline{Pa}^{cs}R^*R^*Pa^{scc}$ (Fig. 4.42	$\underline{Pa}^{cs}\perp R^*\perp^{\|}R^*\|Pa^{scc}$
8	$3\text{-}\underline{Pa}Pa^{cc}$ (Fig. 3.78)	21	$3\text{-}\underline{Pa}^{cs}R^*Pa^{ccs}R^*$ (Fig. 4.43)	$\underline{Pa}^{cs}\|R^*\|Pa^{ccs}\perp R^*$
9	$3\text{-}\underline{Pa}^{cc}Pa$ (Fig. 3.79)	21	$3\text{-}\underline{Pa}^{scc}Pa^{ss}R^*$ (Fig. 4.44)	$\underline{Pa}^{scc}\|Pa^{ss}\|R^*$
10	$3\text{-}\underline{Pa}PaPa$ (Fig. 3.80)	33	$3\text{-}\underline{Pa}^{ss}Pa^{cs}Pa^{ss}$ (Fig. 4.45)	$\underline{Pa}^{ss}\perp Pa^{cs}\perp^{\|}Pa^{ss}$
11	$3\text{-}\underline{Pa}PaPa$ (Fig. 3.81)	33	$3\text{-}\underline{Pa}^{cs}Pa^{ss}Pa^{ss}$ (Fig. 4.46)	$\underline{Pa}^{cs}\perp Pa^{ss}\perp^{\perp}Pa^{ss}$
12	$3\text{-}\underline{Pa}PaPa$ (Fig. 3.82	33	$3\text{-}\underline{Pa}^{ss}Pa^{cs}Pa^{ss}$ (Fig. 4.47	$\underline{Pa}^{ss}\|Pa^{cs}\perp Pa^{ss}$
13	$3\text{-}\underline{R}RC$ (Fig. 3.83)	3	$3\text{-}\underline{R}RR^*C$ (Fig. 4.48)	$\underline{R}\|R\perp R^*\perp^{\|}C$
14	$3\text{-}\underline{R}RC$ (Fig. 3.84)	3	$3\text{-}\underline{R}R^*RC$ (Fig. 4.49	$\underline{R}\perp R^*\perp^{\|}R\|C$
15	$3\text{-}\underline{R}CR$ (Fig. 3.85a)	3	$3\text{-}\underline{R}R^*CR$ (Fig. 4.50a)	$\underline{R}\perp R^*\perp^{\|}C\|R$
16	$3\text{-}\underline{R}PPR$ (Fig. 3.85b)	3	$3\text{-}\underline{R}PR^*RR$ (Fig. 4.50b)	$\underline{R}\|P\perp R^*\perp^{\|}R\|R$
17	$3\text{-}\underline{R}PC$ (Fig. 3.86a)	3	$3\text{-}\underline{R}C^*C$ (Fig. 4.51a)	$\underline{R}\perp C^*\perp^{\|}C$
18	$3\text{-}\underline{R}PPR$ (Fig. 3.86b)	3	$3\text{-}\underline{R}PC^*R$ (Fig. 4.51b)	$\underline{R}\|P\perp C^*\perp^{\|}R$
19	$3\text{-}\underline{Pa}RC$ (Fig. 3.87)	12	$3\text{-}\underline{Pa}^{cs}R^*RC$ (Fig. 4.52)	$\underline{Pa}^{cs}\perp R^*\perp^{\|}R\|C$
20	$3\text{-}\underline{Pa}CR$ (Fig. 3.88)	12	$3\text{-}\underline{Pa}^{cs}R^*CR$ (Fig. 4.53)	$\underline{Pa}^{cs}\perp R^*\perp^{\|}C\|R$

Table 4.11. (cont.)

21	3-$\underline{Pa}PaRR$ (Fig. 3.89)	*21*	3-$\underline{Pa}^{ss}Pa^{ss}R$ (Fig. 4.54)	$\underline{Pa}^{ss} \perp Pa^{ss} \perp^{\perp} R$
22	3-$\underline{Pa}PaRR$ (Fig. 3.90)	*21*	3-$\underline{Pa}^{ss}Pa^{ss}R$ (Fig. 4.55)	$\underline{Pa}^{ss} \perp Pa^{ss} \perp^{\parallel} R$
23	3-$\underline{Pa}PaRR$ (Fig. 3.91)	*21*	3-$\underline{Pa}^{ss}Pa^{ss}R$ (Fig. 4.56)	$\underline{Pa}^{ss} \perp Pa^{ss} \perp^{\perp} R$
24	3-$\underline{Pa}RRPa$ (Fig. 3.92)	*21*	3-$\underline{Pa}^{ss}RPa^{ss}$ (Fig. 4.57)	$\underline{Pa}^{ss} \parallel R \perp Pa^{ss}$
25	3-$\underline{Pa}RRPa$ (Fig. 3.93)	*21*	3-$\underline{Pa}^{ss}RPa^{ss}$ (Fig. 4.58)	$\underline{Pa}^{ss} \perp R \perp^{\perp} Pa^{ss}$
26	3-$\underline{Pa}RRPa$ (Fig. 3.94)	*21*	3-$\underline{Pa}^{ss}RPa^{ss}$ (Fig. 4.59)	$\underline{Pa}^{ss} \perp R \perp^{\parallel} Pa^{ss}$
27	3-$\underline{Pa}RPaR$ (Fig. 3.95)	*21*	3-$\underline{Pa}^{ss}RPa^{ss}$ (Fig. 4.60a)	$\underline{Pa}^{ss} \perp R \perp Pa^{ss}$
28	3-$\underline{Pa}RPaR$ (Fig. 3.96)	*21*	3-$\underline{Pa}^{ss}RPa^{ss}$ (Fig. 4.60b)	$\underline{Pa}^{ss} \perp^{\parallel} R \perp Pa^{ss}$
29	3-$\underline{R}RPaP$ (Fig. 3.97)	*12*	3-$\underline{R}RPa^{ss}P$ (Fig. 4.61)	$\underline{R} \parallel R \parallel Pa^{ss} \parallel P$
30	3-$\underline{R}PRPa$ (Fig. 3.98)	*12*	3-$\underline{R}PRPa^{ss}$ (Fig. 4.62)	$\underline{R} \parallel P \parallel R \parallel Pa^{ss}$
31	3-$\underline{R}CPa$ (Fig. 3.99)	*12*	3-$\underline{R}CPa^{s}$ (Fig. 4.63)	$\underline{R} \parallel C \parallel Pa^{ss}$
32	3-$\underline{R}PaRR$ (Fig. 3.100a)	*12*	3-$\underline{R}Pa^{ss}RR*$ (Fig. 4.64a)	$\underline{R} \perp Pa^{ss} \perp^{\parallel} R \perp R$
33	3-$\underline{R}PaRR$ (Fig. 3.100b)	*12*	3-$\underline{R}Pa^{ss}R*R$ (Fig. 4.64b)	$\underline{R} \perp Pa^{ss}$-$R* \perp R$
34	3-$\underline{R}RPaR$ (Fig. 3.101)	*12*	3-$\underline{R}Pa^{4s}$ (Fig. 4.65)	$\underline{R}$-Pa^{4s}
35	3-$\underline{R}PaPaR$ (Fig. 3.102)	*21*	3-$\underline{R}Pa^{ss}Pa^{ss}$ (Fig. 4.66)	$\underline{R} \perp Pa^{ss} \parallel Pa^{ss}$
36	3-$\underline{R}PaRPa$ (Fig. 3.103)	*21*	3-$\underline{R}Pa^{ss}Pa^{ss}$ (Fig. 4.67)	$\underline{R} \perp Pa^{ss} \parallel Pa^{ss}$
37	3-$\underline{R}PaRPa$ (Fig. 3.104)	*21*	3-$\underline{R}Pa^{ss}Pa^{ss}$ (Fig. 4.68)	$\underline{R} \perp Pa^{ss} \parallel Pa^{ss}$
38	3-$\underline{R}PaPaR$ (Fig. 3.105)	*21*	3-$\underline{R}Pa^{*}Pa^{ss}R*$ (Fig. 4.69)	$\underline{R} \perp Pa* \parallel Pa^{ss} \perp^{\parallel} R*$
39	3-$\underline{R}RPa^{cc}$ (Fig. 3.106)	*9*	3-$\underline{R}RPa^{ccs}R*$ (Fig. 4.70)	$\underline{R} \parallel R \parallel Pa^{ccs} \perp R*$
40	3-$\underline{R}RPa^{cc}$ (Fig. 3.107)	*9*	3-$\underline{R}R*RPa^{scc}$ (Fig. 4.71)	$\underline{R} \perp R* \perp^{\parallel} R \parallel Pa^{scc}$
41	3-$\underline{Pa}^{cc}RR$ (Fig. 3.108)	*9*	3-$\underline{Pa}^{scc}RR*R$ (Fig. 4.72)	$\underline{Pa}^{scc} \parallel R \perp R* \perp^{\parallel} R$
42	3-$\underline{Pa}Pr$ (Fig. 3.109a)	*21*	3-$\underline{Pa}^{ss}Pr^{ss}R*$ (Fig. 4.73a)	$\underline{Pa}^{ss}$-Pr^{ss}-$R*$

Table 4.11. (cont.)

43	$3\text{-}\underline{R}RPr$ (Fig. 3.109b)	9	$3\text{-}\underline{R}RPr^{ss}R^*$ (Fig. 4.73b)	$\underline{R}\Vert R\text{-}Pr^{ss}\text{-}R^*$
44	$3\text{-}\underline{Pa}RRRR$ (Fig. 3.110a)	9	$3\text{-}\underline{Pa}^{cs}RRRR$ (Fig. 4.74a)	$\underline{Pa}^{cs}\Vert R\Vert R\perp R\Vert R$
45	$3\text{-}\underline{Pa}RRRR$ (Fig. 3.110b)	9	$3\text{-}\underline{Pa}^{cs}RRRR$ (Fig. 4.74b)	$\underline{Pa}^{cs}\perp R\perp R\Vert R\perp R$
46	$3\text{-}\underline{Pa}RRRR$ (Fig. 3.111a)	9	$3\text{-}\underline{Pa}^{ss}RRR$ (Fig. 4.75a)	$\underline{Pa}^{ss}\perp R\perp R\Vert R$
47	$3\text{-}\underline{Pa}RRRR$ (Fig. 3.111b)	9	$3\text{-}\underline{Pa}^{ss}RRR$ (Fig. 4.75b)	$\underline{Pa}^{ss}\Vert R\Vert R\perp R$
48	$3\text{-}\underline{Pa}RRRR$ (Fig. 3.112a)	9	$3\text{-}\underline{Pa}^{cs}RRRR$ (Fig. 4.76a)	$\underline{Pa}\Vert R\perp R\Vert R\perp R$
49	$3\text{-}\underline{R}RPaRR$ (Fig. 3.112b)	9	$3\text{-}\underline{R}Pa^{ss}RR$ (Fig. 4.76b)	$\underline{R}\Vert Pa^{ss}\perp R\perp^{\Vert}R$
50	$3\text{-}\underline{R}PaRRR$ (Fig. 3.113a)	9	$3\text{-}\underline{R}Pa^{cs}RRR$ (Fig. 4.77a)	$\underline{R}\perp Pa^{cs}\Vert R\Vert R\perp^{\Vert}R$
51	$3\text{-}\underline{R}PaRRR$ (Fig. 3.113b)	9	$3\text{-}\underline{R}Pa^{ss}RR$ (Fig. 4.77b)	$\underline{R}\perp Pa^{ss}\perp^{\perp}R\perp^{\perp}R$
52	$3\text{-}\underline{R}PaRRR$ (Fig. 3.114a)	9	$3\text{-}\underline{R}Pa^{cs}RRR$ (Fig. 4.78a)	$\underline{R}\perp Pa^{cs}\perp^{\Vert}R\perp R\Vert R$
53	$3\text{-}\underline{R}PaRRR$ (Fig. 3.114b)	9	$3\text{-}\underline{R}Pa^{cs}RRR$ (Fig. 4.78b)	$\underline{R}\perp Pa^{cs}\Vert R\Vert R\perp^{\Vert}R$
54	$3\text{-}\underline{R}RPaRR$ (Fig. 3.115a)	9	$3\text{-}\underline{R}RPa^{ss}R$ (Fig. 4.79a)	$\underline{R}\Vert R\Vert Pa^{ss}\perp R$
55	$3\text{-}\underline{R}RPaRR$ (Fig. 3.115b)	9	$3\text{-}\underline{R}RPa^{ss}R$ (Fig. 4.79b)	$\underline{R}\Vert R\perp Pa^{ss}\perp^{\perp}R$
56	$3\text{-}\underline{R}RRRPa$ (Fig. 3.116a)	9	$3\text{-}\underline{R}RRPa^{ss}$ (Fig. 4.80a)	$\underline{R}\Vert R\perp R\perp^{\perp}Pa^{ss}$
57	$3\text{-}\underline{R}RRRPa$ (Fig. 3.116b)	9	$3\text{-}\underline{R}RRRPa^{cs}$ (Fig. 4.80b)	$\underline{R}\Vert R\perp R\Vert R\perp^{\perp}Pa^{cs}$
58	$3\text{-}\underline{R}RRPaR$ (Fig. 3.117a)	9	$3\text{-}\underline{R}RRPa^{ss}$ (Fig. 4.81a)	$\underline{R}\Vert R\perp R\perp Pa^{ss}$
59	$3\text{-}\underline{R}RRRPa$ (Fig. 3.117b)	9	$3\text{-}\underline{R}RRRPa^{cs}$ (Fig. 4.81b)	$\underline{R}\perp R\Vert R\perp^{\Vert}R\perp Pa^{cs}$
60	$3\text{-}\underline{R}RRPaR$ (Fig. 3.118a)	9	$3\text{-}\underline{R}RRPa^{cs}R$ (Fig. 4.82a)	$\underline{R}\perp R\Vert R\Vert Pa^{cs}\perp^{\Vert}R$
61	$3\text{-}\underline{R}RRPaR$ (Fig. 3.118b)	9	$3\text{-}\underline{R}RRPa^{ss}$ (Fig. 4.82b)	$\underline{R}\perp R\Vert R\Vert Pa^{ss}$

Table 4.12. Bases of the operational velocities spaces of the limbs isolated from the parallel mechanisms presented in Figs. 4.36–4.82

No.	Parallel mechanism	Basis (R_{G1})	(R_{G2})	(R_{G3})
1	Figs. 4.36–4.44, 4.46, 4.48, 4.49a, 4.52, 4.53, 4.61–4.63, 4.64b, 4.65b, 4.66–4.72, 4.74b, 4.76a, 4.77a, 4.78a, 4.79, 4.80a, 4.81a	$(\boldsymbol{v}_1, \boldsymbol{v}_2, \boldsymbol{v}_3, \boldsymbol{\omega}_\beta, \boldsymbol{\omega}_\delta)$	$(\boldsymbol{v}_1, \boldsymbol{v}_2, \boldsymbol{v}_3, \boldsymbol{\omega}_\alpha, \boldsymbol{\omega}_\delta)$	$(\boldsymbol{v}_1, \boldsymbol{v}_2, \boldsymbol{v}_3, \boldsymbol{\omega}_\alpha, \boldsymbol{\omega}_\beta)$
2	Figs. 4.45, 4.55, 4.56, 4.60, 4.64a, 4.65a, 4.73, 4.74a, 4.75, 4.82b	$(\boldsymbol{v}_1, \boldsymbol{v}_2, \boldsymbol{v}_3, \boldsymbol{\omega}_\alpha, \boldsymbol{\omega}_\beta)$	$(\boldsymbol{v}_1, \boldsymbol{v}_2, \boldsymbol{v}_3, \boldsymbol{\omega}_\beta, \boldsymbol{\omega}_\delta)$	$(\boldsymbol{v}_1, \boldsymbol{v}_2, \boldsymbol{v}_3, \boldsymbol{\omega}_\alpha, \boldsymbol{\omega}_\delta)$
3	Figs. 4.47, 4.54, 4.57–4.59, 4.76b, 4.77b, 4.78b, 4.80b, 4.81b, 4.82a	$(\boldsymbol{v}_1, \boldsymbol{v}_2, \boldsymbol{v}_3, \boldsymbol{\omega}_\alpha, \boldsymbol{\omega}_\delta)$	$(\boldsymbol{v}_1, \boldsymbol{v}_2, \boldsymbol{v}_3, \boldsymbol{\omega}_\alpha, \boldsymbol{\omega}_\beta)$	$(\boldsymbol{v}_1, \boldsymbol{v}_2, \boldsymbol{v}_3, \boldsymbol{\omega}_\beta, \boldsymbol{\omega}_\delta)$
4	Figs. 4.49b, 4.50, 4.51	$(\boldsymbol{v}_1, \boldsymbol{v}_2, \boldsymbol{v}_3, \boldsymbol{\omega}_\beta, \boldsymbol{\omega}_\delta)$	$(\boldsymbol{v}_1, \boldsymbol{v}_2, \boldsymbol{v}_3, \boldsymbol{\omega}_\alpha, \boldsymbol{\omega}_\beta)$	$(\boldsymbol{v}_1, \boldsymbol{v}_2, \boldsymbol{v}_3, \boldsymbol{\omega}_\alpha, \boldsymbol{\omega}_\delta)$

Table 4.13. Structural parameters[a] of translational parallel mechanisms in Figs. 4.36–4.47

No.	Structural parameter	Solution 3-$\underline{Pa}^{cs}Pa^{ss}C^*$ (Figs. 4.36, 4.37) 3-$\underline{Pa}^{cs}C^*Pa^{ss}$ (Figs. 4.38, 4.39) 3-$\underline{Pa}^{scc}Pa^{ss}R^*$ (Fig. 4.44)	3-$\underline{Pa}^{cs}R^*R^*Pa^{scc}$ (Figs. 4.40, 4.42) 3-$\underline{Pa}^{cs}R^*Pa^{ccs}R^*$ (Figs. 4.41, 4.43)	3-$\underline{Pa}^{ss}Pa^{cs}Pa^{ss}$ (Figs. 4.45, 4.47) 3-$\underline{Pa}^{cs}Pa^{ss}Pa^{ss}$ (Fig. 4.46)
1	m	20	23	26
2	p_1	9	10	12
3	p_2	9	10	12
4	p_3	9	10	12
5	p	27	30	36
6	q	8	8	11
7	k_1	0	0	0
8	k_2	3	3	3
9	k	3	3	3
10	(R_{Gi}) $(i = 1,2,3)$	See Table 4.12	See Table 4.12	See Table 4.12
11	S_{G1}	5	5	5
12	S_{G2}	5	5	5
13	S_{G3}	5	5	5
14	r_{G1}	12	12	18
15	r_{G2}	12	12	18
16	r_{G3}	12	12	18
17	M_{G1}	5	5	5
18	M_{G2}	5	5	5
19	M_{G3}	5	5	5
20	(R_F)	$(\boldsymbol{v}_1,\boldsymbol{v}_2,\boldsymbol{v}_3)$	$(\boldsymbol{v}_1,\boldsymbol{v}_2,\boldsymbol{v}_3)$	$(\boldsymbol{v}_1,\boldsymbol{v}_2,\boldsymbol{v}_3)$
21	S_F	3	3	3
22	r_l	36	36	54
23	r_F	48	48	66
24	M_F	3	3	3
25	N_F	0	0	0
26	T_F	0	0	0
27	$\sum_{j=1}^{p_1} f_j$	17	17	23
28	$\sum_{j=1}^{p_2} f_j$	17	17	23
29	$\sum_{j=1}^{p_3} f_j$	17	17	23
30	$\sum_{j=1}^{p} f_j$	51	51	69

[a]See footnote of Table 2.1 for the nomenclature of structural parameters

Table 4.14. Structural parameters[a] of translational parallel mechanisms in Figs. 4.48–4.51

No.	Structural parameter	Solution *3-<u>R</u>RR*C, 3-<u>R</u>R*RC* (Figs. 4.48, 4.49) *3-<u>R</u>R*CR, 3-<u>R</u>PC*R* (Figs. 4.50a, 4.51b)	 *3-<u>R</u>C*C* (Fig. 4.51a)	 *3-<u>R</u>PR*RR* (Fig. 4.50b)
1	m	11	8	14
2	p_1	4	3	5
3	p_2	4	3	5
4	p_3	4	3	5
5	p	12	9	15
6	q	2	2	2
7	k_1	3	3	3
8	k_2	0	0	0
9	k	3	3	3
10	(R_{Gi}) $(i = 1,2,3)$	See Table 4.12	See Table 4.12	See Table 4.12
11	S_{G1}	5	5	5
12	S_{G2}	5	5	5
13	S_{G3}	5	5	5
14	r_{G1}	0	0	0
15	r_{G2}	0	0	0
16	r_{G3}	0	0	0
17	M_{G1}	5	5	5
18	M_{G2}	5	5	5
19	M_{G3}	5	5	5
20	(R_F)	$(\boldsymbol{v}_1,\boldsymbol{v}_2,\boldsymbol{v}_3)$	$(\boldsymbol{v}_1,\boldsymbol{v}_2,\boldsymbol{v}_3)$	$(\boldsymbol{v}_1,\boldsymbol{v}_2,\boldsymbol{v}_3)$
21	S_F	3	3	3
22	r_l	0	0	0
23	r_F	12	12	12
24	M_F	3	3	3
25	N_F	0	0	0
26	T_F	0	0	0
27	$\sum_{j=1}^{p_1} f_j$	5	5	5
28	$\sum_{j=1}^{p_2} f_j$	5	5	5
29	$\sum_{j=1}^{p_3} f_j$	5	5	5
30	$\sum_{j=1}^{p} f_j$	15	15	15

[a]See footnote of Table 2.1 for the nomenclature of structural parameters

Table 4.15. Structural parameters[a] of translational parallel mechanisms in Figs. 4.52–4.64

No.	Structural parameter	Solution		
		$3\text{-}\underline{Pa}^{cs}R^{*}RC$ (Fig. 4.52) $3\text{-}\underline{Pa}^{cs}R^{*}CR$ (Fig. 4.53) $3\text{-}\underline{R}RPa^{ss}P$ (Fig. 4.61) $3\text{-}\underline{R}PRPa^{ss}$ (Fig. 4.62) $3\text{-}\underline{R}Pa^{ss}RR^{*}$ (Fig. 4.64a) $3\text{-}\underline{R}Pa^{ss}R^{*}R$ (Fig. 4.64b)	$3\text{-}\underline{Pa}^{ss}Pa^{ss}R$ (Figs. 4.54–4.56) $3\text{-}\underline{Pa}^{ss}RPa^{ss}$ (Figs. 4.57–4.60)	$3\text{-}\underline{R}CPa^{ss}$ (Fig. 4.63)
1	m	17	20	14
2	p_1	7	9	6
3	p_2	7	9	6
4	p_3	7	9	6
5	p	21	27	18
6	q	5	8	5
7	k_1	0	0	0
8	k_2	3	3	3
9	k	3	3	3
10	(R_{Gi}) $(i = 1,2,3)$	See Table 4.12	See Table 4.12	See Table 4.12
11	S_{G1}	5	5	5
12	S_{G2}	5	5	5
13	S_{G3}	5	5	5
14	r_{G1}	6	12	6
15	r_{G2}	6	12	6
16	r_{G3}	6	12	6
17	M_{G1}	5	5	5
18	M_{G2}	5	5	5
19	M_{G3}	5	5	5
20	(R_F)	$(\boldsymbol{v}_1,\boldsymbol{v}_2,\boldsymbol{v}_3)$	$(\boldsymbol{v}_1,\boldsymbol{v}_2,\boldsymbol{v}_3)$	$(\boldsymbol{v}_1,\boldsymbol{v}_2,\boldsymbol{v}_3)$
21	S_F	3	3	3
22	r_l	18	26	18
23	r_F	30	48	30
24	M_F	3	3	3
25	N_F	0	0	0
26	T_F	0	0	0
27	$\sum_{j=1}^{p_1} f_j$	11	17	11
28	$\sum_{j=1}^{p_2} f_j$	11	17	11
29	$\sum_{j=1}^{p_3} f_j$	11	17	
30	$\sum_{j=1}^{p} f_j$	33	51	

[a]See footnote of Table 2.1 for the nomenclature of structural parameters

Table 4.16. Structural parameters[a] of translational parallel mechanisms in Figs. 4.65–4.69

No.	Structural parameter	Solution *3-RPa^4s* (Fig. 4.65)	*3-RPa^ss Pa^ss* (Figs. 4.66–4.68)	*3-RPa^* Pa^ss R* (Fig. 4.69)
1	m	11	20	23
2	p_1	5	9	10
3	p_2	5	9	10
4	p_3	5	9	10
5	p	15	27	30
6	q	5	8	8
7	k_1	0	0	0
8	k_2	3	3	3
9	k	3	3	3
10	(R_{Gi}) $(i = 1,2,3)$	See Table 4.12	See Table 4.12	See Table 4.12
11	S_{G1}	5	5	5
12	S_{G2}	5	5	5
13	S_{G3}	5	5	5
14	r_{G1}	6	12	12
15	r_{G2}	6	12	12
16	r_{G3}	6	12	12
17	M_{G1}	7	5	5
18	M_{G2}	7	5	5
19	M_{G3}	7	5	5
20	(R_F)	$(\boldsymbol{v}_1,\boldsymbol{v}_2,\boldsymbol{v}_3)$	$(\boldsymbol{v}_1,\boldsymbol{v}_2,\boldsymbol{v}_3)$	$(\boldsymbol{v}_1,\boldsymbol{v}_2,\boldsymbol{v}_3)$
21	S_F	3	3	3
22	r_l	18	36	36
23	r_F	30	48	48
24	M_F	9	3	3
25	N_F	0	0	0
26	T_F	6	0	0
27	$\sum_{j=1}^{p_1} f_j$	13	17	17
28	$\sum_{j=1}^{p_2} f_j$	13	17	17
29	$\sum_{j=1}^{p_3} f_j$	13	17	17
30	$\sum_{j=1}^{p} f_j$	39	51	51

[a]See footnote of Table 2.1 for the nomenclature of structural parameters

Table 4.17. Structural parameters[a] of translational parallel mechanisms in Figs. 4.70–4.73

No.	Structural parameter	Solution *3-<u>R</u>RPa^{ccs}R** (Fig. 4.70) *3-<u>R</u>R*RPa^{scc}* (Fig. 4.71) *3-<u>Pa</u>^{scc}RR*R* (Fig. 4.72)	*3-<u>Pa</u>^{ss}Pr^{ss}R** (Fig. 4.73a)	*3-<u>R</u>RPr^{ss}R** (Fig. 4.73b)
1	m	17	23	20
2	p_1	7	11	9
3	p_2	7	11	9
4	p_3	7	11	9
5	p	21	33	27
6	q	5	11	8
7	k_1	0	0	0
8	k_2	3	3	3
9	k	3	3	3
10	(R_{Gi}) $(i = 1,2,3)$	See Table 4.12	See Table 4.12	See Table 4.12
11	S_{G1}	5	5	5
12	S_{G2}	5	5	5
13	S_{G3}	5	5	5
14	r_{G1}	6	18	12
15	r_{G2}	6	18	12
16	r_{G3}	6	18	12
17	M_{G1}	5	5	5
18	M_{G2}	5	5	5
19	M_{G3}	5	5	5
20	(R_F)	$(\boldsymbol{v}_1,\boldsymbol{v}_2,\boldsymbol{v}_3)$	$(\boldsymbol{v}_1,\boldsymbol{v}_2,\boldsymbol{v}_3)$	$(\boldsymbol{v}_1,\boldsymbol{v}_2,\boldsymbol{v}_3)$
21	S_F	3	3	3
22	r_l	18	54	36
23	r_F	30	66	48
24	M_F	3	3	3
25	N_F	0	0	0
26	T_F	0	0	0
27	$\sum_{j=1}^{p_1} f_j$	11	23	17
28	$\sum_{j=1}^{p_2} f_j$	11	23	17
29	$\sum_{j=1}^{p_3} f_j$	11	23	17
30	$\sum_{j=1}^{p} f_j$	33	69	51

[a]See footnote of Table 2.1 for the nomenclature of structural parameters

Table 4.18. Structural parameters[a] of translational parallel mechanisms in Figs. 4.74–4.82

No.	Structural parameter	Solution *3-<u>Pa</u>^cs^RRRR* (Figs. 4.74, 4.76a) *3-<u>R</u>Pa^cs^RRR* (Figs. 4.77a, 4.78) *3-<u>R</u>RRRPa^cs^* (Figs. 4.80b, 4.81b) *3-<u>R</u>RRPa^cs^R* (Fig. 4.82a)	 *3-<u>Pa</u>^ss^RRR* (Fig. 4.75) *3-<u>R</u>Pa^ss^RR* (Figs. 4.76b, 4.77b) *3-<u>R</u>RPa^ss^R* (Fig. 4.79) *3-<u>R</u>RRPa^ss^* (Figs. 4.80a, 4.81a, 4.82b)
1	M	20	17
2	p_1	8	7
3	p_2	8	7
4	p_3	8	7
5	P	24	21
6	Q	5	5
7	k_1	0	0
8	k_2	3	3
9	K	3	3
10	(R_{Gi}) $(i = 1,2,3)$	See Table 4.12	See Table 4.12
11	S_{G1}	5	5
12	S_{G2}	5	5
13	S_{G3}	5	5
14	r_{G1}	6	6
15	r_{G2}	6	6
16	r_{G3}	6	6
17	M_{G1}	5	5
18	M_{G2}	5	5
19	M_{G3}	5	5
20	(R_F)	$(\boldsymbol{v}_1,\boldsymbol{v}_2,\boldsymbol{v}_3)$	$(\boldsymbol{v}_1,\boldsymbol{v}_2,\boldsymbol{v}_3)$
21	S_F	3	3
22	r_l	18	18
23	r_F	30	30
24	M_F	3	3
25	N_F	0	0
26	T_F	0	0
27	$\sum_{j=1}^{p_1} f_j$	11	11
28	$\sum_{j=1}^{p_2} f_j$	11	11
29	$\sum_{j=1}^{p_3} f_j$	11	11
30	$\sum_{j=1}^{p} f_j$	33	33

[a]See footnote of Table 2.1 for the nomenclature of structural parameters

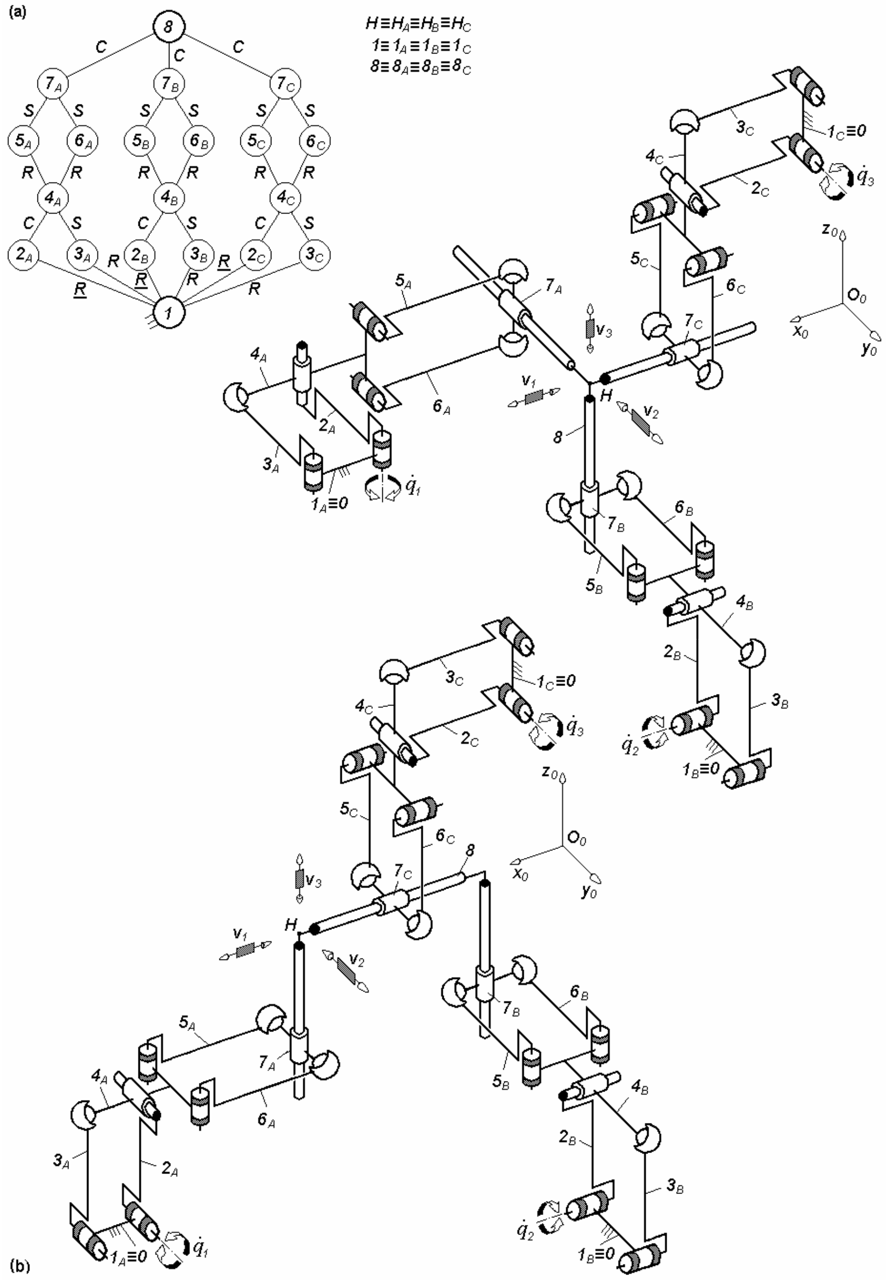

Fig. 4.36. *3-$\underline{Pa}^{cs}Pa^{ss}C^*$*-type non overconstrained TPMs with coupled motions and rotating actuators mounted on the fixed base, limb topology $\underline{Pa}^{cs} \perp Pa^{ss} || C^*$

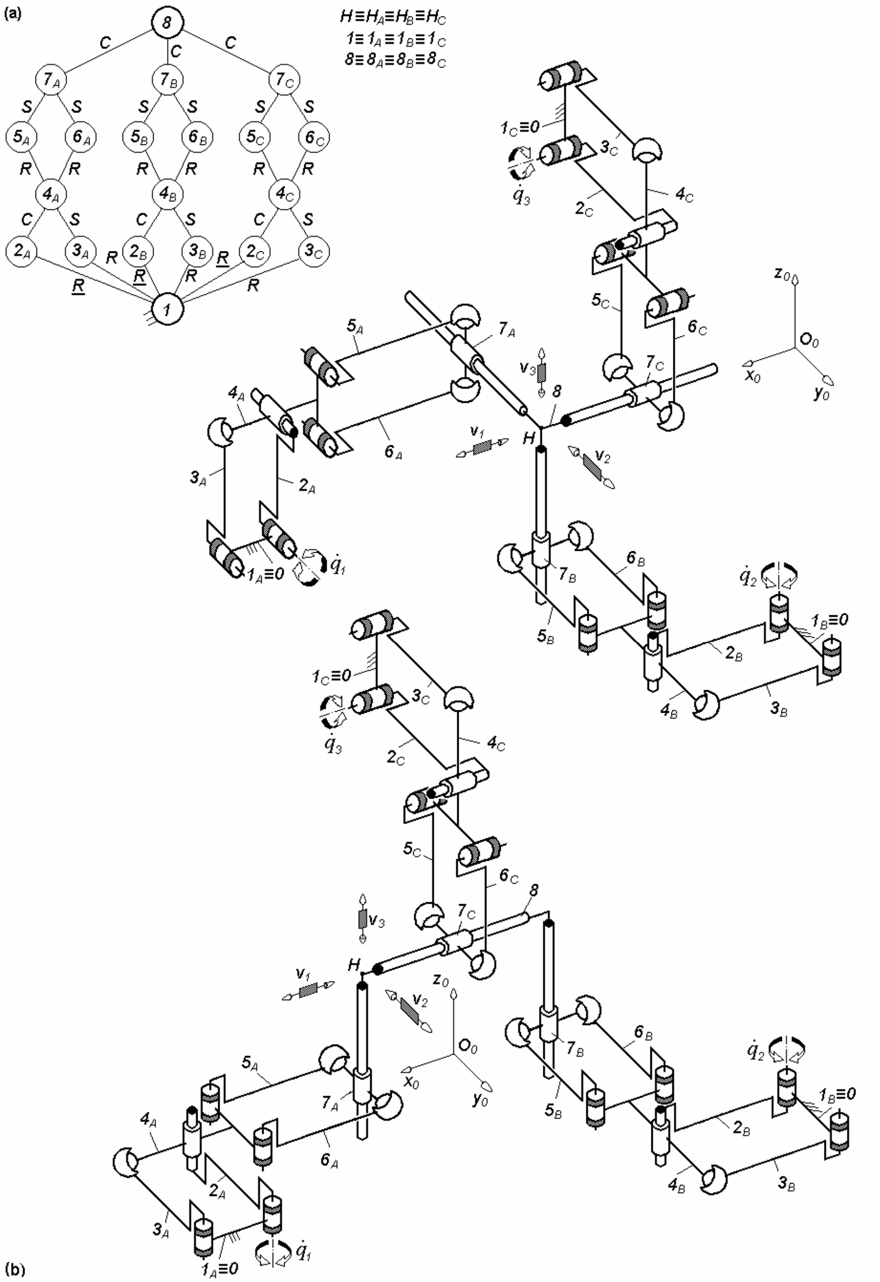

Fig. 4.37. *3-$\underline{Pa}^{cs}Pa^{ss}C$**-type non overconstrained TPMs with coupled motions and rotating actuators mounted on the fixed base, limb topology $\underline{Pa}^{cs}||Pa^{ss}||C$*

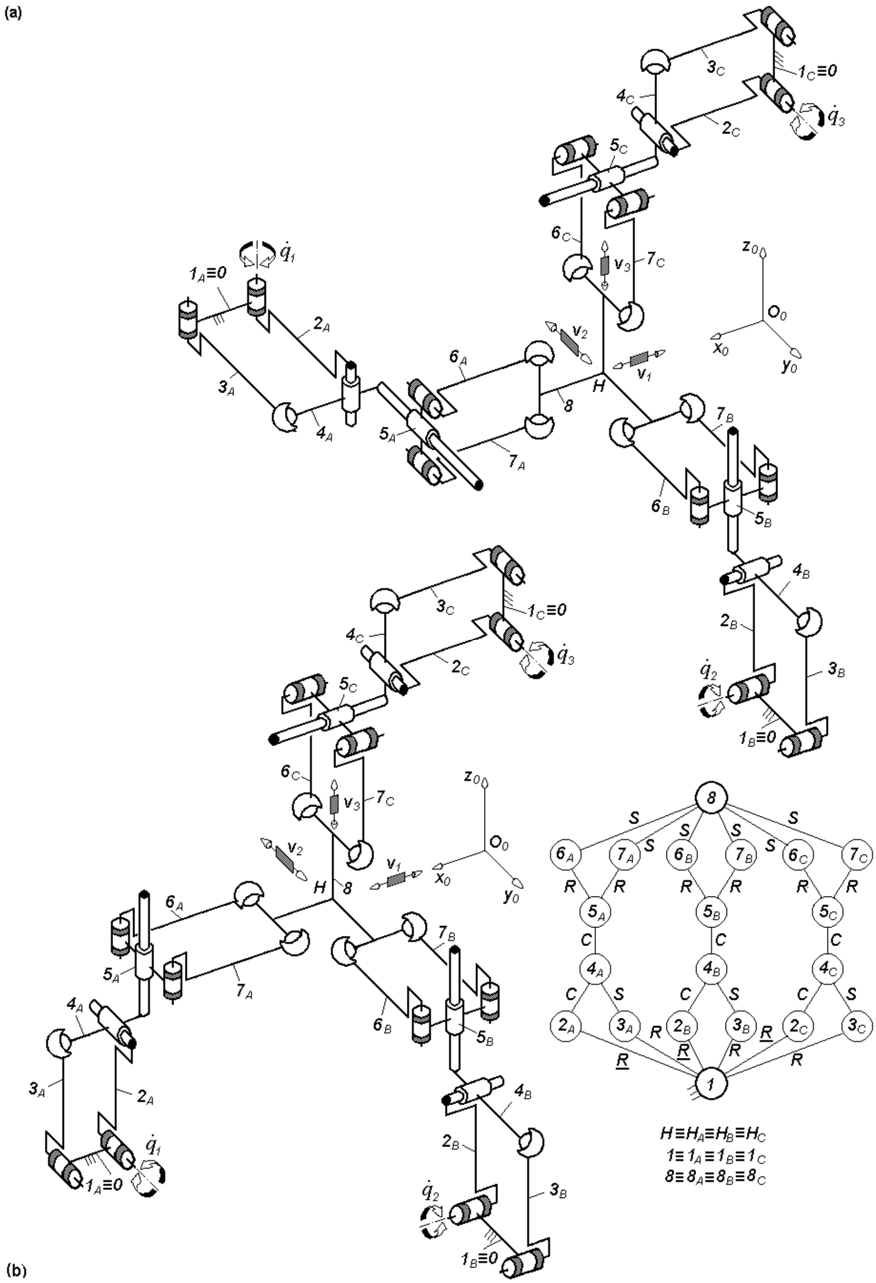

Fig. 4.38. *3-$\underline{Pa}^{cs}C^*Pa^{ss}$*-type non overconstrained TPMs with coupled motions and rotating actuators mounted on the fixed base, limb topology $\underline{Pa}^{cs} \perp C^*||Pa^{ss}$

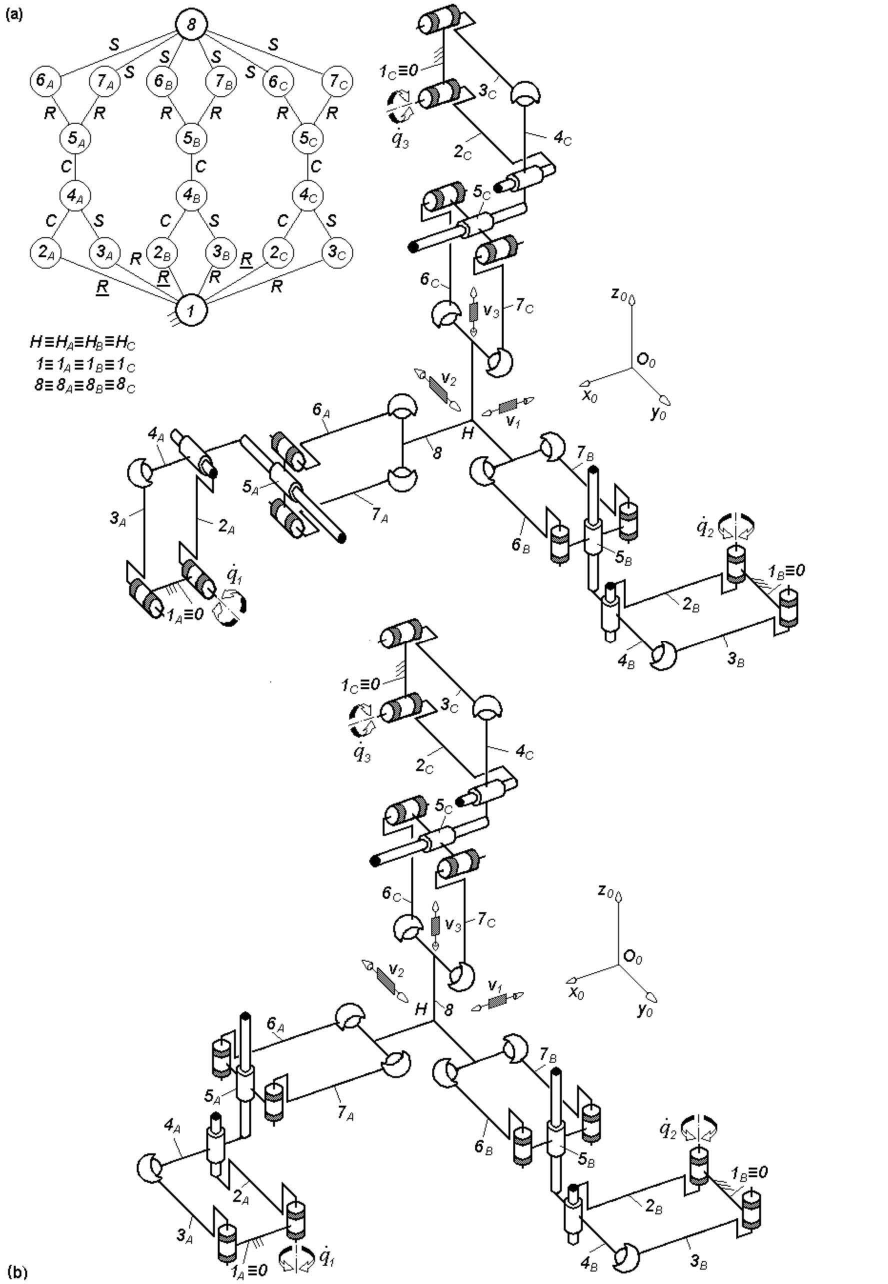

Fig. 4.39. *3-$\underline{Pa}^{cs}$C*Pa^{ss}*-type non overconstrained TPMs with coupled motions and rotating actuators mounted on the fixed base, limb topology $\underline{Pa}^{cs}||C^*||Pa^{ss}$

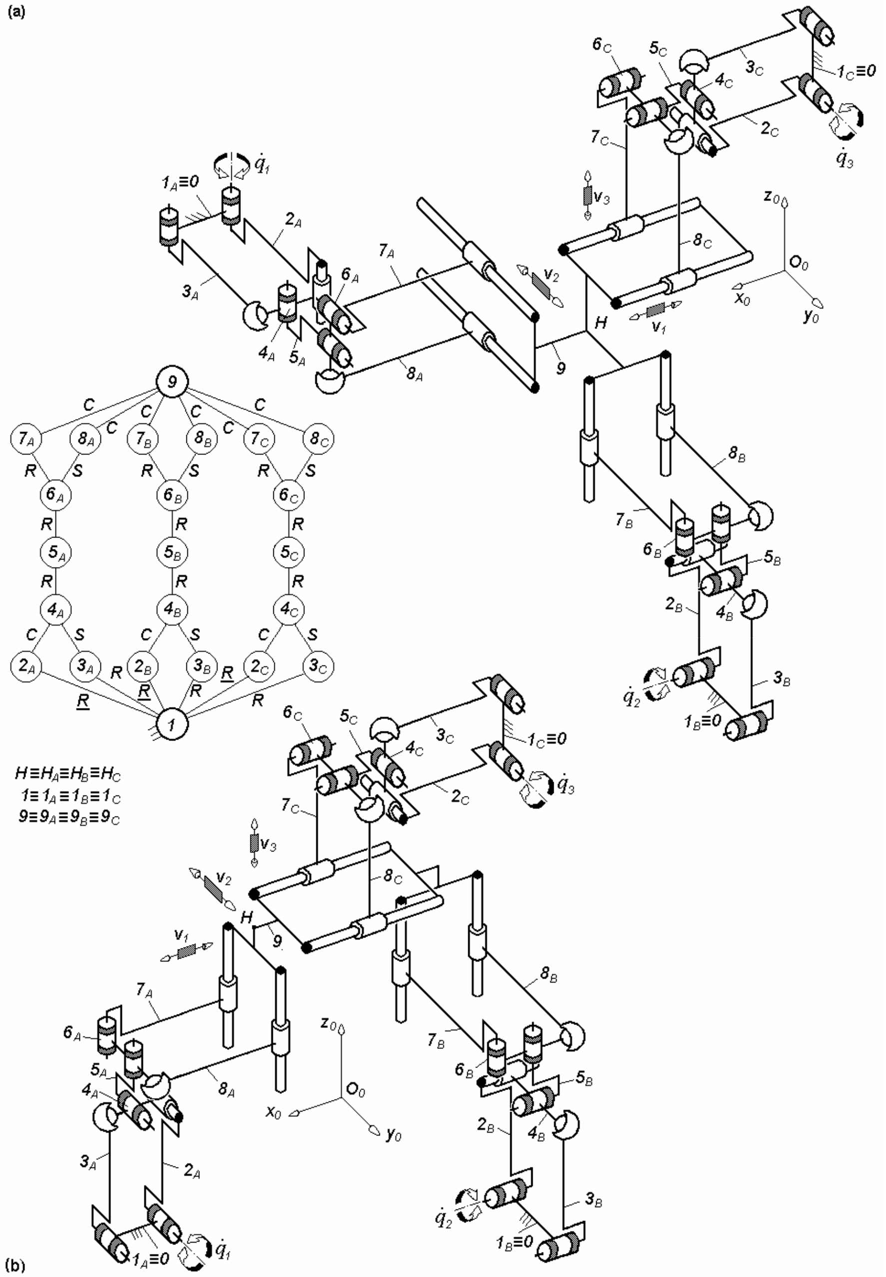

Fig. 4.40. $3\text{-}\underline{Pa}^{cs}R^*R^*Pa^{scc}$-type non overconstrained TPMs with coupled motions and rotating actuators mounted on the fixed base, limb topology $\underline{Pa}^{cs}||R^*\perp R^*||Pa^{scc}$

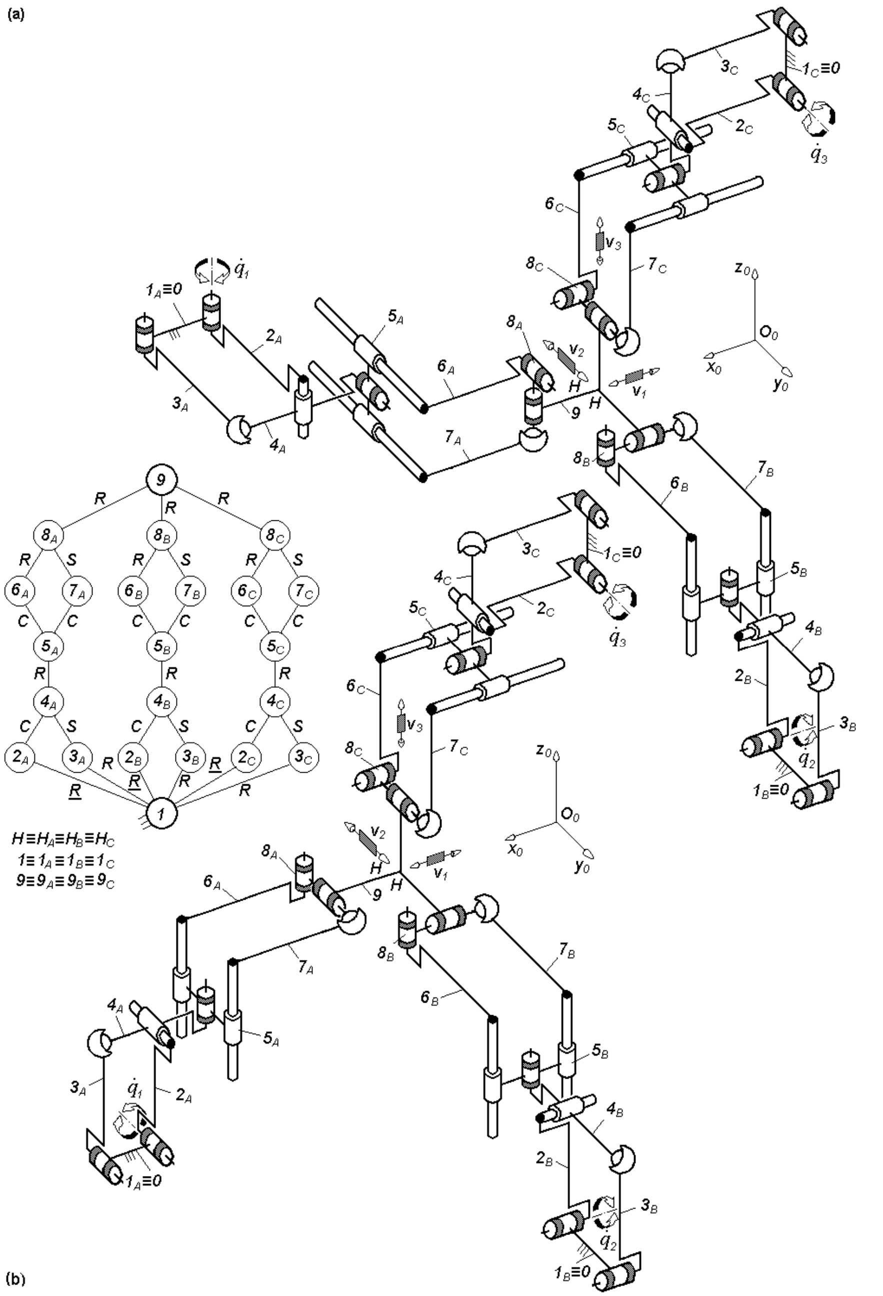

Fig. 4.41. 3-$\underline{Pa}^{cs}R^*Pa^{ccs}R^*$-type non overconstrained TPMs with coupled motions and rotating actuators mounted on the fixed base, limb topology $\underline{Pa}^{cs}\perp R^*||Pa^{ccs}\perp^{||}R^*$

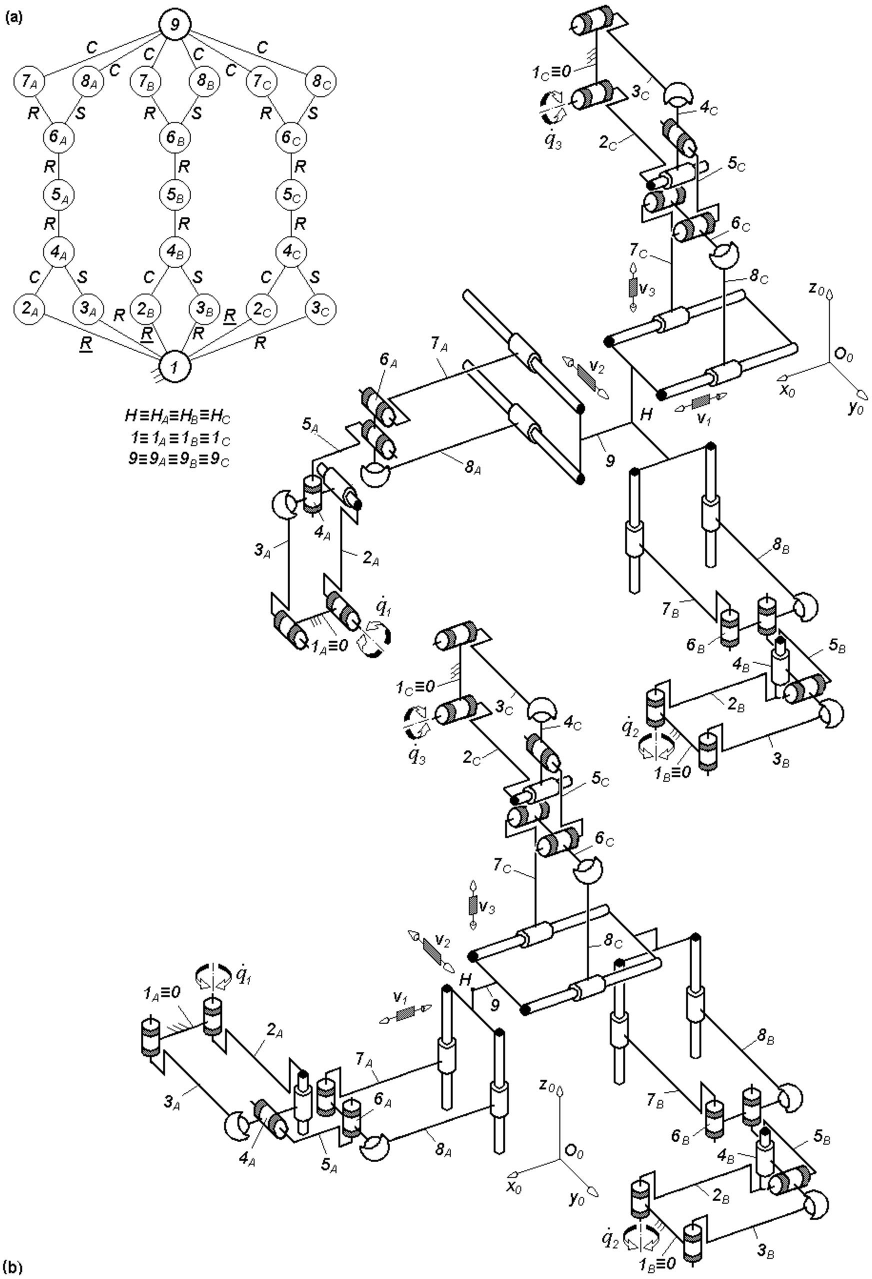

Fig. 4.42. *3-$\underline{Pa}^{cs}R^*R^*Pa^{scc}$*-type non overconstrained TPMs with coupled motions and rotating actuators mounted on the fixed base, limb topology $\underline{Pa}^{cs}\perp R^*\perp^{||}R^*||Pa^{scc}$

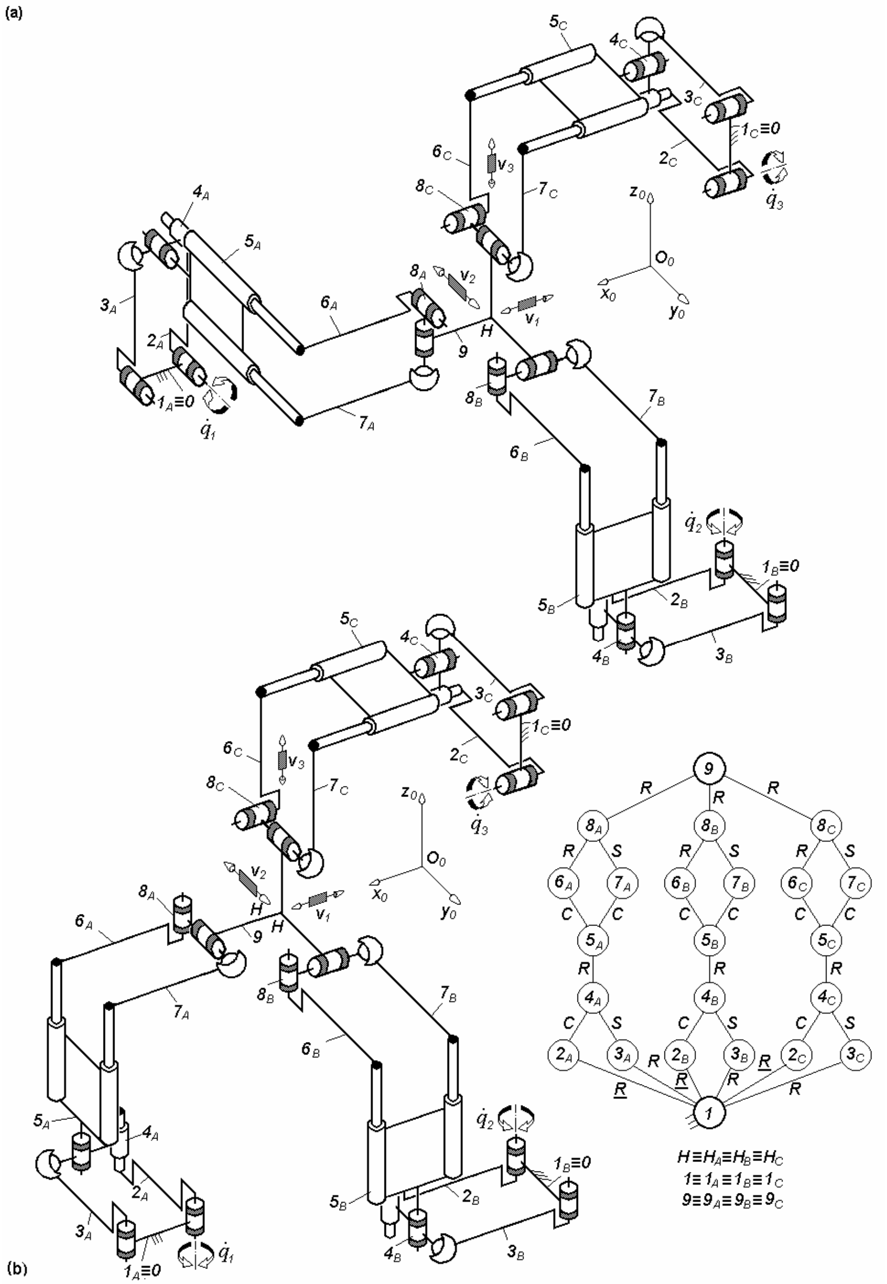

Fig. 4.43. $3\text{-}\underline{Pa}^{cs}R^*Pa^{ccs}R^*$-type non overconstrained TPMs with coupled motions and rotating actuators mounted on the fixed base, limb topology $\underline{Pa}^{cs}||R^*||Pa^{ccs} \perp R^*$

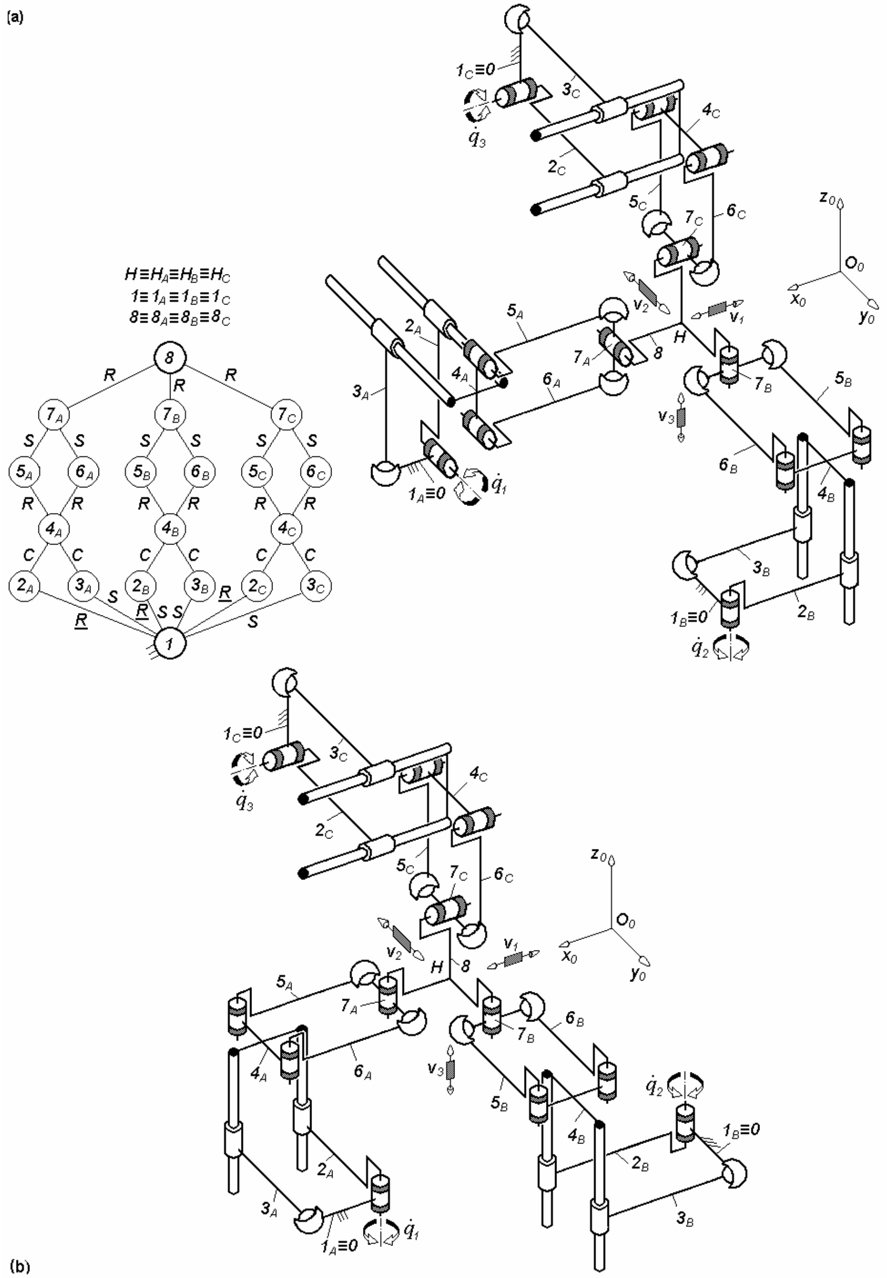

Fig. 4.44. *3-$\underline{Pa}^{scc}Pa^{ss}R$*-type* non overconstrained TPMs with coupled motions and rotating actuators mounted on the fixed base, limb topology $\underline{Pa}^{scc}||Pa^{ss}||R$*

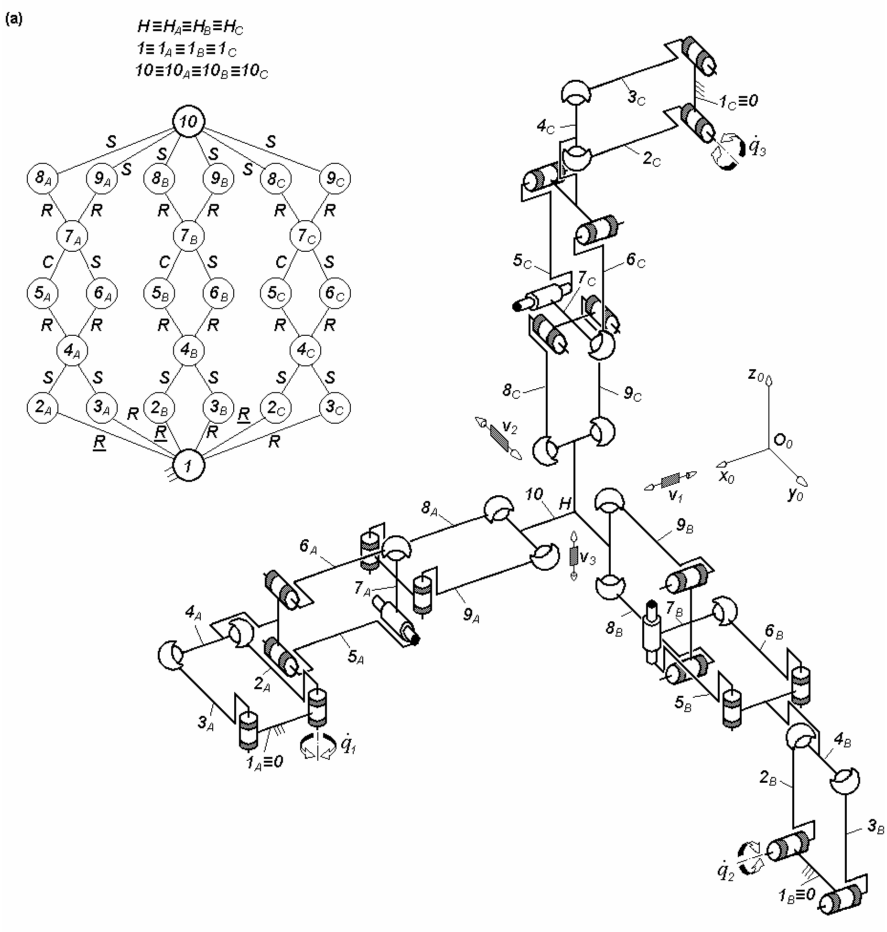

Fig. 4.45. *3-*$\underline{Pa}^{ss}Pa^{cs}Pa^{ss}$-type non overconstrained TPM with coupled motions and rotating actuators mounted on the fixed base, limb topology $\underline{Pa}^{ss} \perp Pa^{cs} \perp^{\|} Pa^{ss}$

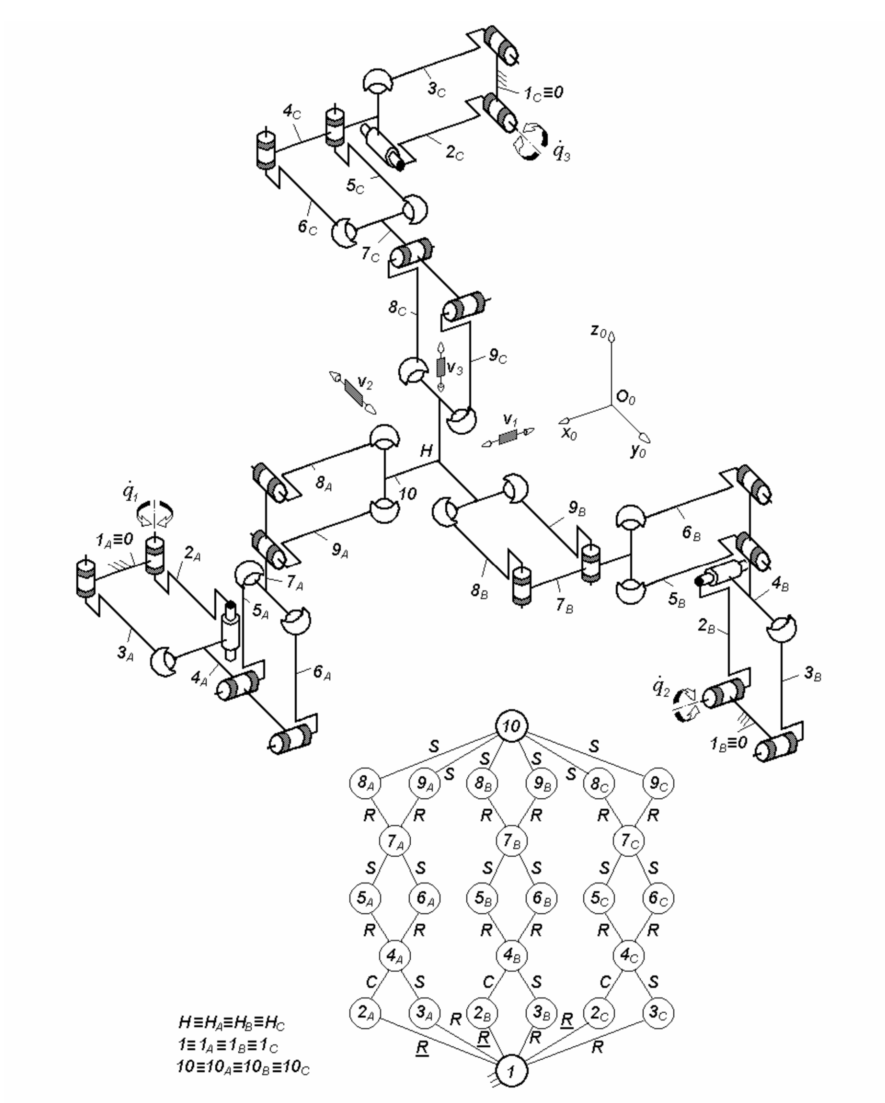

Fig. 4.46. *3-*$\underline{Pa}^{cs}Pa^{ss}Pa^{ss}$-type non overconstrained TPM with coupled motions and rotating actuators mounted on the fixed base, limb topology $\underline{Pa}^{cs} \perp Pa^{ss} \perp^{\perp} Pa^{ss}$

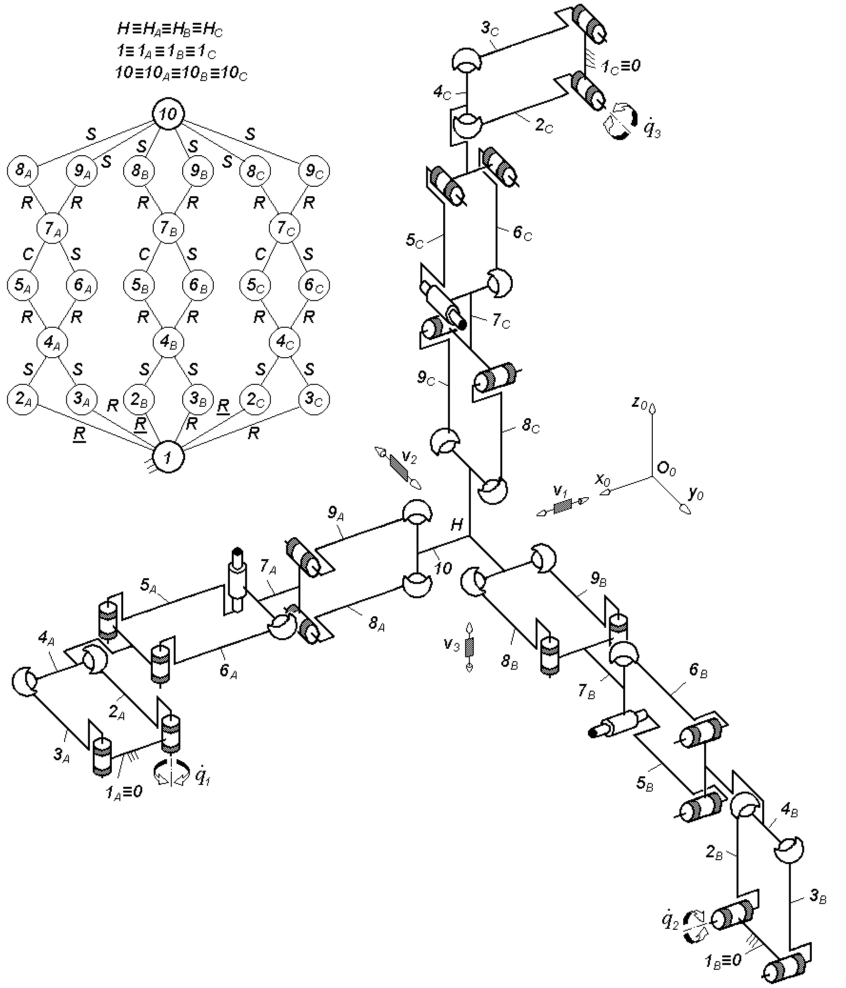

Fig. 4.47. *3-$\underline{Pa}^{ss}Pa^{cs}Pa^{ss}$*-type non overconstrained TPM with coupled motions and rotating actuators mounted on the fixed base, limb topology $\underline{Pa}^{ss}||Pa^{cs}\perp Pa^{ss}$

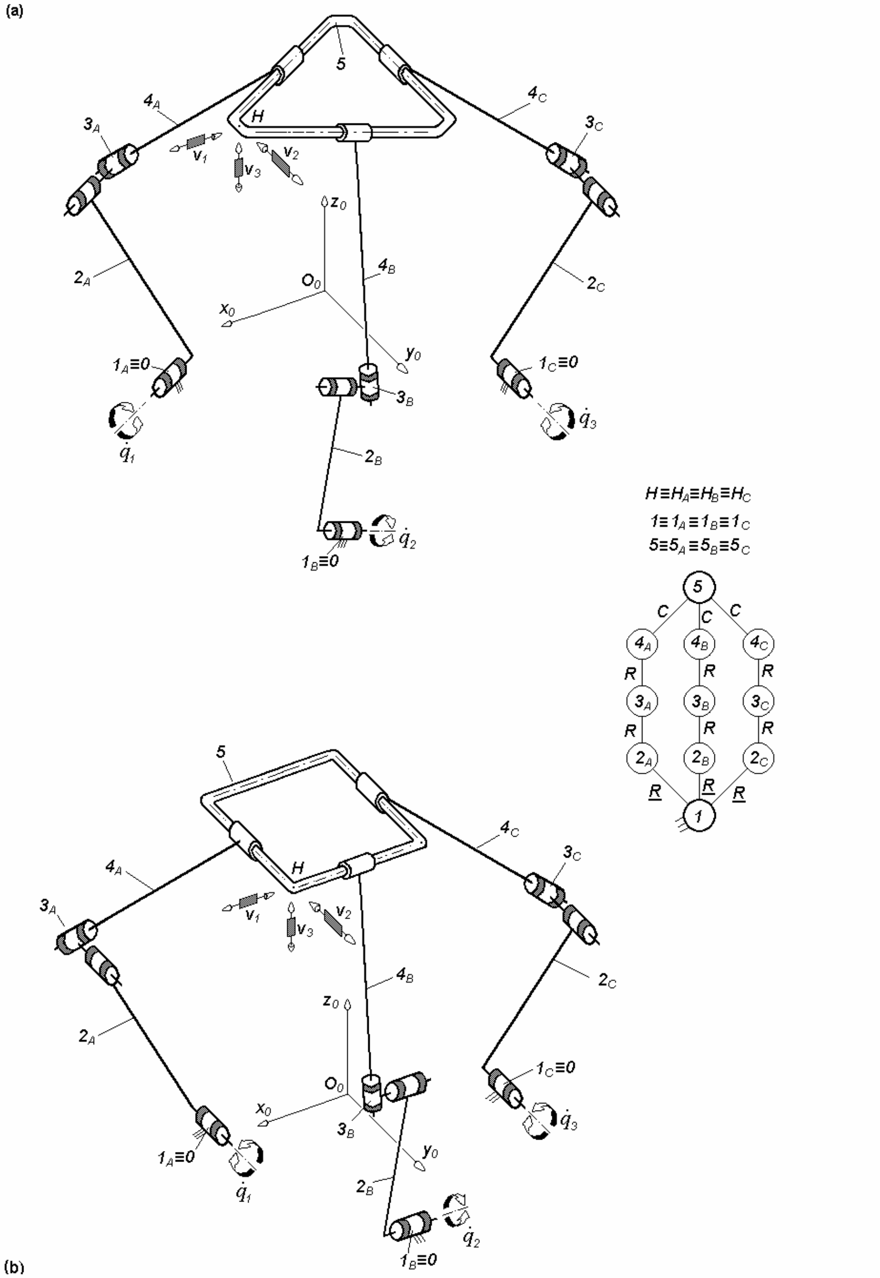

Fig. 4.48. *3-$\underline{R}$RR*C*-type non overconstrained TPMs with coupled motions and rotating actuators mounted on the fixed base, limb topology $\underline{R}||R\perp R^*\perp^{||}C$

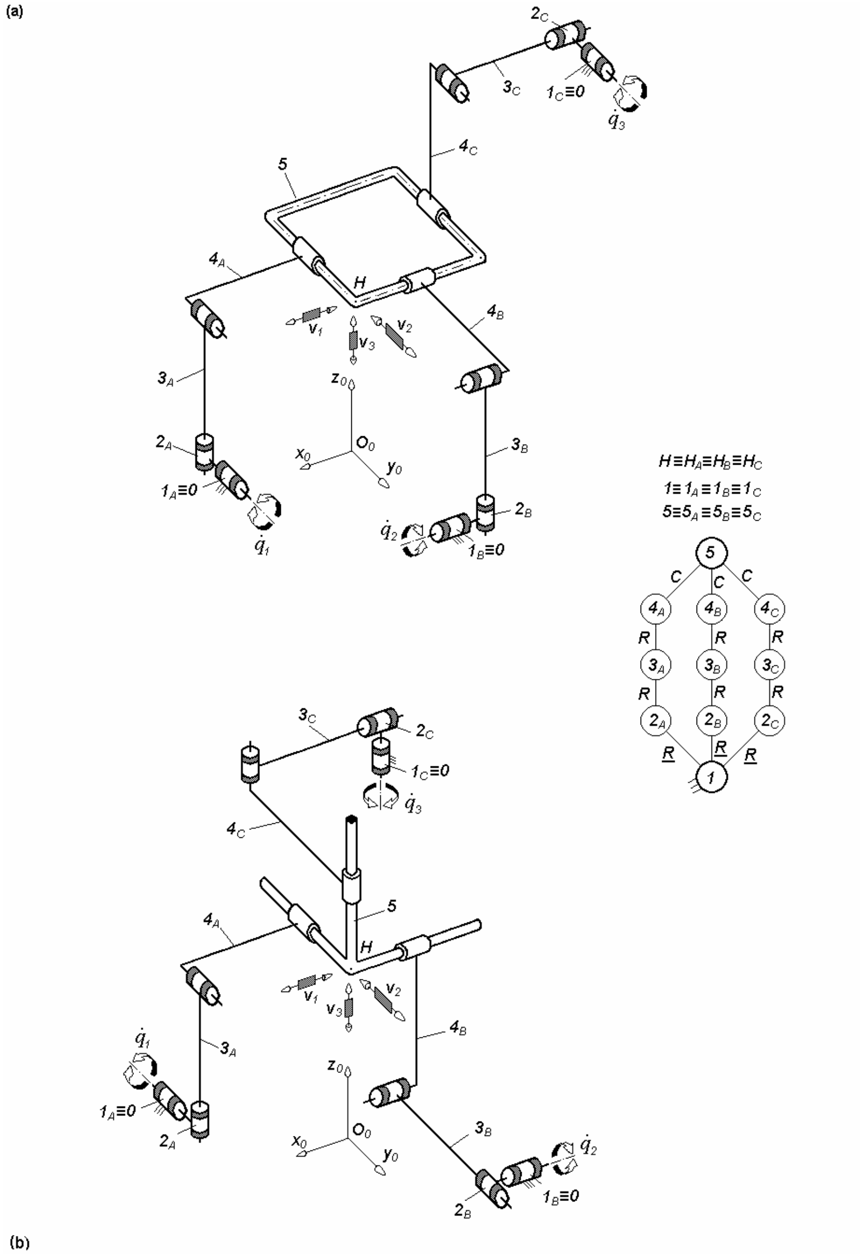

Fig. 4.49. *3-*$\underline{R}$*R*RC*-type non overconstrained TPMs with coupled motions and rotating actuators mounted on the fixed base, limb topology $\underline{R}\perp R^{*}\perp^{\parallel}R\parallel C$

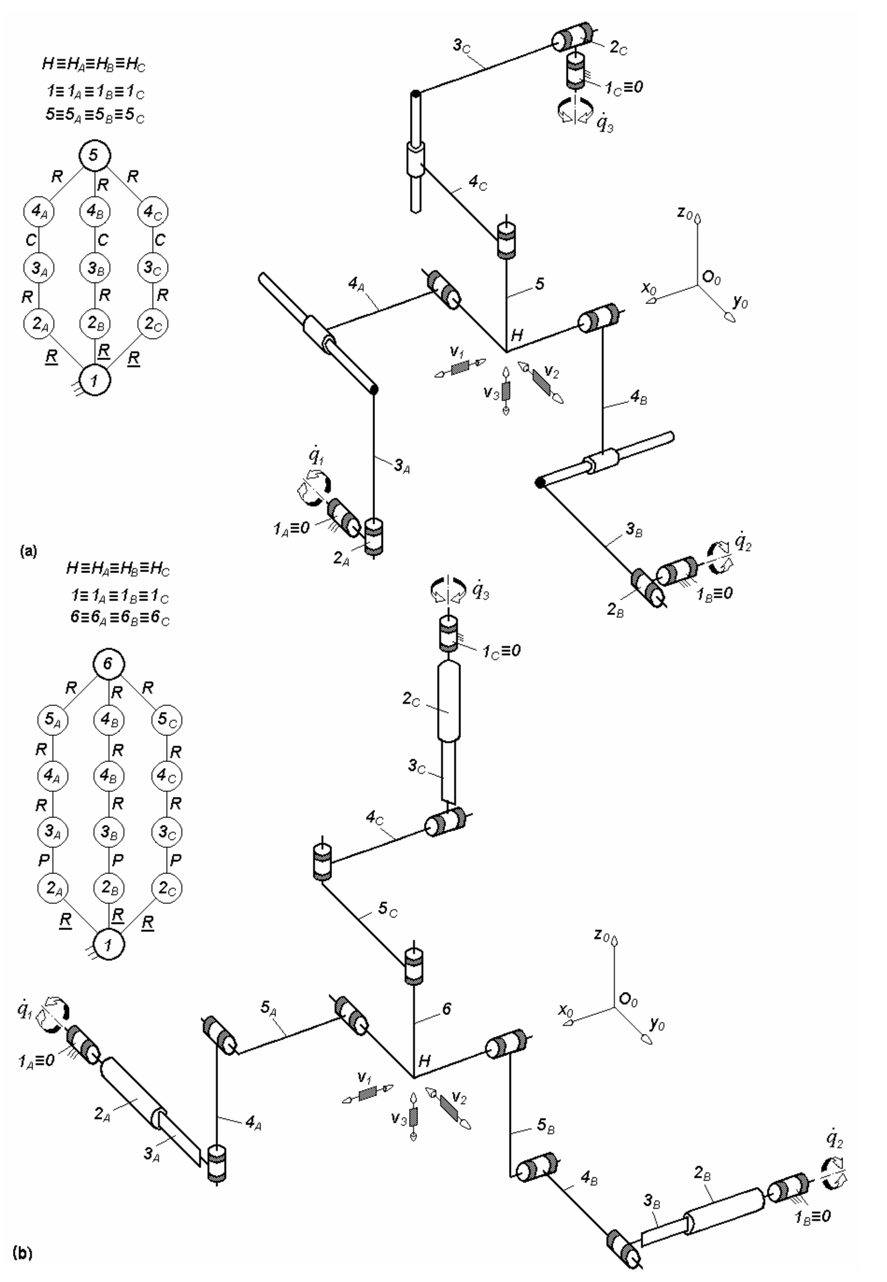

Fig. 4.50. Non overconstrained TPMs of types *3-$\underline{R}$R*CR* (**a**) and *3-$\underline{R}$PR*RR* (**b**) with coupled motions and rotating actuators mounted on the fixed base, limb toplogy $\underline{R} \perp R^* \perp {}^{\|}C\|R$ (**a**) and $\underline{R} \| P \perp R^* \perp {}^{\|}R\|R$ (**b**)

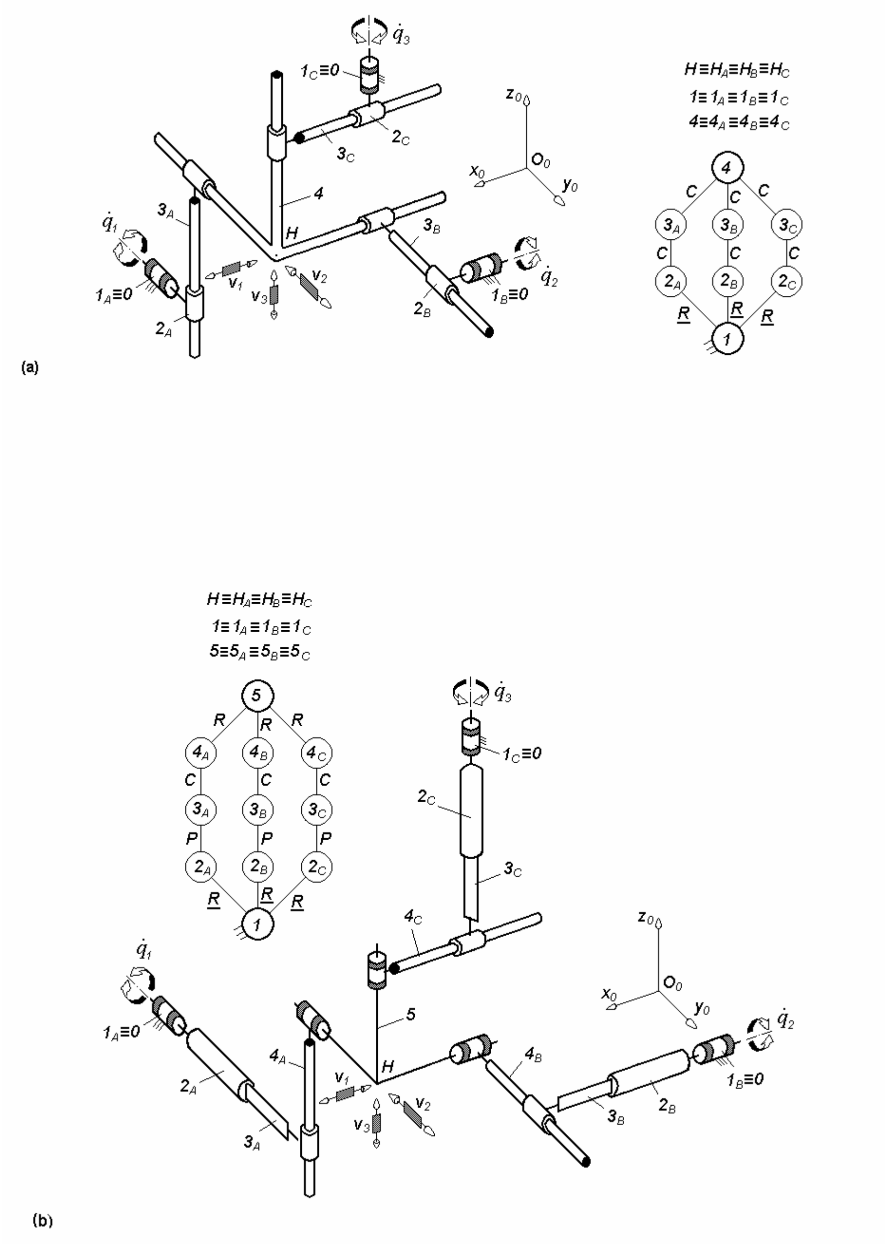

Fig. 4.51. Non overconstrained TPMs with coupled motions of types *3-$\underline{R}$C*C* (**a**) and *3-$\underline{R}$PC*R* (**b**) and rotating actuators mounted on the fixed base, limb topology $\underline{R}\perp C^{*}\perp^{\parallel}C$ (**a**) and $\underline{R}\parallel P\perp C^{*}\perp^{\parallel}R$ (**b**)

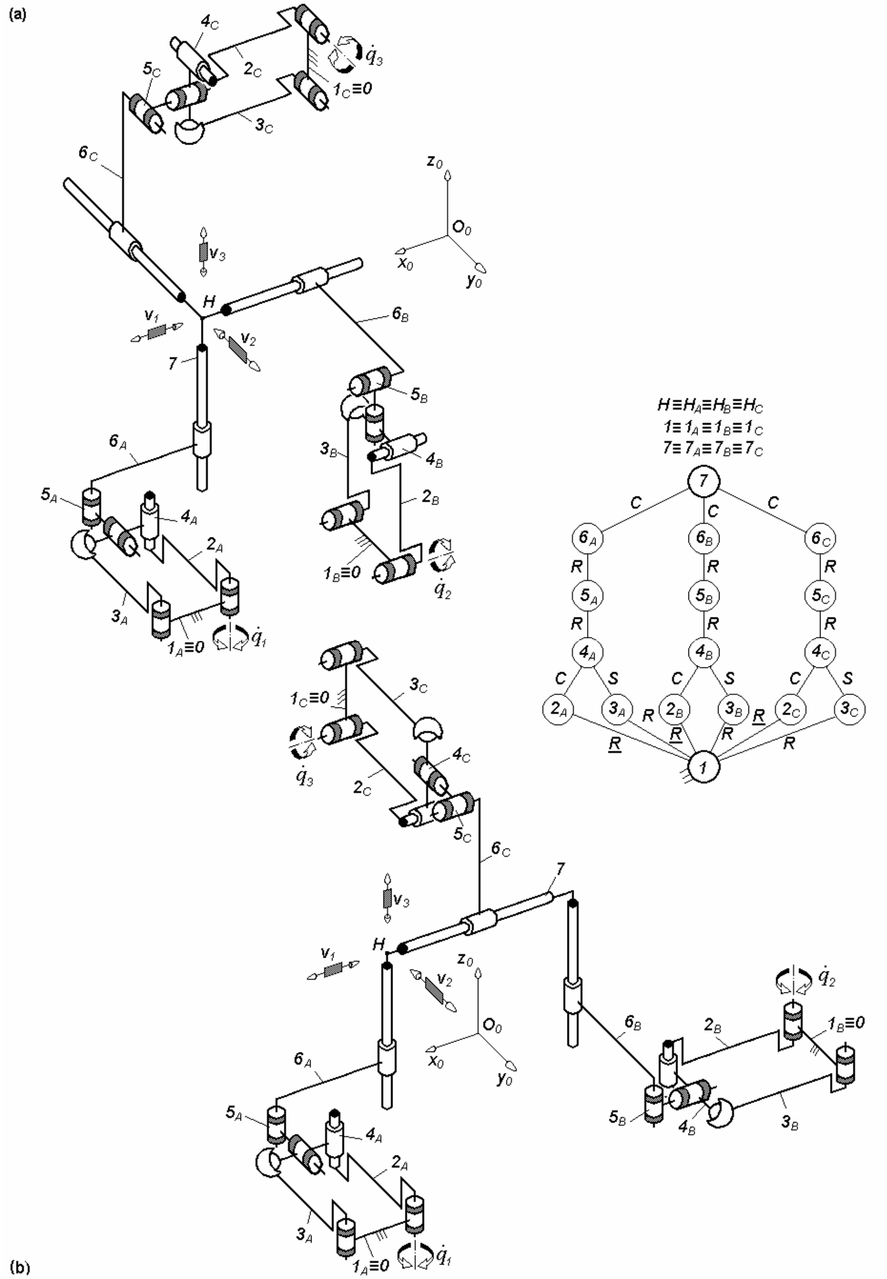

Fig. 4.52. *3-$\underline{Pa}^{cs}R{*}RC$*-type non overconstrained TPMs with coupled motions and rotating actuators mounted on the fixed base, limb topology $\underline{Pa}^{cs} \perp R{*} \perp^{||} R||C$

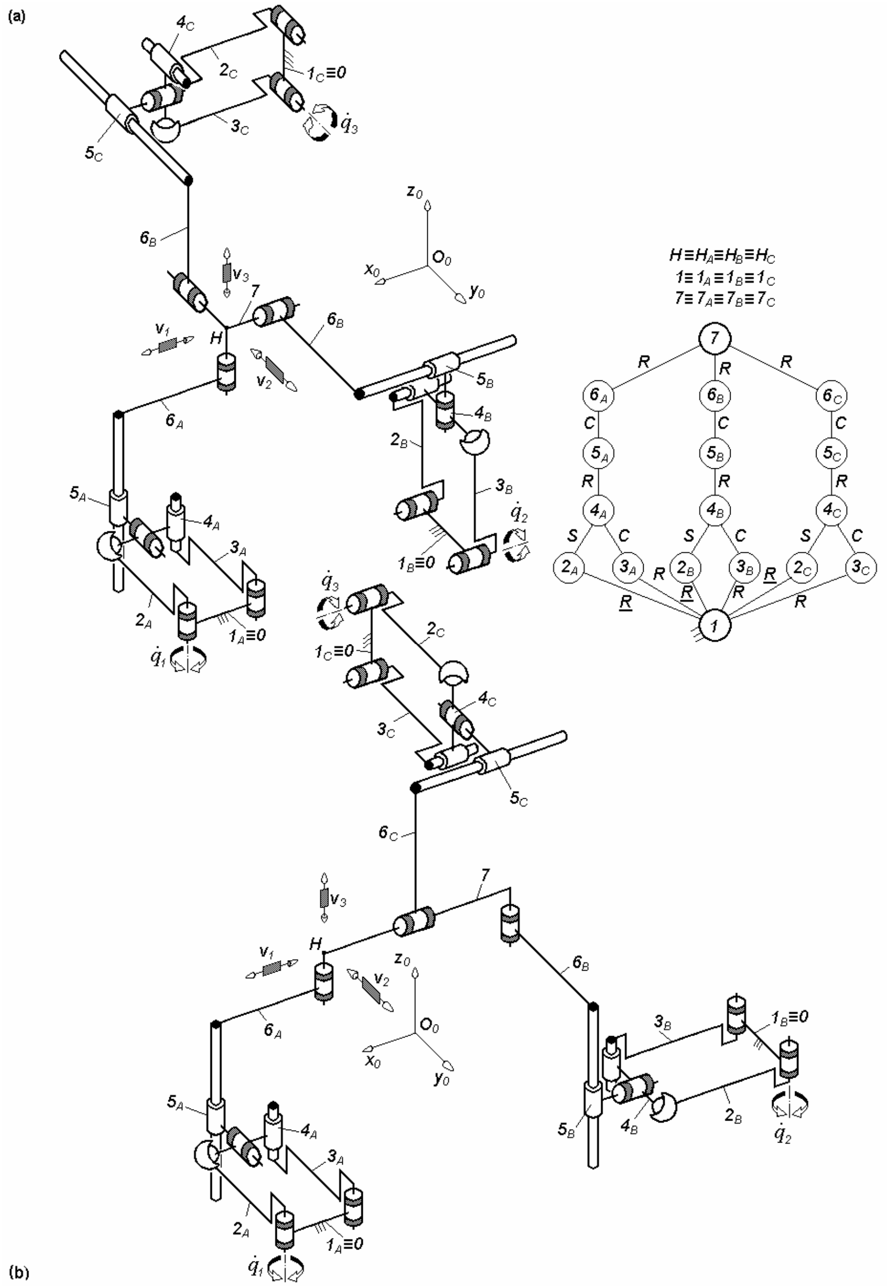

Fig. 4.53. *3-*$\underline{Pa}^{cs}$*R*CR*-type non overconstrained TPMs with coupled motions and rotating actuators mounted on the fixed base, limb topology $\underline{Pa}^{cs} \perp R^* \perp^{||} C || R$

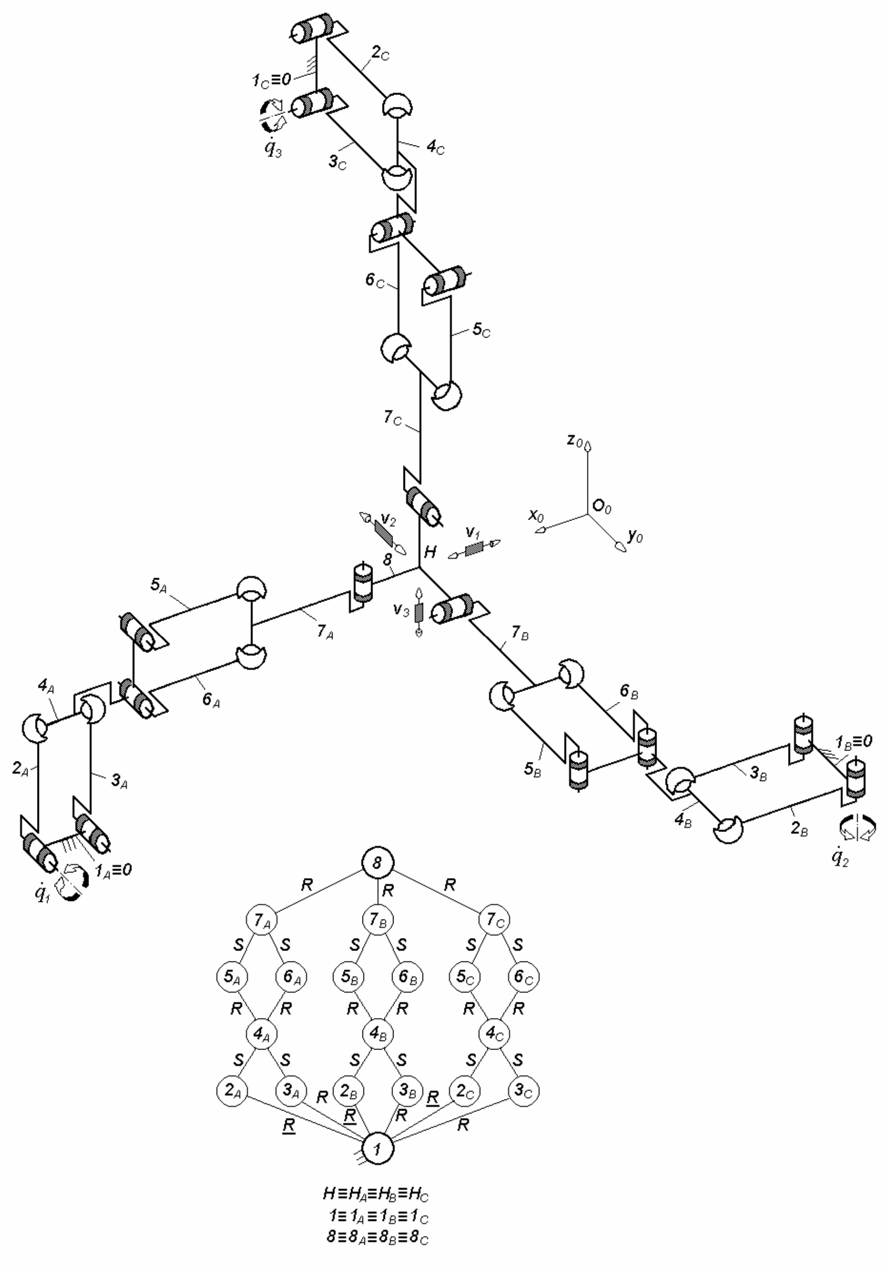

Fig. 4.54. *3-$\underline{Pa}^{ss}Pa^{ss}R$*-type non overconstrained TPM with coupled motions and rotating actuators mounted on the fixed base, limb topology $\underline{Pa}^{ss} \perp Pa^{ss} \perp^{\perp} R$

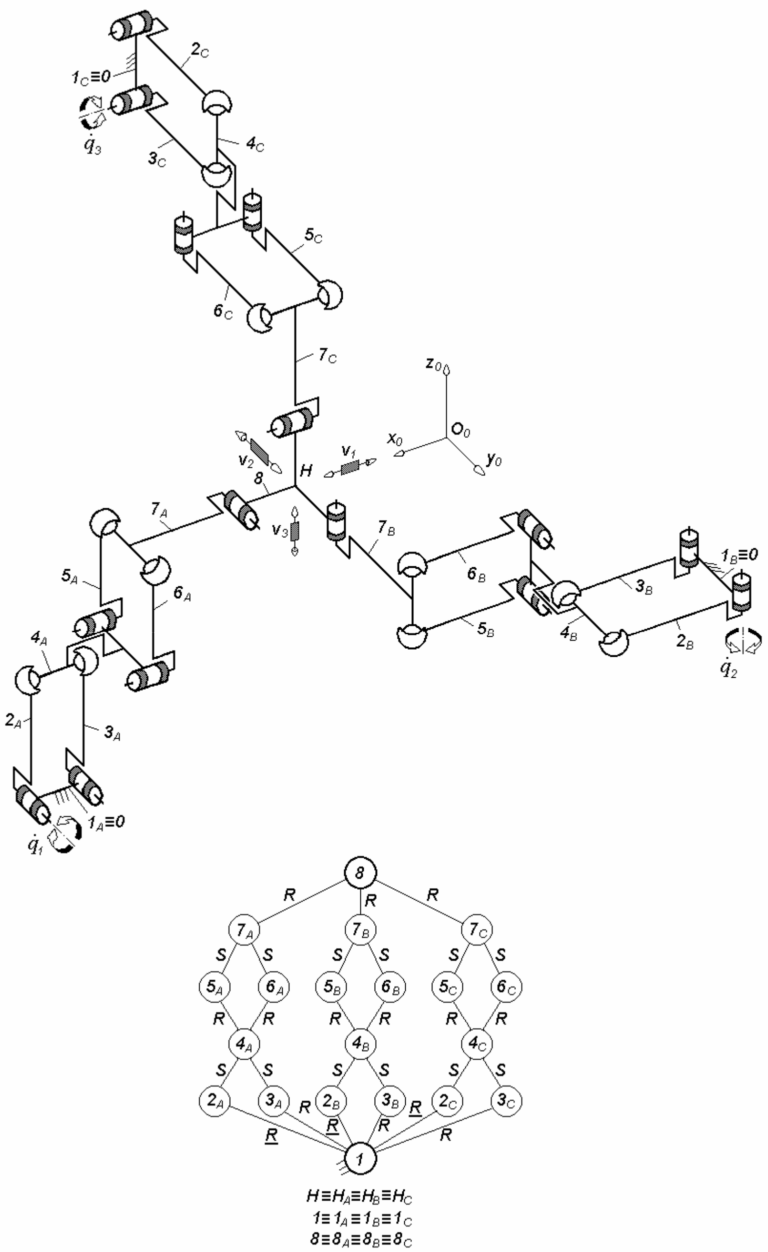

Fig. 4.55. $3\text{-}\underline{Pa}^{ss}Pa^{ss}R$-type non overconstrained TPM with coupled motions and rotating actuators mounted on the fixed base, limb topology $\underline{Pa}^{ss} \perp Pa^{ss} \perp^{\parallel} R$

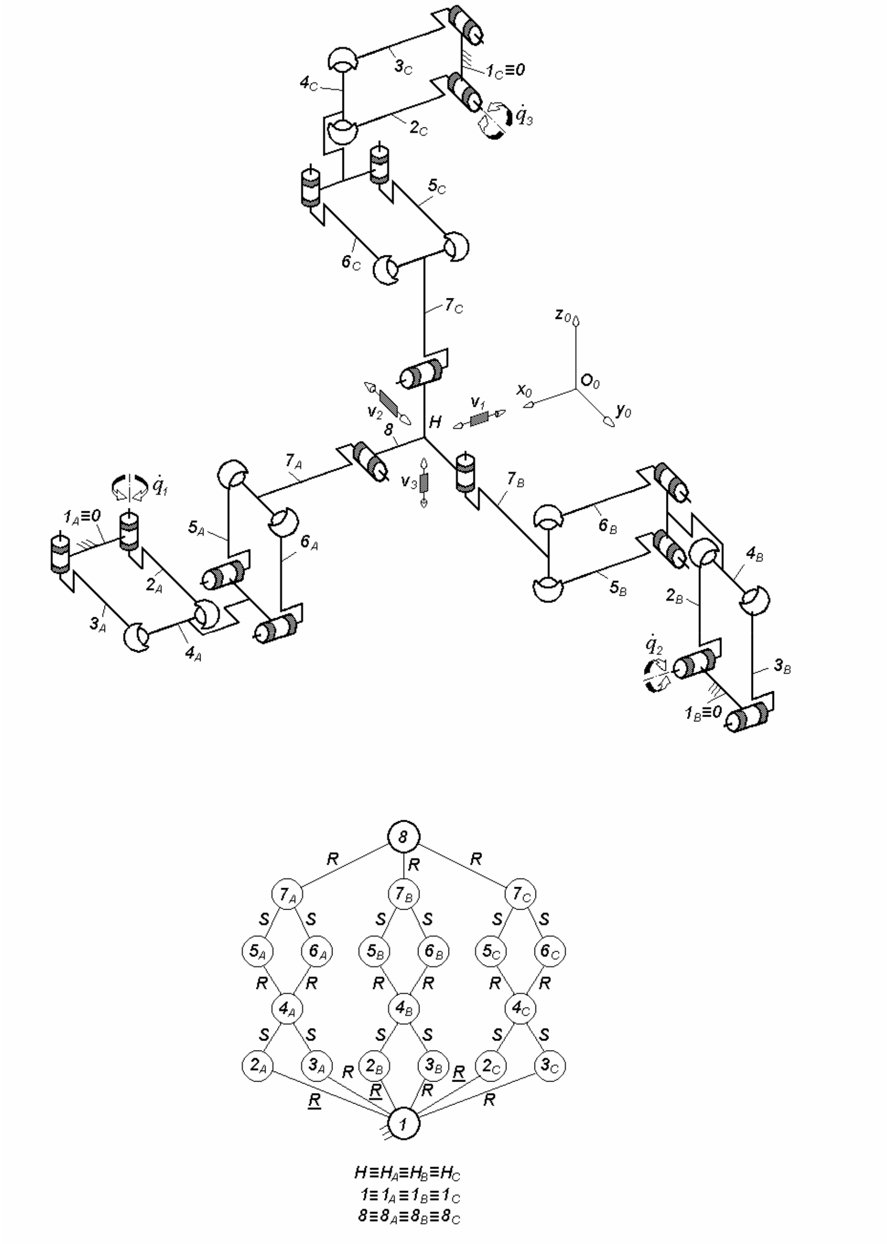

Fig. 4.56. *3-*$\underline{Pa}^{ss}Pa^{ss}R$-type non overconstrained TPM with coupled motions and rotating actuators mounted on the fixed base, limb topology $\underline{Pa}^{ss} \perp Pa^{ss} \perp^{\perp} R$

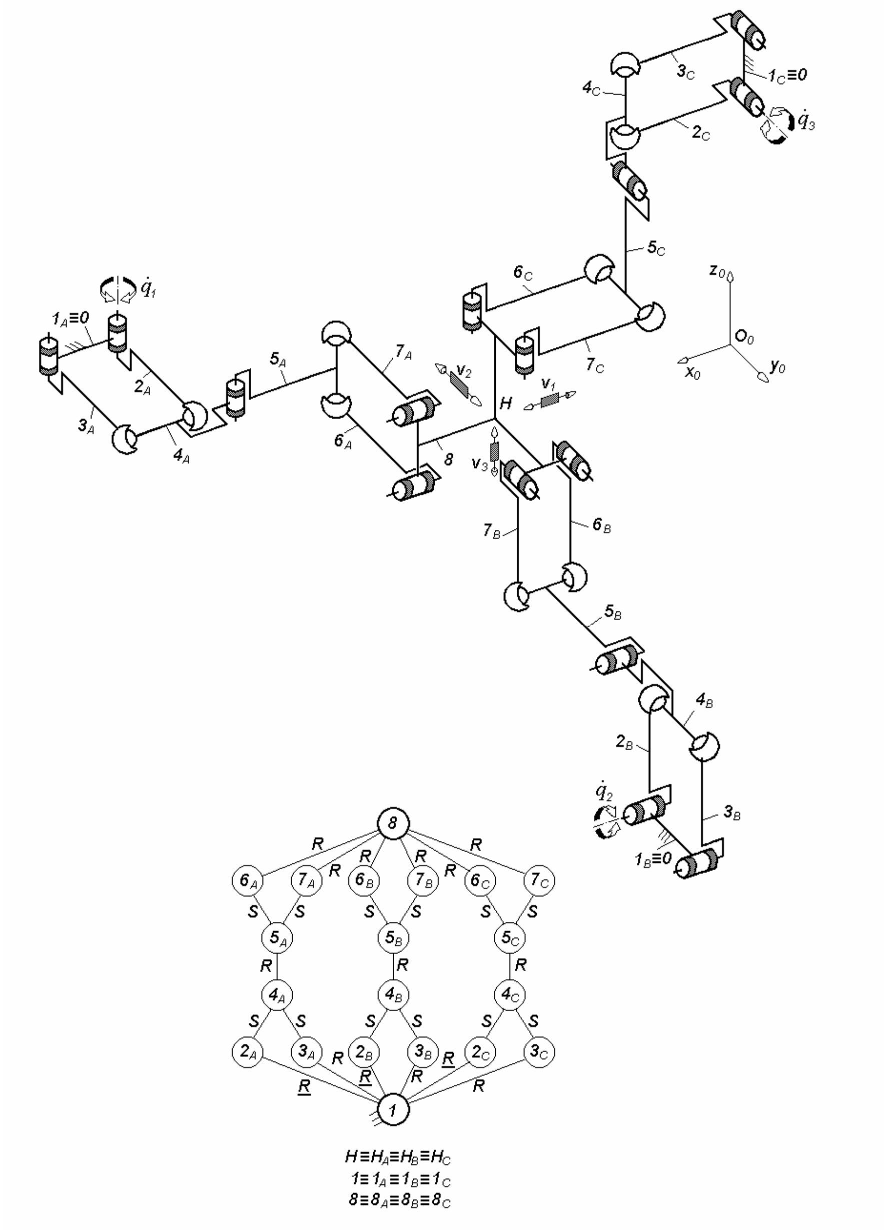

Fig. 4.57. *3-*$\underline{Pa}^{ss}RPa^{ss}$-type non overconstrained TPM with coupled motions and rotating actuators mounted on the fixed base, limb topology $\underline{Pa}^{ss} || R \perp Pa^{ss}$

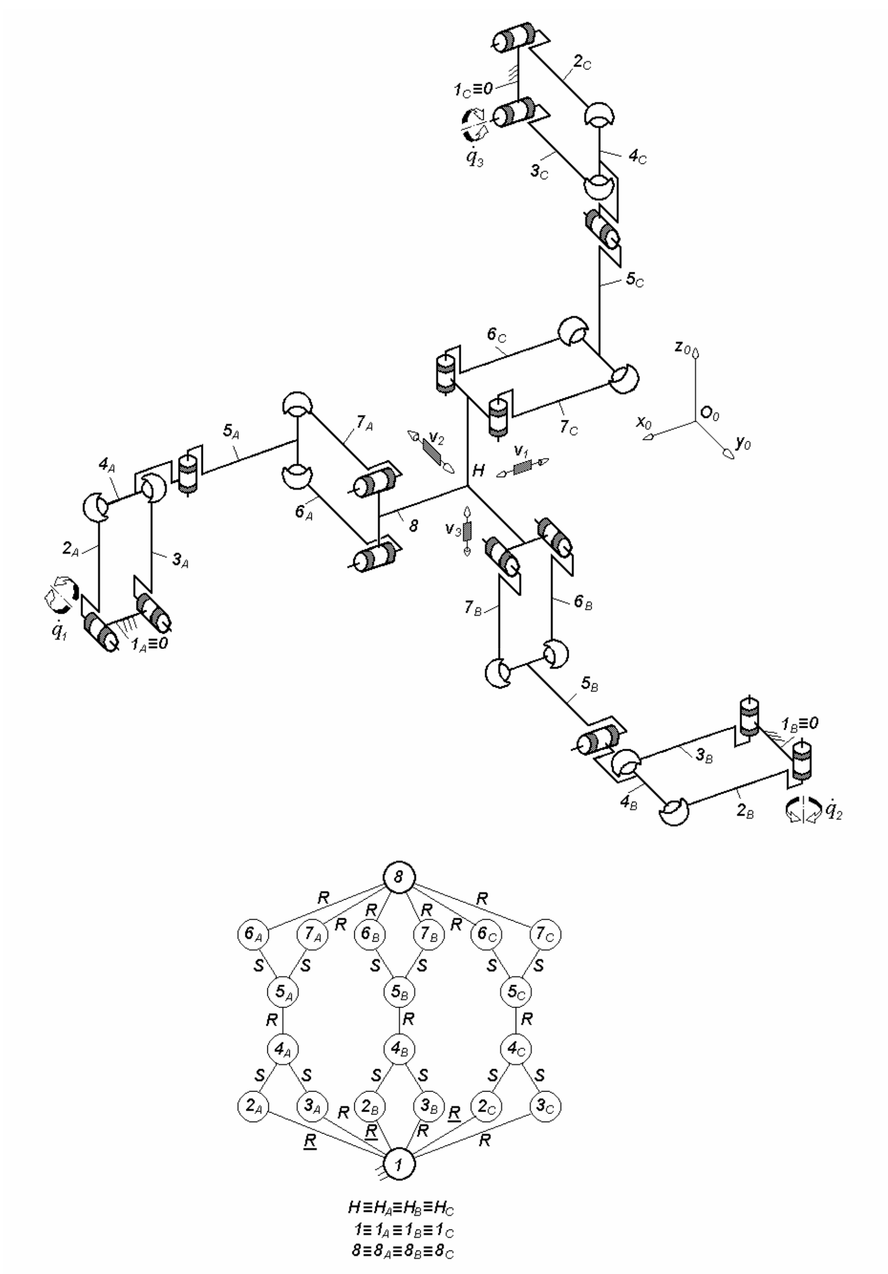

Fig. 4.58. *3-$\underline{Pa}^{ss}RPa^{ss}$*-type non overconstrained TPM with coupled motions and rotating actuators mounted on the fixed base, limb topology $\underline{Pa}^{ss} \perp R \perp^{\perp} Pa^{ss}$

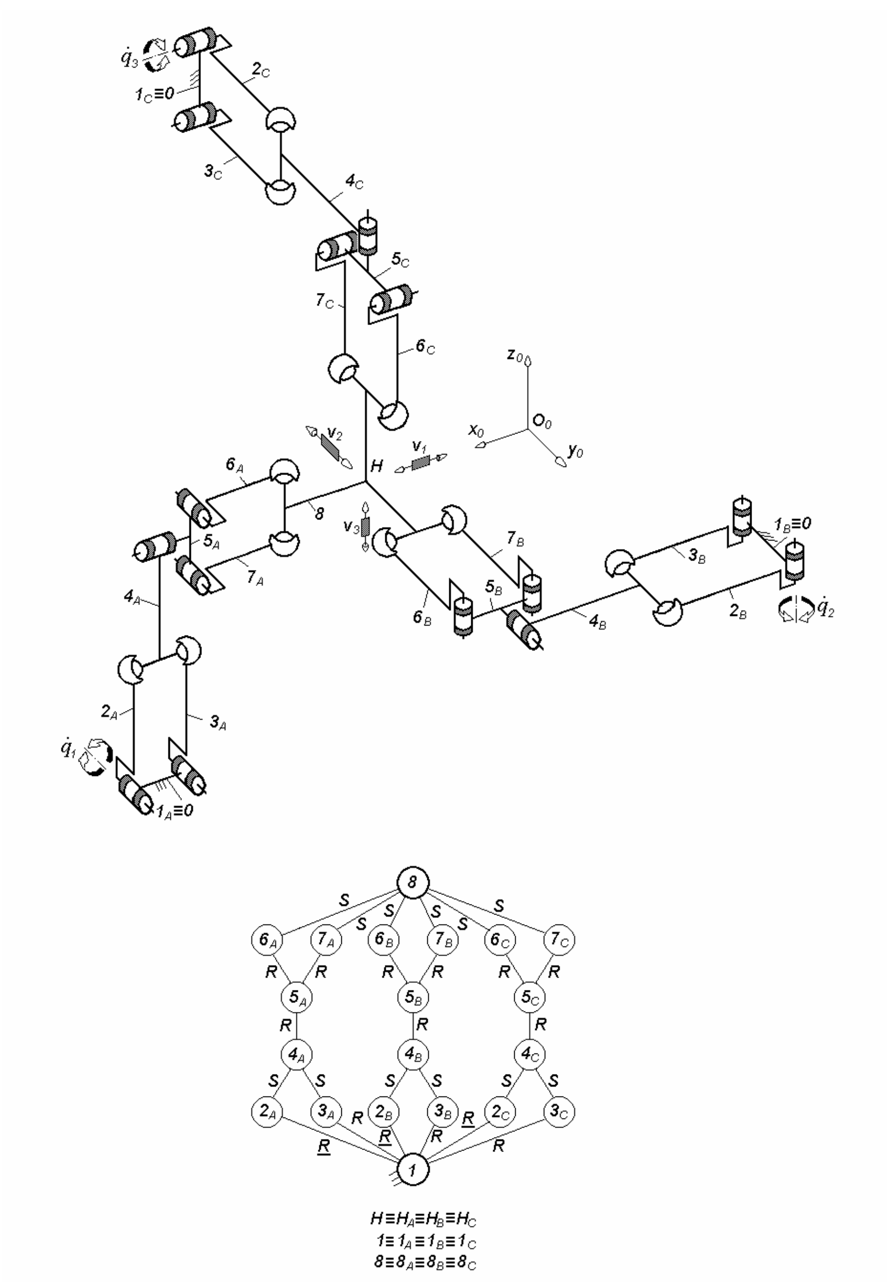

Fig. 4.59. *3-$\underline{Pa}^{ss}RPa^{ss}$*-type non overconstrained TPM with coupled motions and rotating actuators mounted on the fixed base, limb topology $\underline{Pa}^{ss} \perp R \perp^{||} Pa^{ss}$

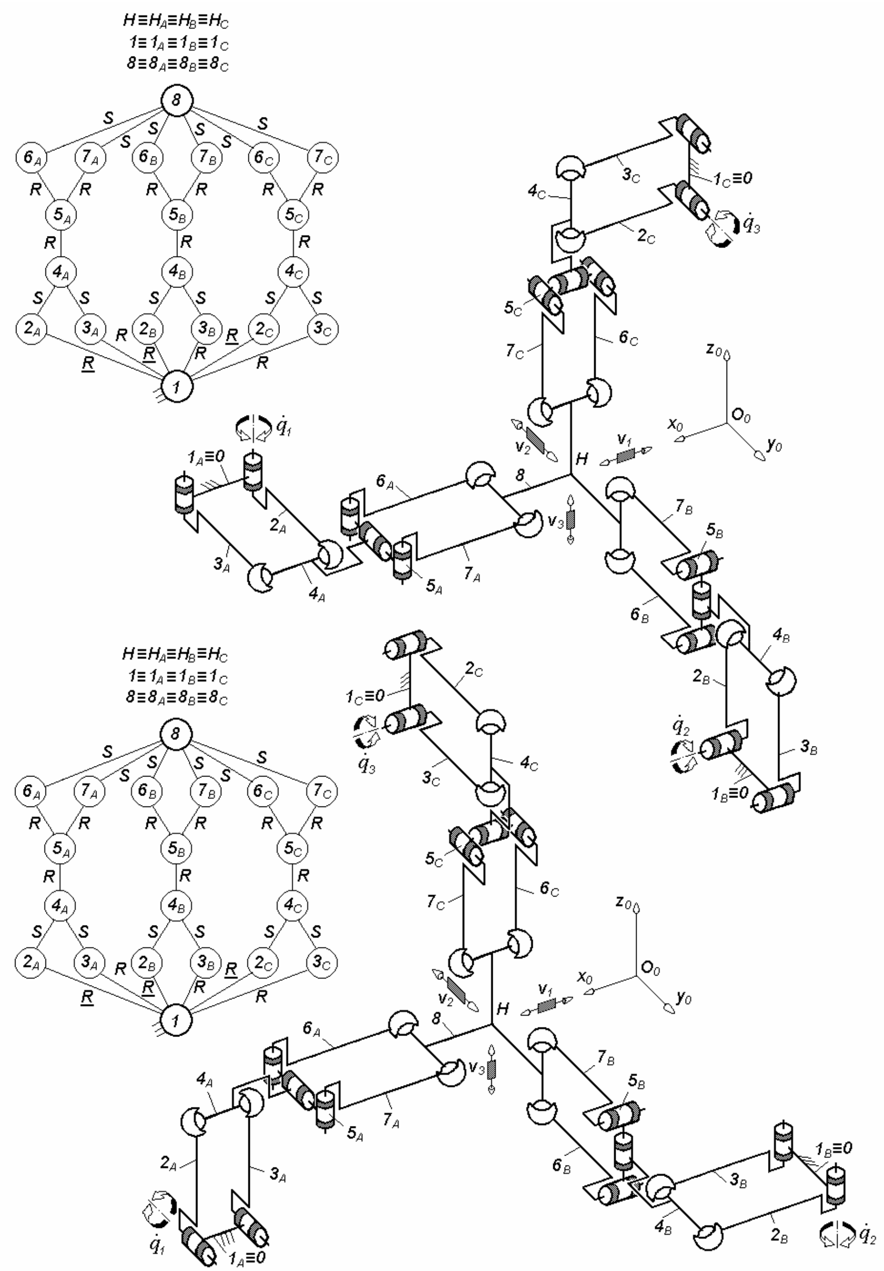

Fig. 4.60. *3-$\underline{Pa}^{ss}RPa^{ss}$*-type non overconstrained TPMs with coupled motions and rotating actuators mounted on the fixed base, limb topology $\underline{Pa}^{ss} \perp R \perp Pa^{ss}$ (**a**) and $\underline{Pa}^{ss} \perp^{\parallel} R \perp Pa^{ss}$ (**b**)

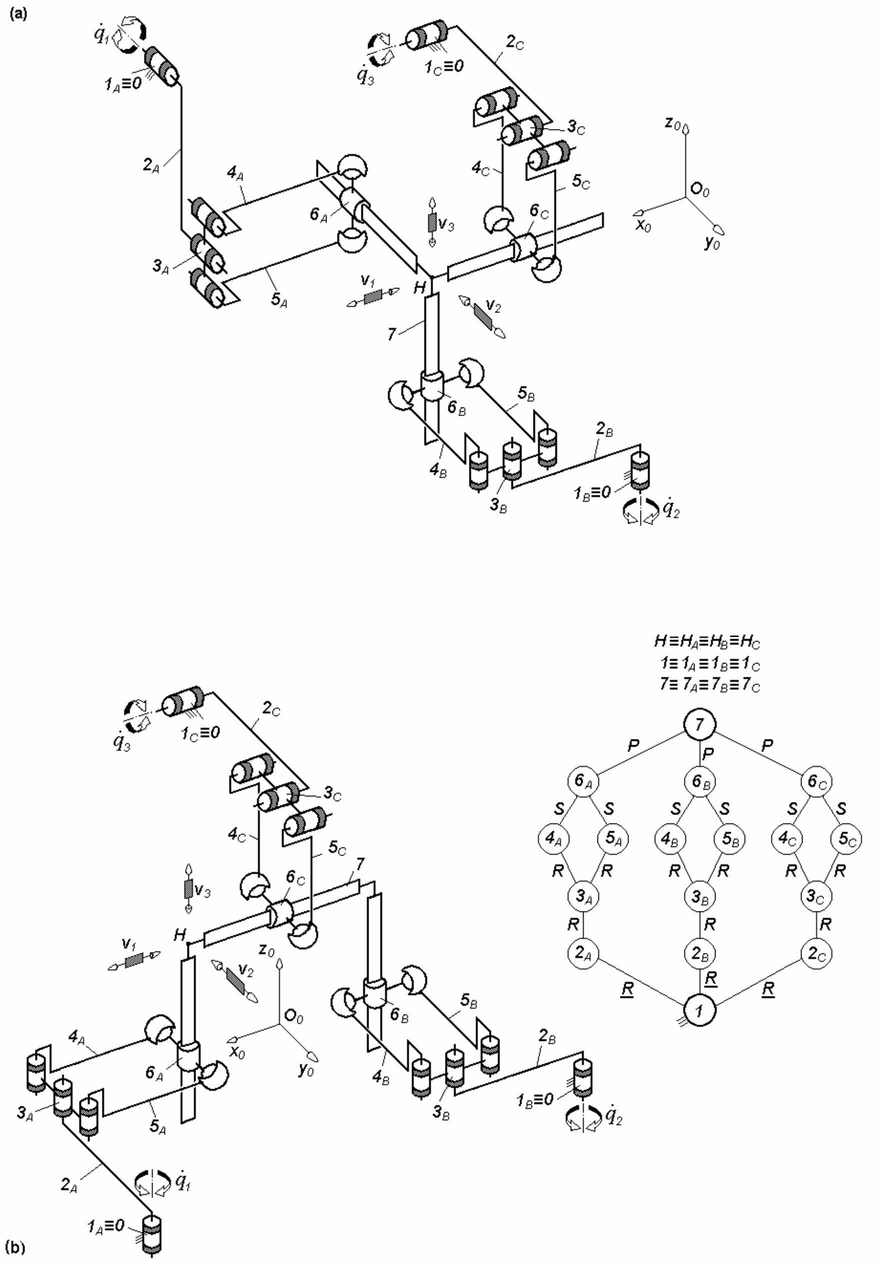

Fig. 4.61. *3-RRPa^ss P*-type non overconstrained TPMs with co-upled motions and rotating actuators mounted on the fixed base, limb topology *R*||*R*||*Pa^ss*||*P*

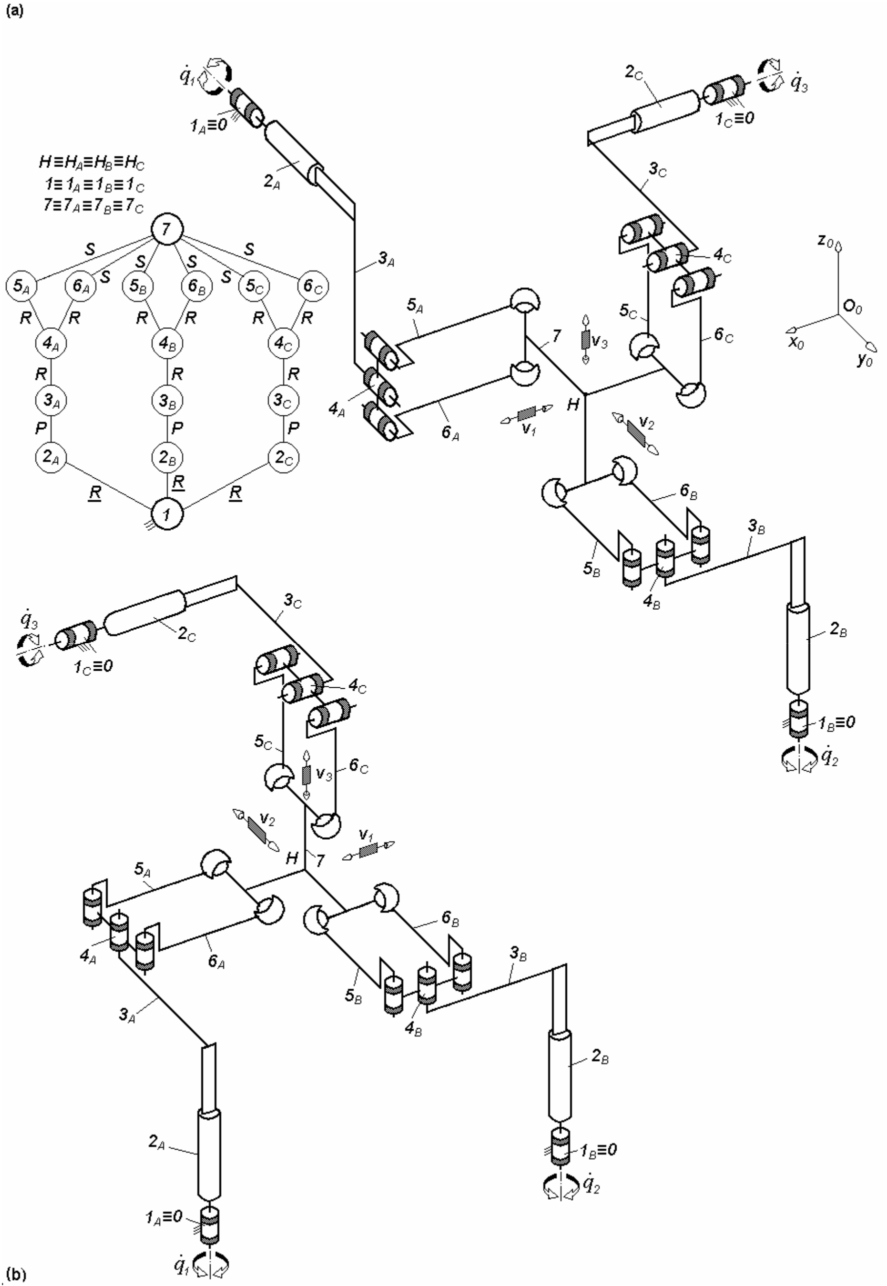

Fig. 4.62. *3-RPRPa^ss*-type non overconstrained TPMs with coupled motions and rotating actuators mounted on the fixed base, limb topology $\underline{R}||P||R||Pa^{ss}$

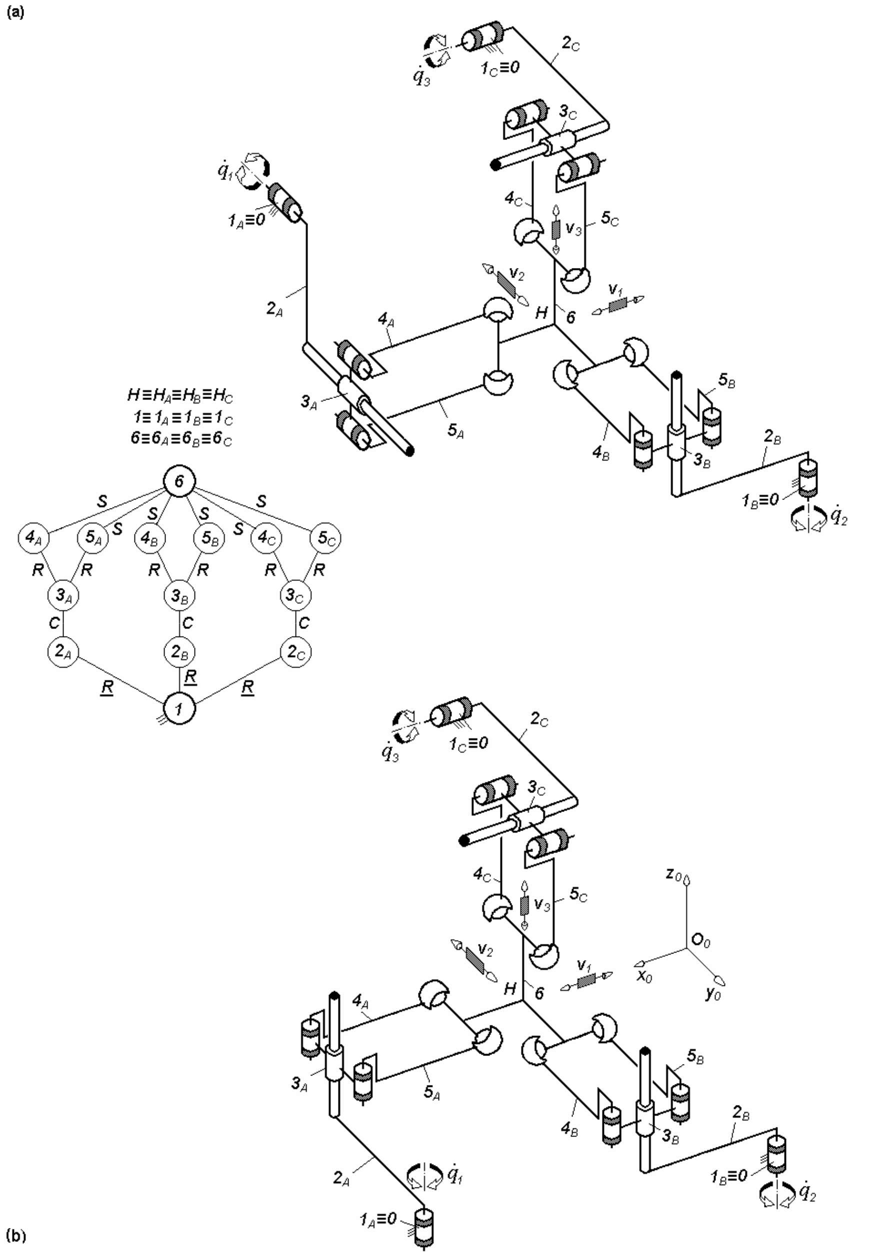

Fig. 4.63. *3-RCPa^ss*-type non overconstrained TPMs with coupled motions and rotating actuators mounted on the fixed base, limb topology $\underline{R}||C||Pa^{ss}$

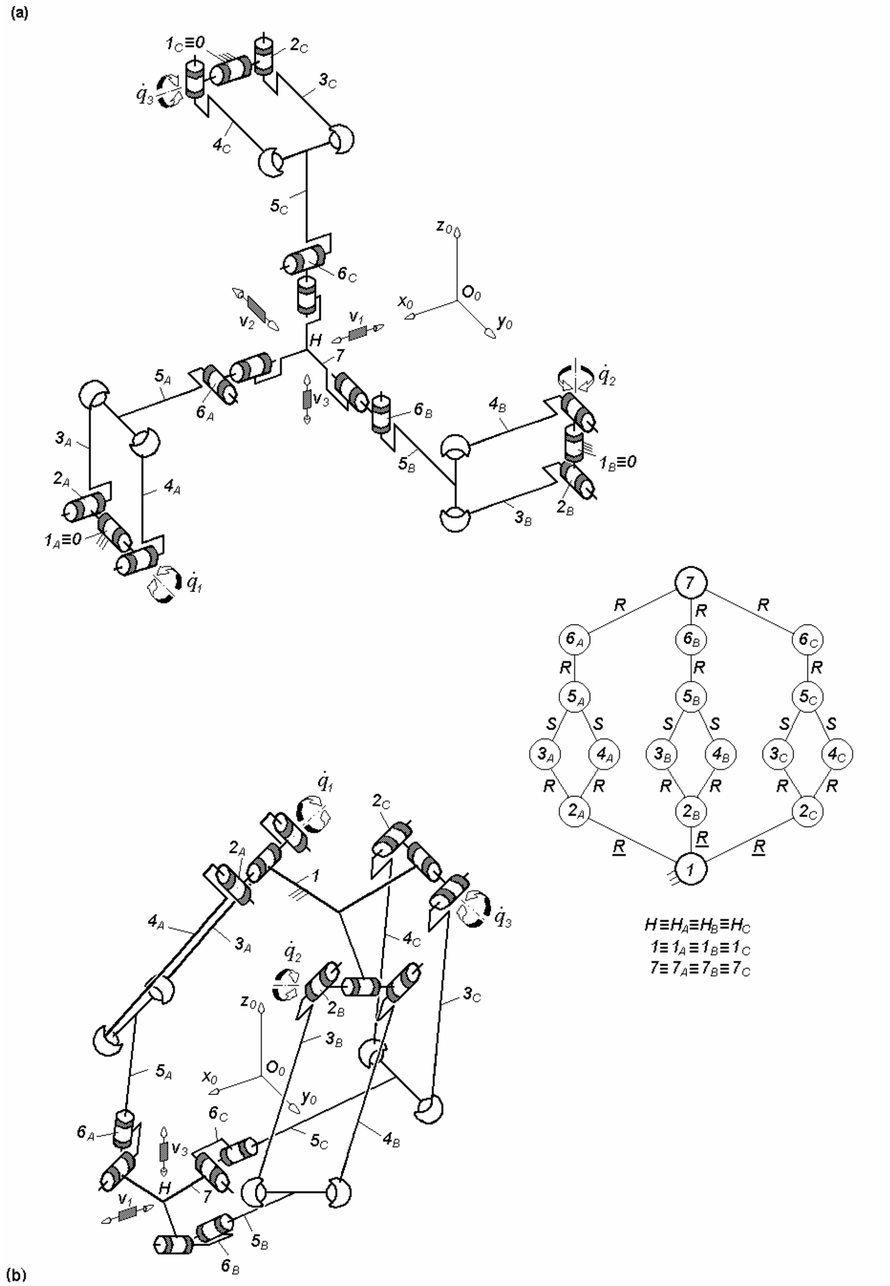

Fig. 4.64. Non overconstrained TPMs of types *3-*$\underline{R}Pa^{ss}RR^*$ (**a**) and *3-*$\underline{R}Pa^{ss}R^*R$ (**b**) with coupled motions and rotating actuators mounted on the fixed base, limb topology $\underline{R}\perp Pa^{ss}\perp^{\parallel}R\perp R$ (a) and $\underline{R}\perp Pa^{ss\text{-}}R^*\perp R$ (**b**)

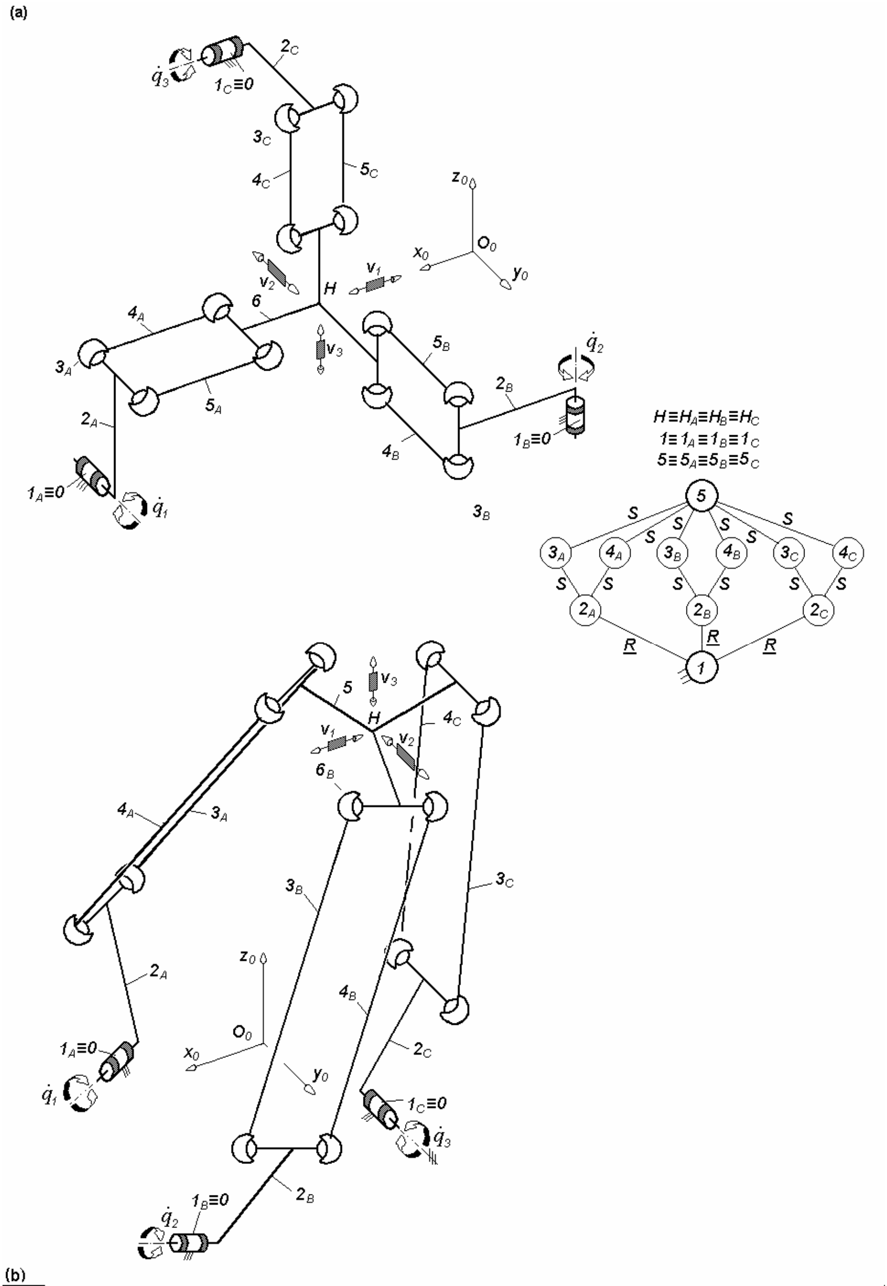

Fig. 4.65. *3-<u>R</u>Pa*^{4s}-type non overconstrained TPMs with coupled motions and rotating actuators mounted on the fixed base and six internal rotational mobilities of links 2_A, 3_A, 2_B, 3_B, 2_C, 3_C

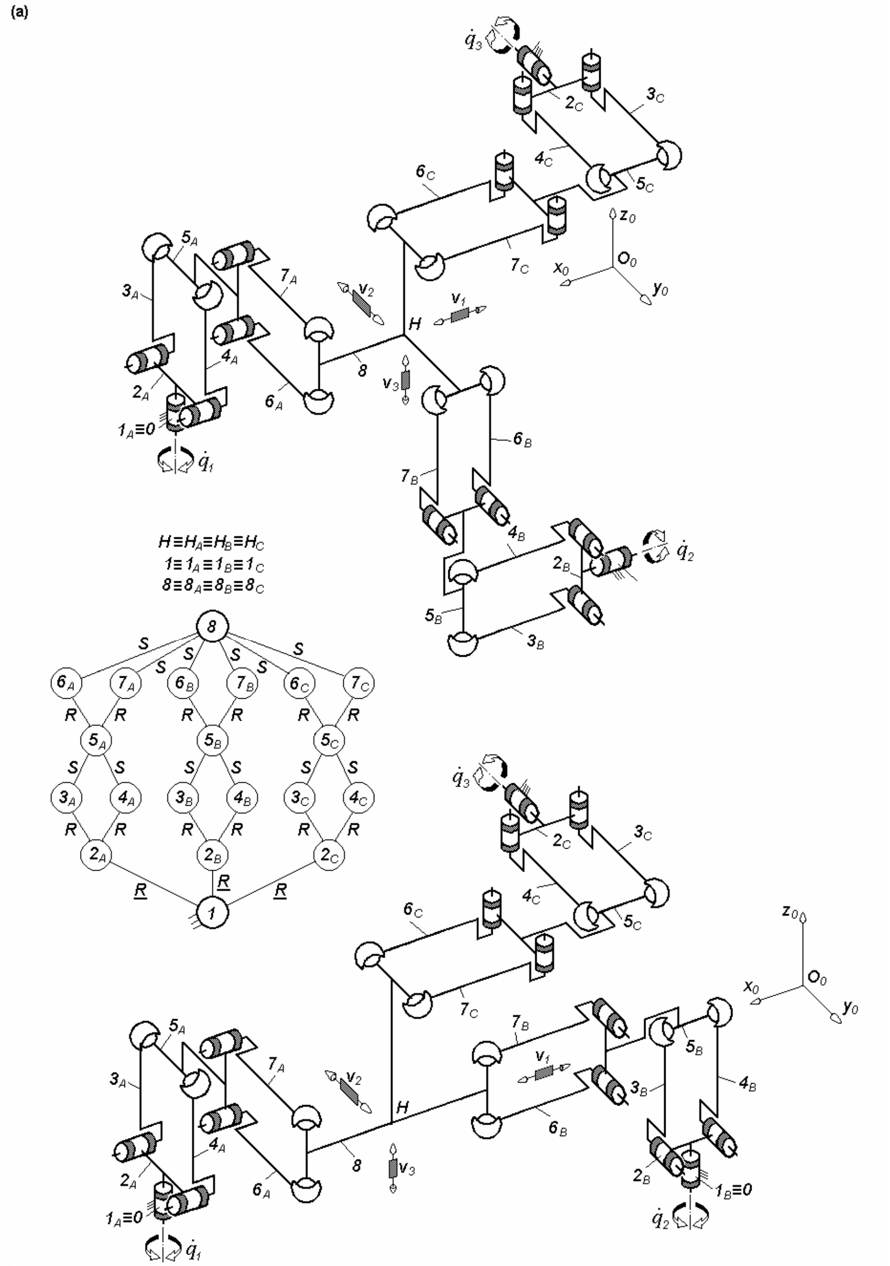

Fig. 4.66. *3-$\underline{R}Pa^{ss}Pa^{ss}$*-type non overconstrained TPMs with coupled motions and rotating actuators mounted on the fixed base, limb topology $\underline{R} \perp Pa^{ss}||Pa^{ss}$

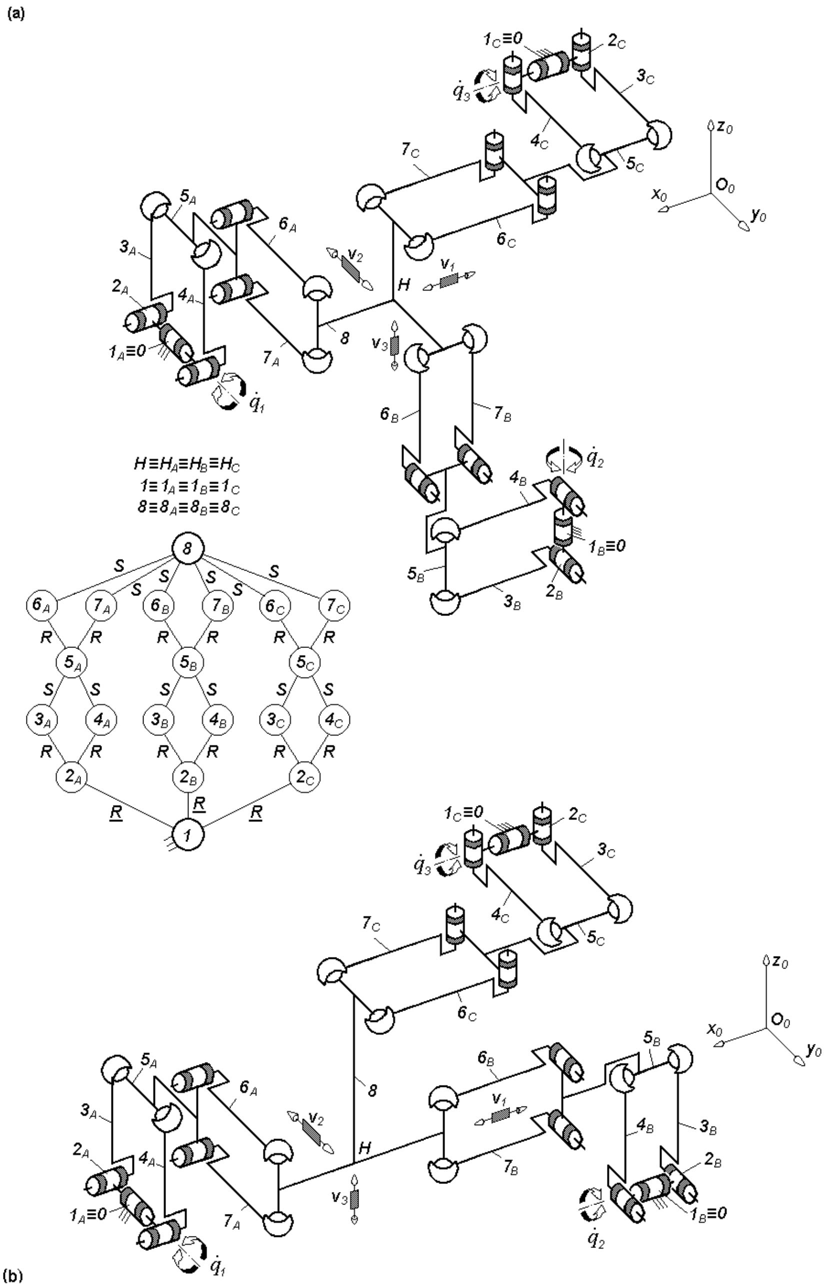

Fig. 4.67. *3-*$\underline{R}Pa^{ss}Pa^{ss}$-type non overconstrained TPMs with coupled motions and rotating actuators mounted on the fixed base, limb topology $\underline{R} \perp Pa^{ss}||Pa^{ss}$

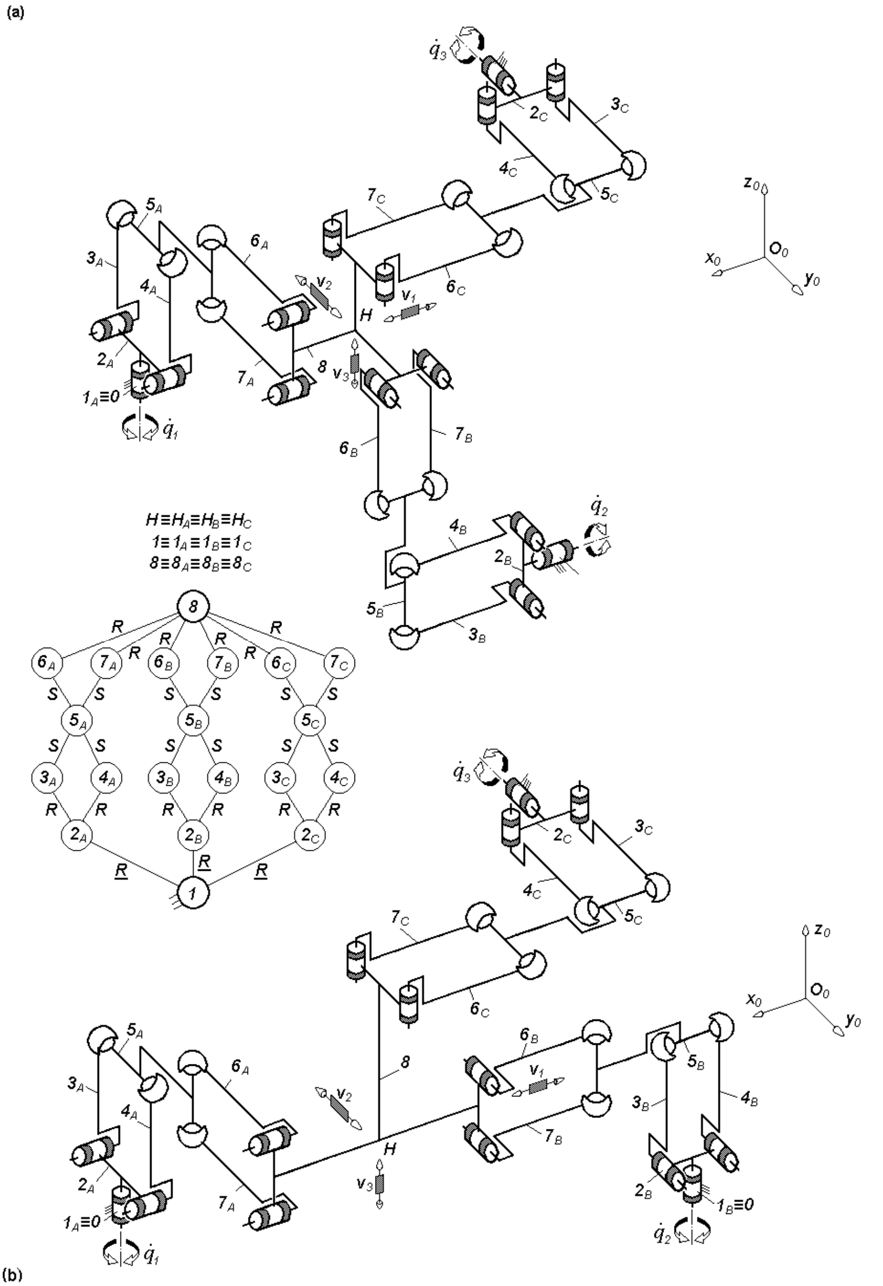

Fig. 4.68. *3-*$\underline{R}Pa^{ss}Pa^{ss}$-type non overconstrained TPMs with coupled motions and rotating actuators mounted on the fixed base, limb topology $\underline{R} \perp Pa^{ss}||Pa^{ss}$

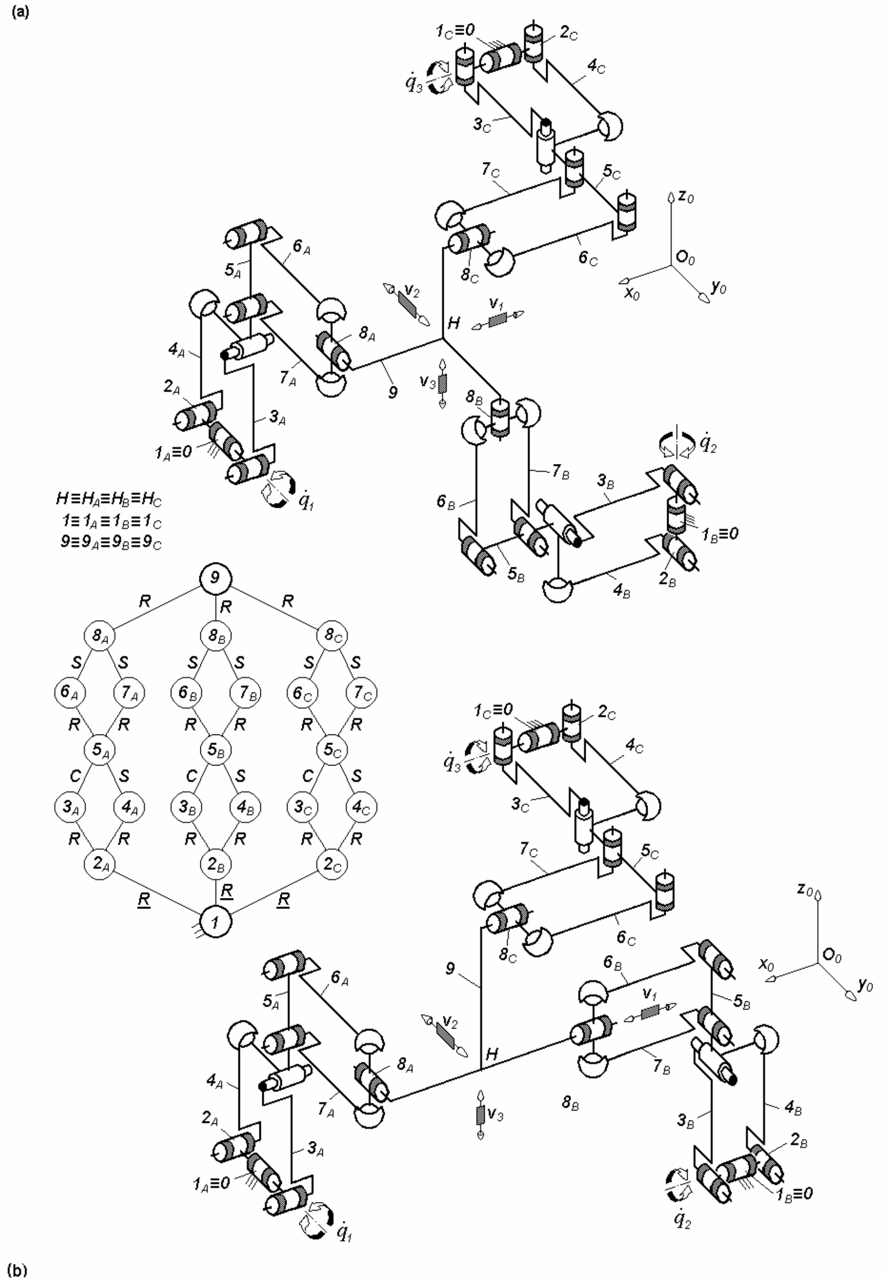

Fig. 4.69. *3-$\underline{R}Pa^{*}Pa^{ss}R$*-type non overconstrained TPMs with coupled motions and rotating actuators mounted on the fixed base, limb topology $\underline{R} \perp Pa^{*} || Pa^{ss} \perp^{||} R$

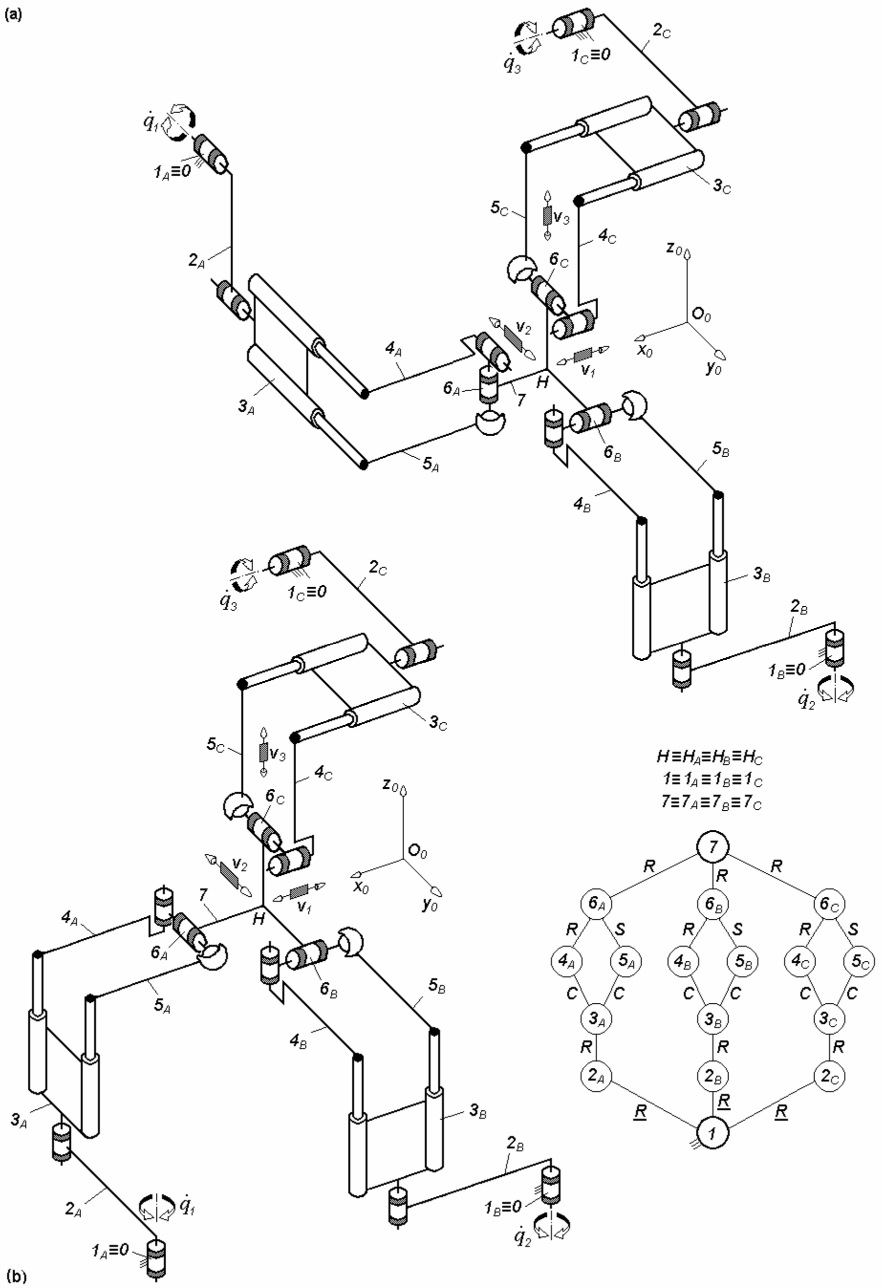

Fig. 4.70. *3-*$\underline{R}RPa^{ccs}R*$-type non overconstrained TPMs with coupled motions and rotating actuators mounted on the fixed base, limb topology $\underline{R}||R||Pa^{ccs}\perp R*$

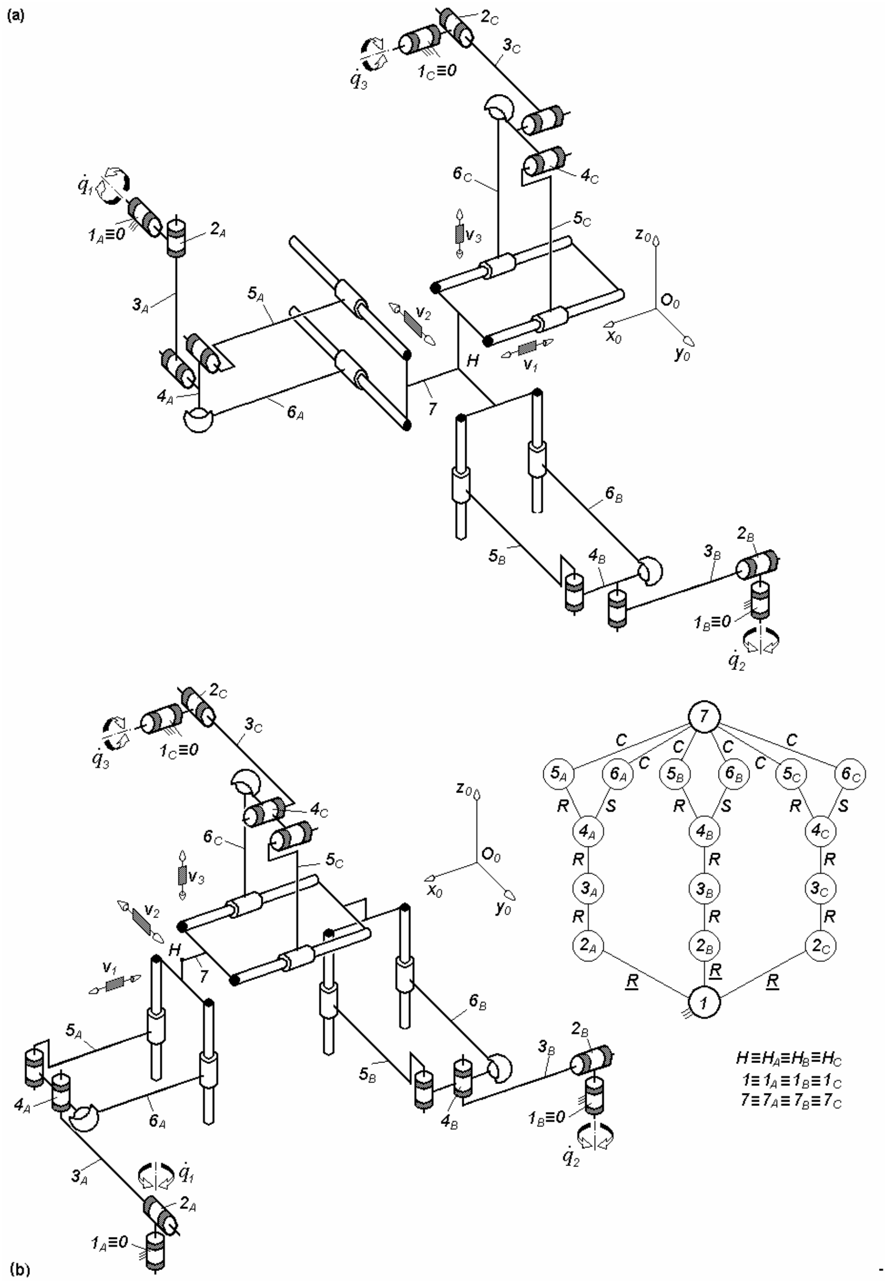

Fig. 4.71. $3\text{-}\underline{R}R^*RPa^{scc}$-type non overconstrained TPMs with coupled motions and rotating actuators mounted on the fixed base, limb topology $\underline{R}\perp R^*\perp^{||}R||Pa^{scc}$

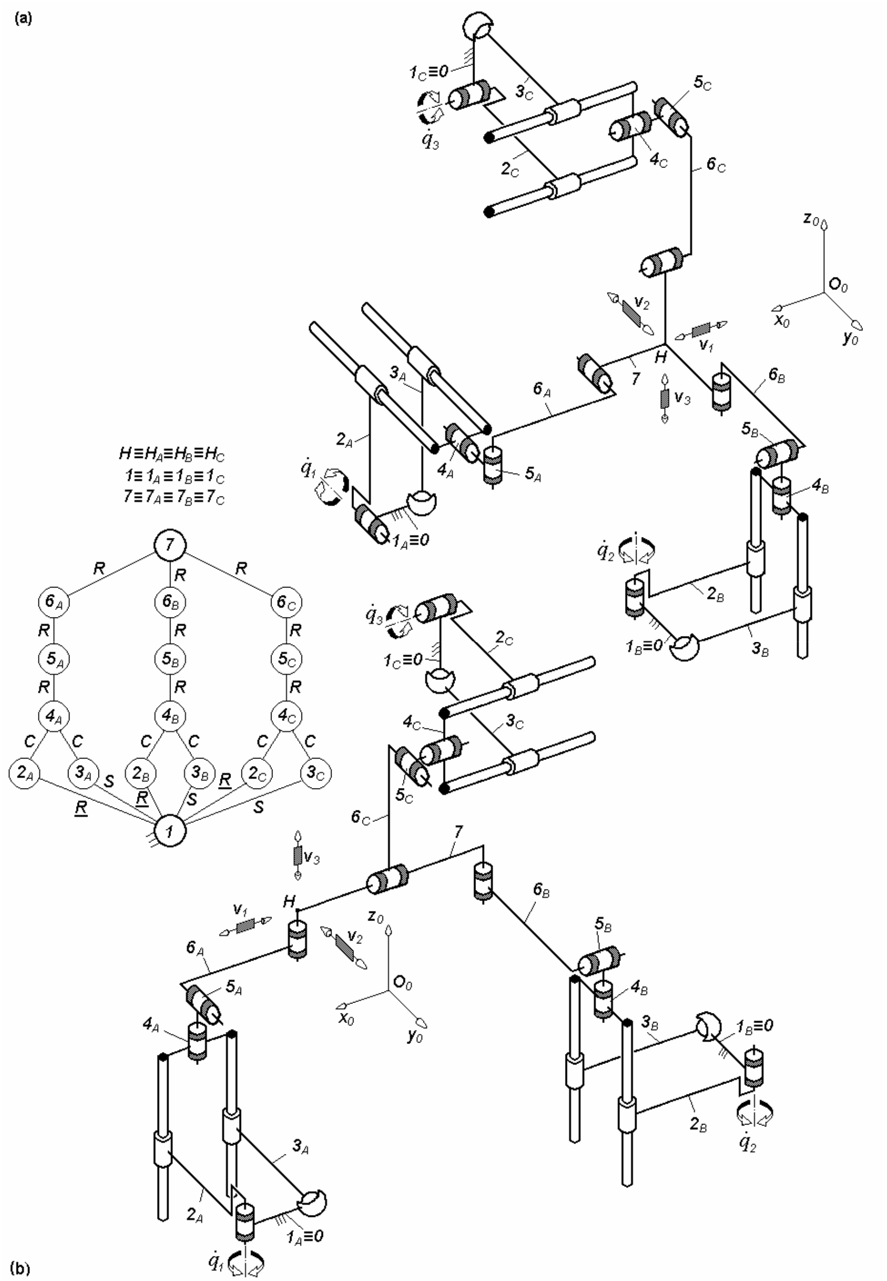

Fig. 4.72. *3-*$\underline{Pa}^{scc}$*RR*R*-type non overconstrained TPMs with coupled motions and rotating actuators mounted on the fixed base, limb topology $\underline{Pa}^{scc}||R \perp R^* \perp^{||} R$

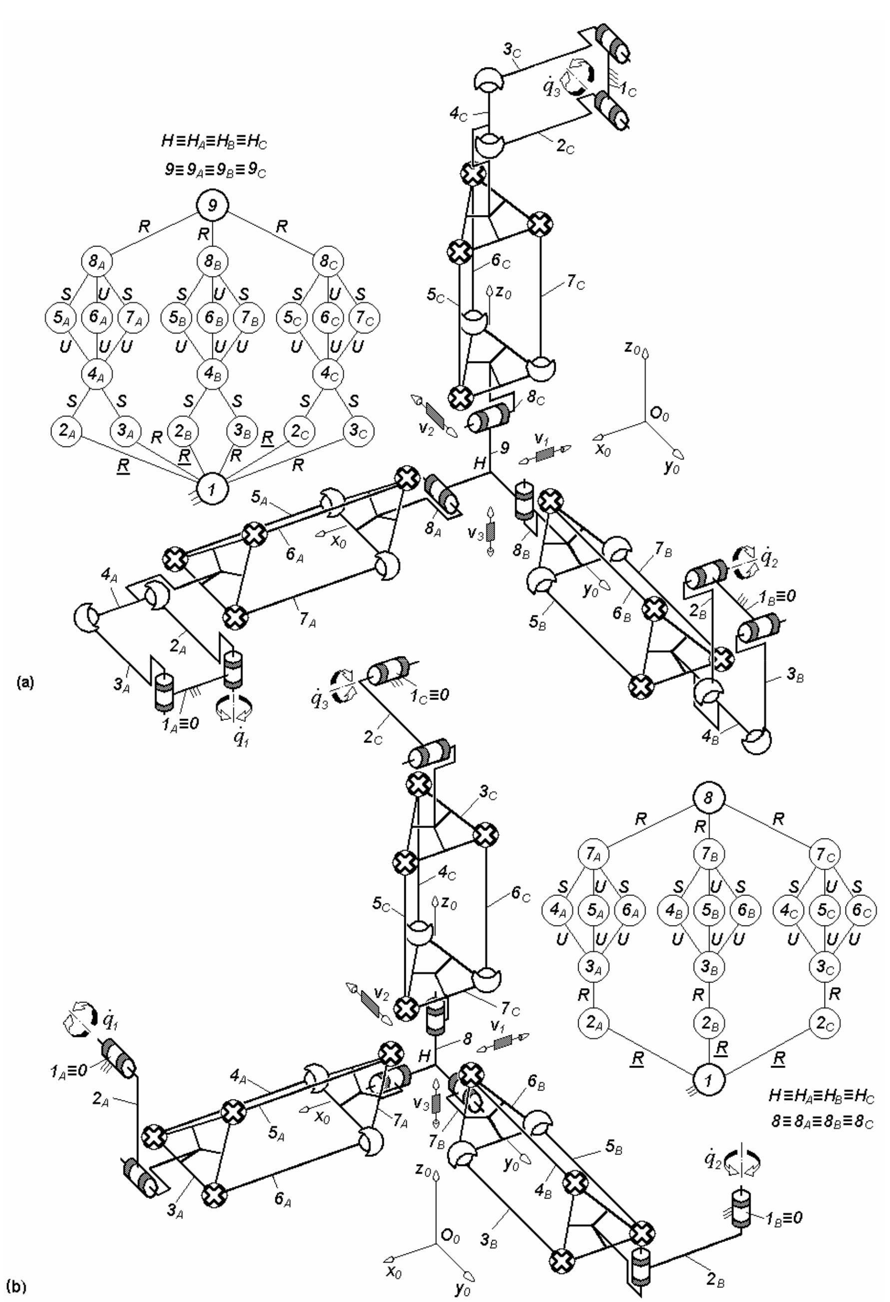

Fig. 4.73. Non overconstrained TPMs of types *3-<u>Pa</u>^{ss}Pr^{ss}R** (**a**) and *3-<u>R</u>RPr^{ss}R** (**b**) with coupled motions and rotating actuators mounted on the fixed base

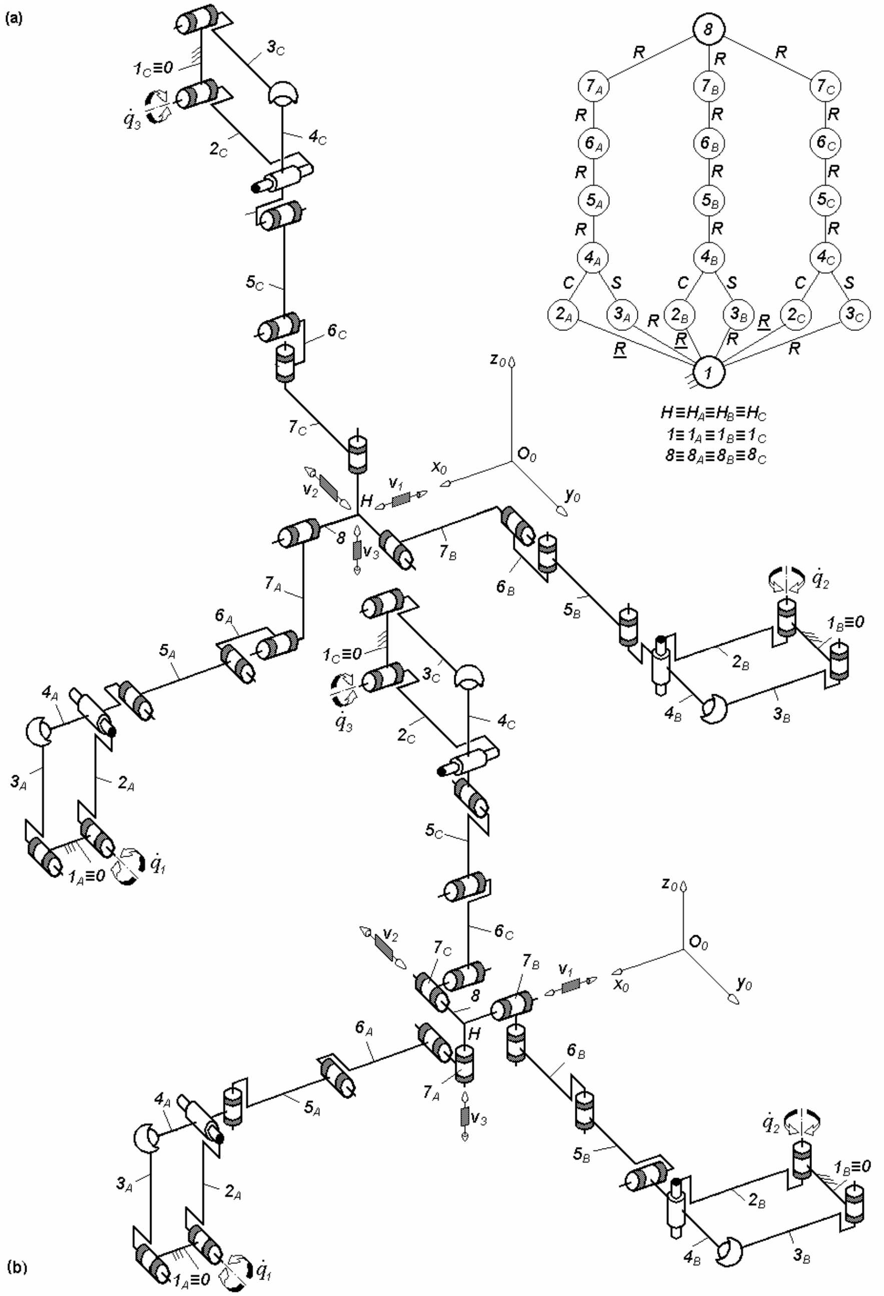

Fig. 4.74. *3-$\underline{Pa}^{cs}$RRRR* -type non overconstrained TPMs with coupled motions and rotating actuators on the fixed base, limb topology $\underline{Pa}^{cs}||R||R\perp R||R$ (**a**) and $\underline{Pa}^{cs}\perp R\perp R||R\perp R$ (**b**)

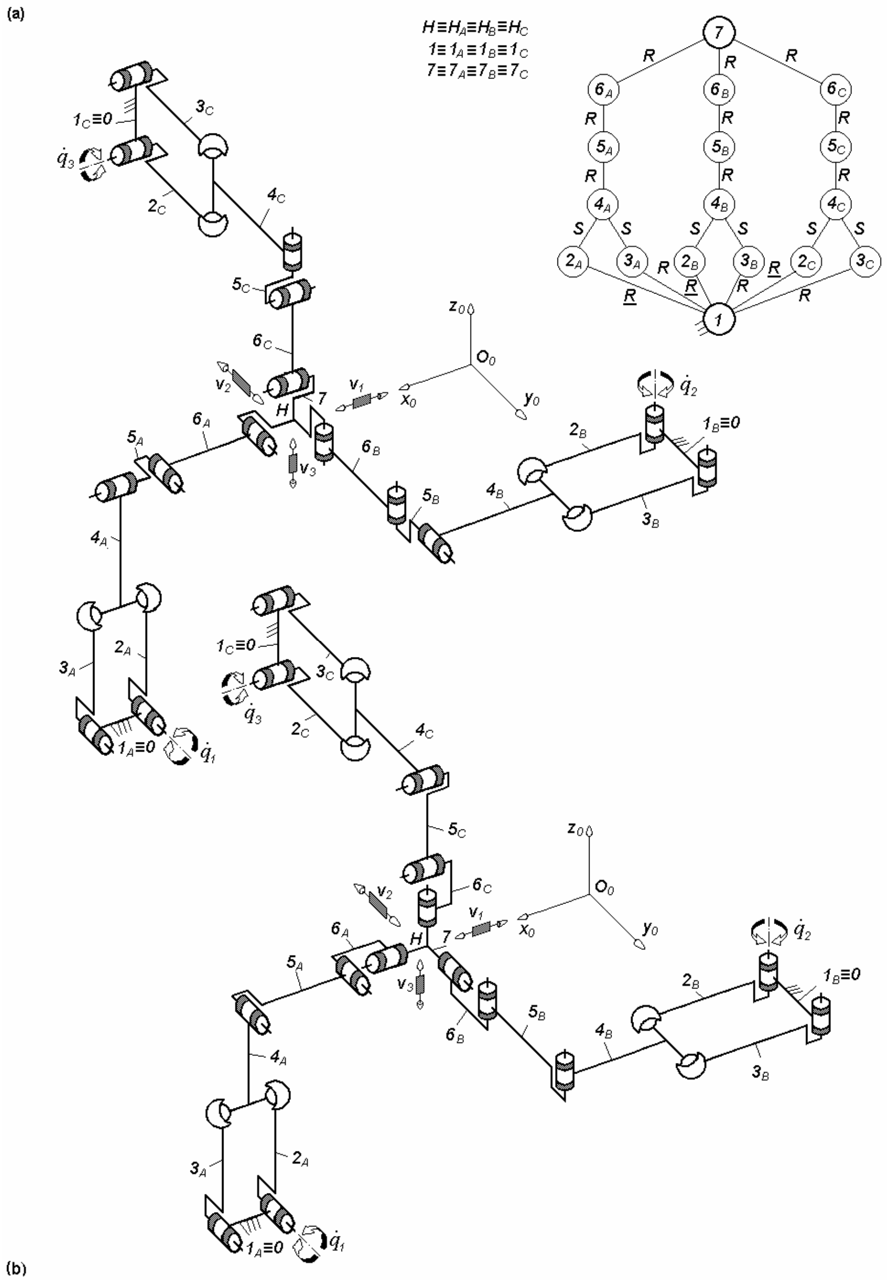

Fig. 4.75. *3-*$\underline{Pa}^{ss}RRR$ -type non overconstrained TPMs with coupled motions and rotating actuators on the fixed base, limb topology $\underline{Pa}^{ss}\perp R\perp R||R$ (**a**) and $\underline{Pa}^{ss}||R||R\perp R$ (**b**)

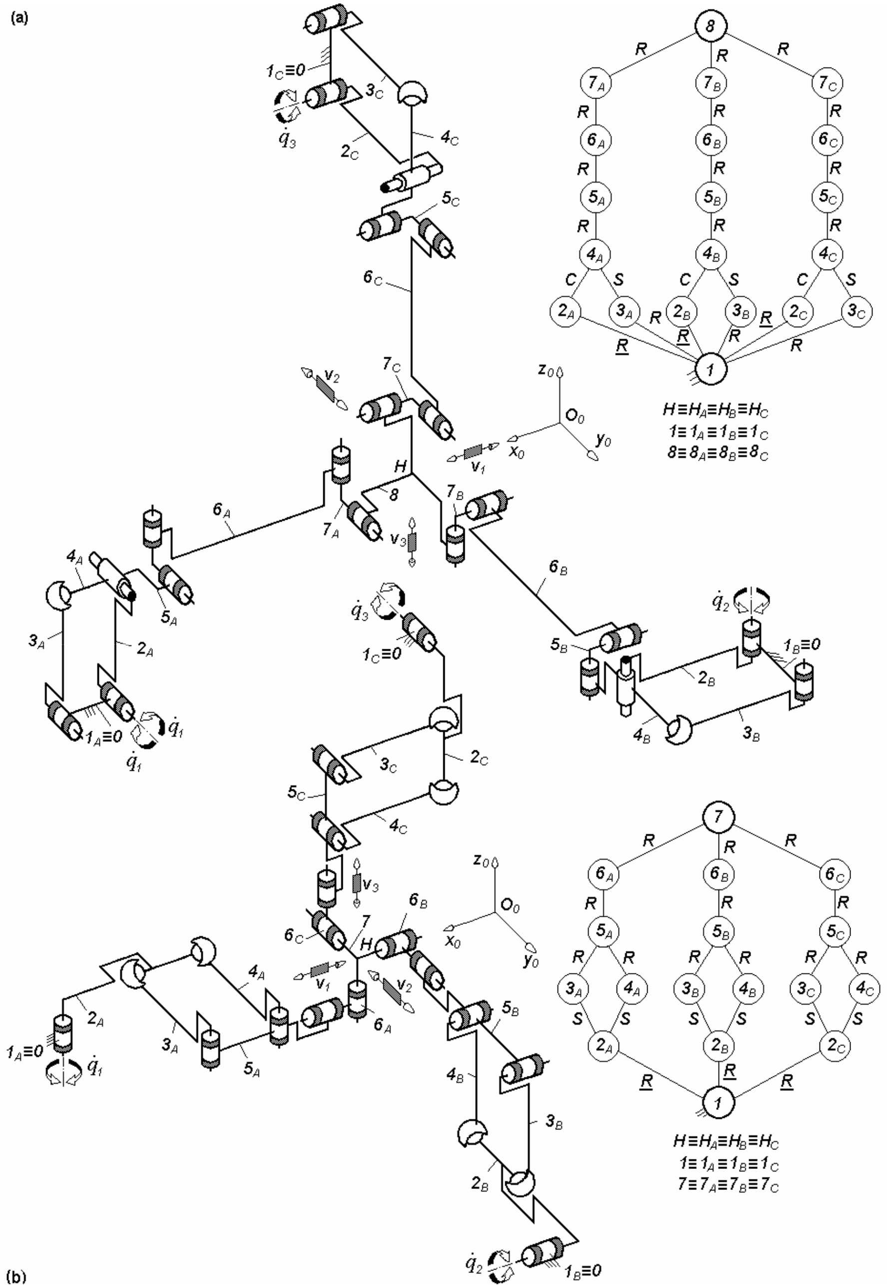

Fig. 4.76. Non overconstrained TPMs of types *3-*$\underline{Pa}^{cs}$*RRRR* (**a**) and *3-*$\underline{R}Pa^{ss}RR$ (**b**) with coupled motions and rotating actuators on the fixed base, limb topology $\underline{Pa}^{cs}||R \perp R||R \perp R$ (**a**) and $\underline{R}||Pa^{ss} \perp R \perp^{||} R$ (**b**)

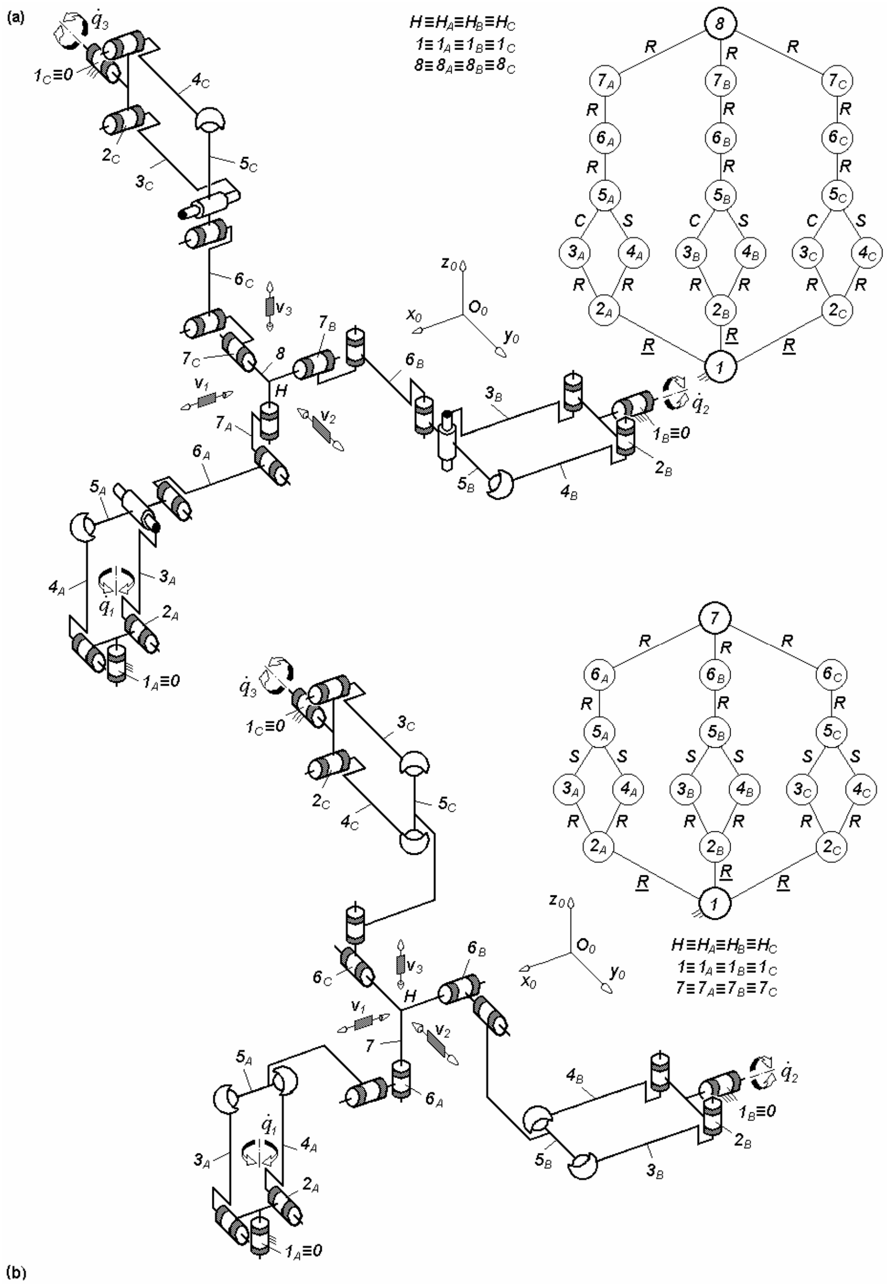

Fig. 4.77. Non overconstrained TPMs of types *3-*$\underline{R}Pa^{cs}RRR$ (**a**) and *3-*$\underline{R}Pa^{ss}RR$ (**b**) non overconstrained TPMs with coupled motions and rotating actuators on the fixed base, limb topology $\underline{R}\perp Pa^{cs}||R||R\perp^{||}R$ (**a**) and $\underline{R}\perp Pa^{ss}\perp^{\perp}R\perp^{\perp}R$ (**b**)

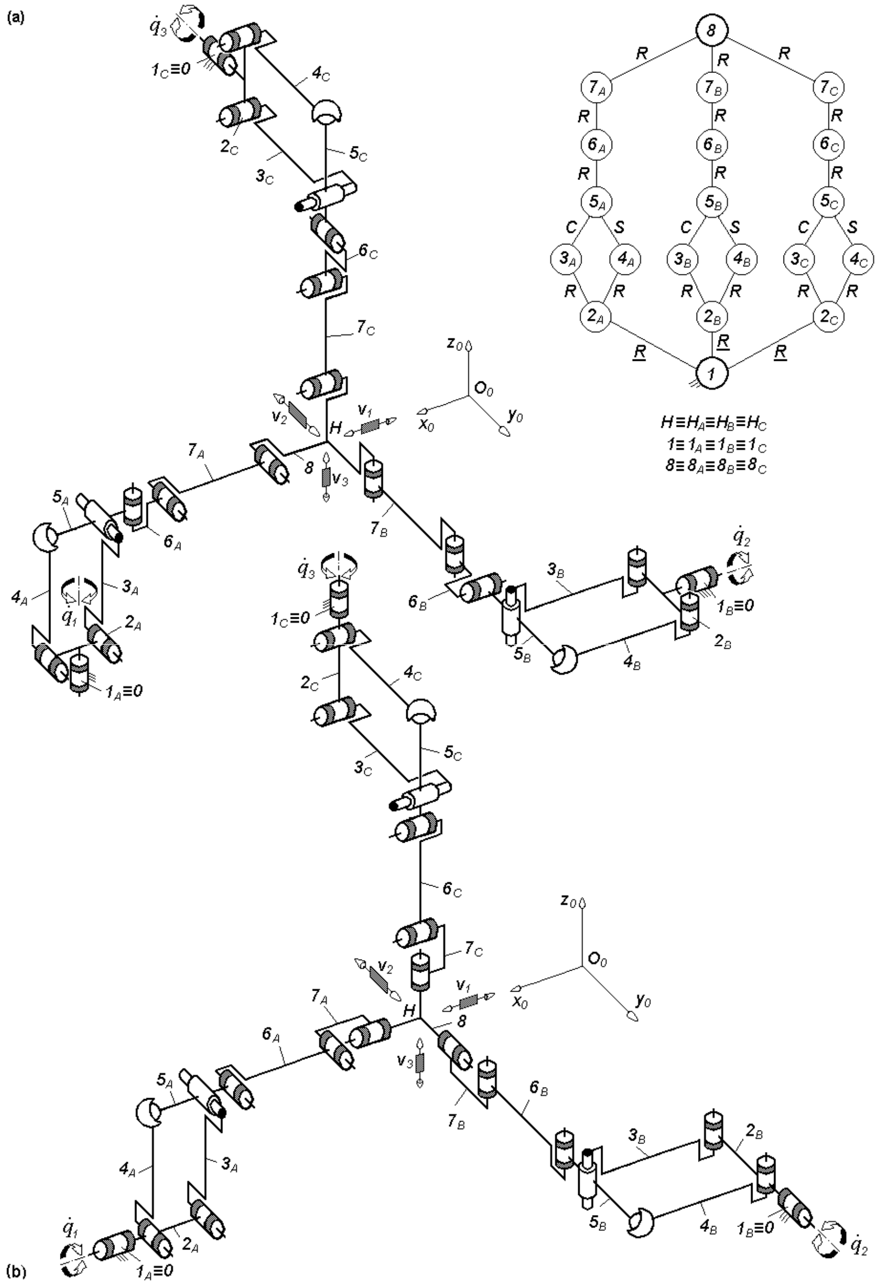

Fig. 4.78. *3-$\underline{R}Pa^{cs}RRR$* -type non overconstrained TPMs with coupled motions and rotating actuators on the fixed base, limb topology $\underline{R}\perp Pa^{cs}\perp^{\parallel}R\perp R\parallel R$ (**a**) and $\underline{R}\perp Pa^{cs}\parallel R\parallel R\perp^{\parallel}R$ (**b**)

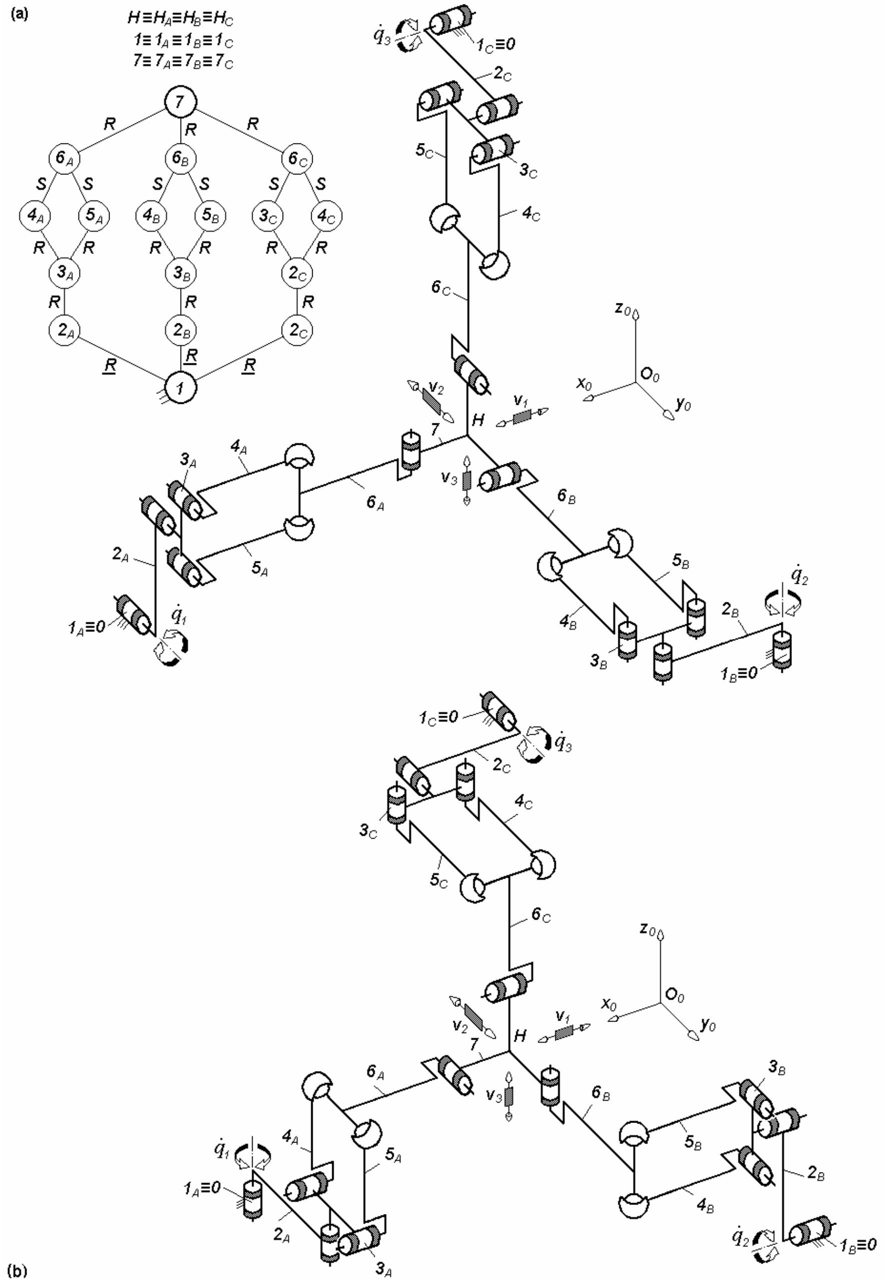

Fig. 4.79. *3-$\underline{R}RPa^{ss}R$*-type overconstrained TPMs with coupled motions and rotating actuators on the fixed base, limb topology $\underline{R}||R||Pa^{ss}\perp R$ (**a**) and $\underline{R}||R\perp Pa^{ss}\perp^{\perp} R$ (**b**)

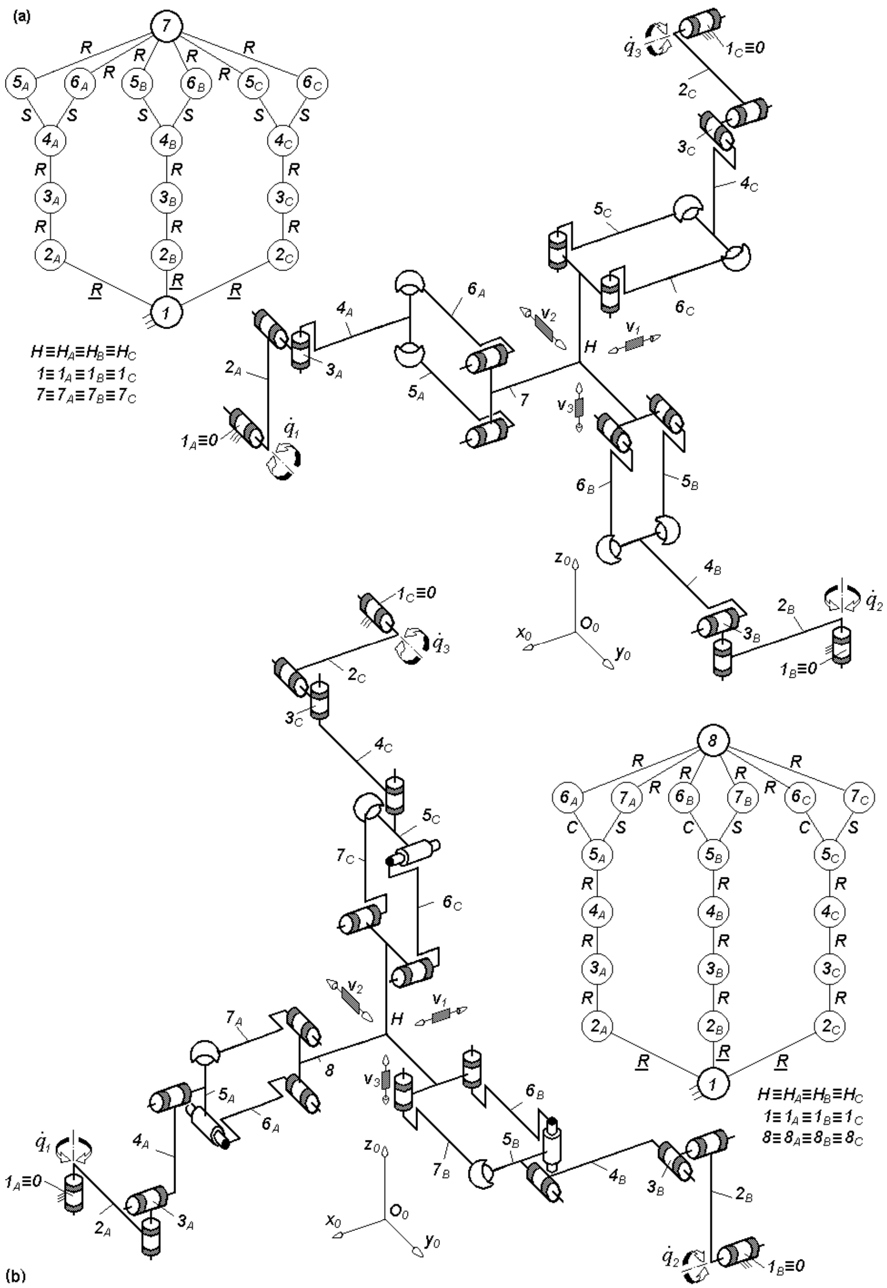

Fig. 4.80. Non overconstrained TPMs of types *3-$\underline{R}RRPa^{ss}$* (**a**) and *3-$\underline{R}RRRPa^{cs}$* (**b**) with coupled motions and rotating actuators on the fixed base, limb topology $\underline{R}||R\perp R\perp^{\perp} Pa^{ss}$ (**a**) and $\underline{R}||R\perp R||R\perp^{\perp} Pa^{cs}$ (**b**)

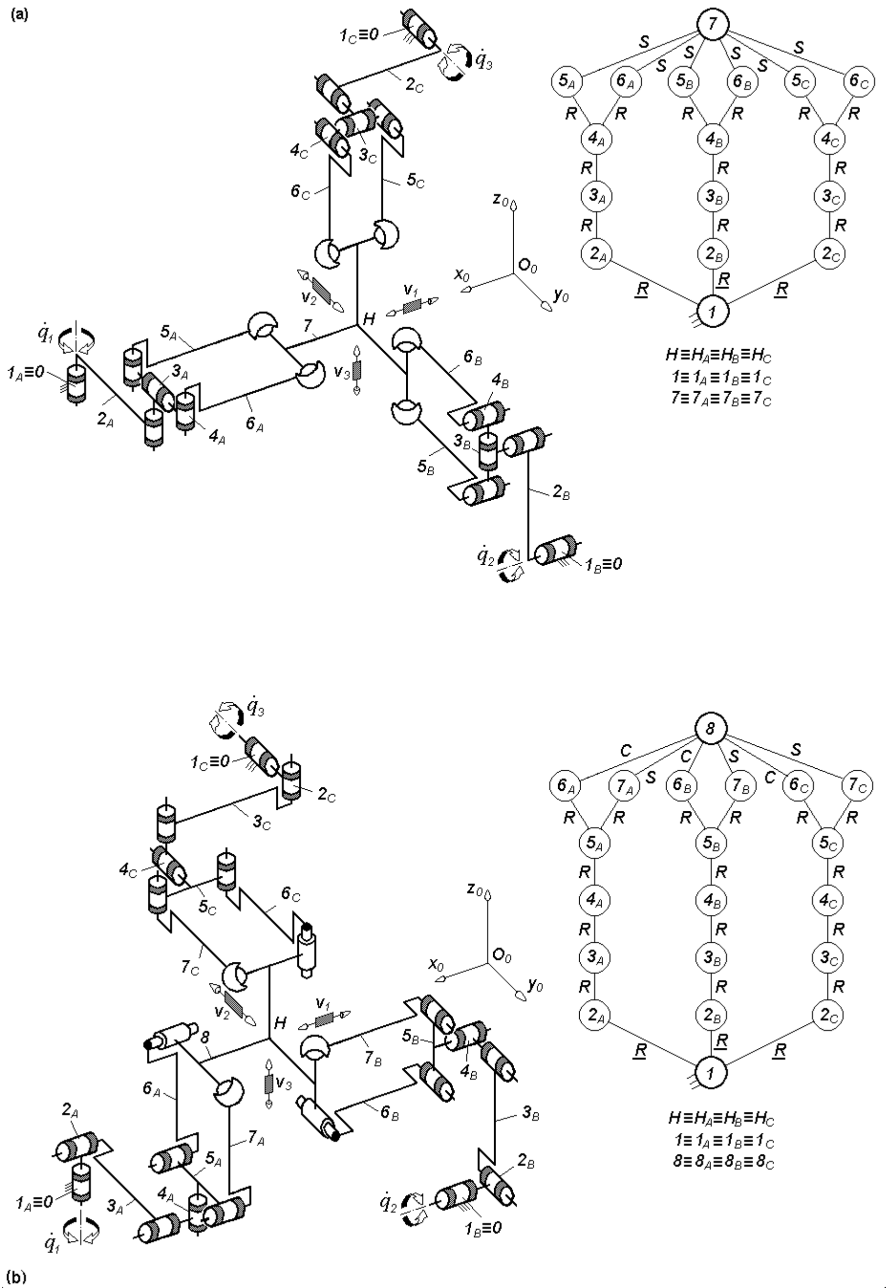

Fig. 4.81. Non overconstrained TPMs of types *3-*$\underline{R}RRPa^{ss}$ (**a**) and *3-*$\underline{R}RRRPa^{cs}$ (**b**) with coupled motions and rotating actuators on the fixed base, limb topology $\underline{R}||R\perp R\perp Pa^{ss}$ (**a**) and $\underline{R}\perp R||R\perp^{||}R\perp Pa^{cs}$ (**b**)

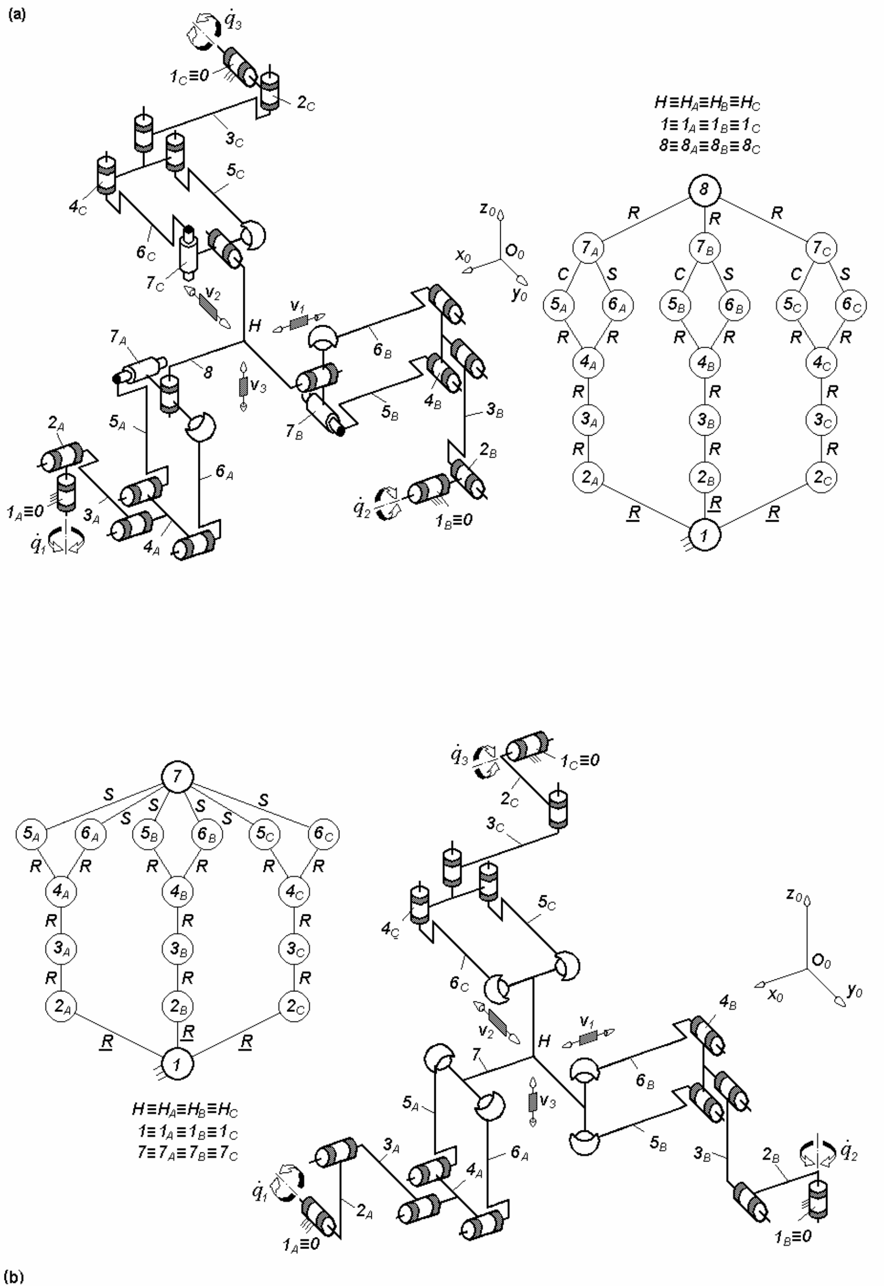

Fig. 4.82. Non overconstrained TPMs of types *3-$\underline{R}$RRPa^{cs}R* (**a**) and *3-$\underline{R}$RRPa^{ss}* (**b**) with coupled motions and rotating actuators on the fixed base, limb topology $\underline{R} \perp R||R||Pa^{cs} \perp^{||} R$ (**a**) and $\underline{R} \perp R||R||Pa^{ss}$ (**b**)